Volume 45, Number 3

Proceedings of the West Virginia Academy of Science 1973

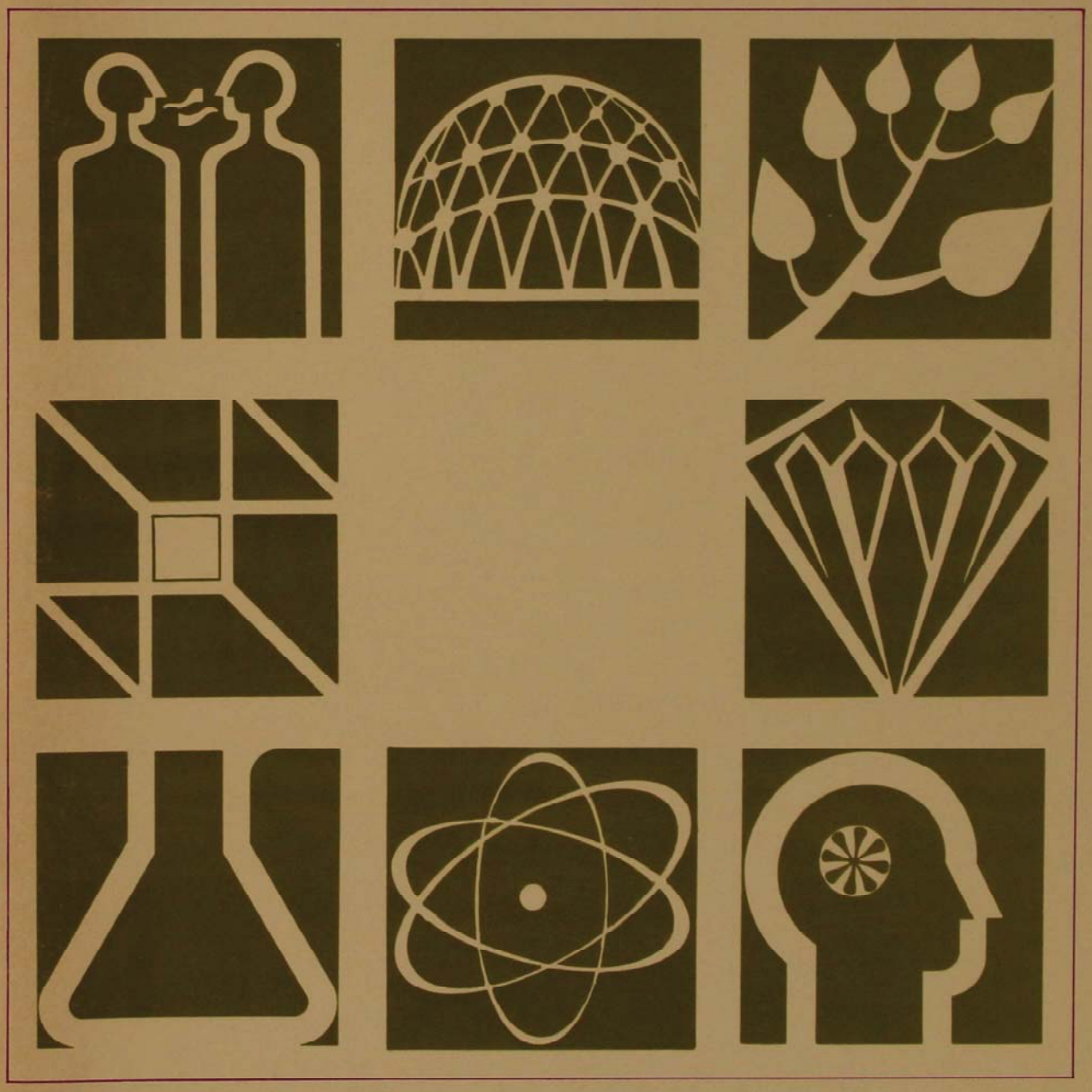

Proceedings of the West Virginia Academy of Science 1973

Vol. 45—No. 3

THE FORTY-EIGHTH ANNUAL SESSION

Fairmont State College

Fairmont, West Virginia

APRIL 5, 6, 7, 1973

Printed by
McClain Printing Company
Parsons, West Virginia

Cover Design
Meredith Pearce
West Virginia University
Office of Publications
Morgantown

West Virginia Academy of Science, Inc.

The West Virginia Academy of Science was founded at Morgantown, November 28, 1924. The Academy was incorporated under the Code of West Virginia on May 9, 1959 as "a nonstock corporation, which is not organized for profit but for the advancement of learning and scientific knowledge."

Proceedings of the West Virginia Academy of Science

Published quarterly by the West Virginia Academy of Science, Inc. Manuscripts for publication should be sent to the Editor, Anthony Winston, Department of Chemistry, West Virginia University, Morgantown, West Virginia 26506. Proof, edited manuscripts, and all correspondence regarding papers for publication should be directed to the Editor.

Applications for membership in the Academy and dues should be sent to Joseph Glencoe, West Virginia Wesleyan College, Buckhannon, West Virginia 26201. Changes of address should be sent to Elizabeth Ann Bartholomew, Department of Biology, West Virginia University, Morgantown, West Virginia 26506. Correspondence concerning library exchanges should be directed to Director of Libraries, West Virginia University, Morgantown, West Virginia 26506.

Contents

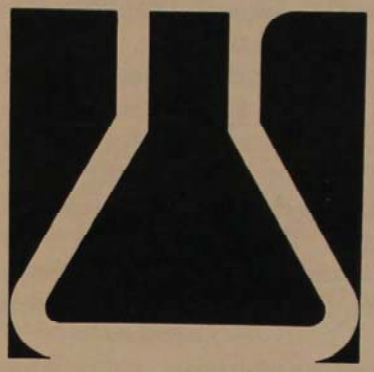

Chemistry Section

Isolation and Inhibition Studies of Lectins a Preliminary Report

Linda Sue Adkins, Gary R. Beasley, Diana G. Childers, Karla Jean Hixon, Mary Jane Hutchinson McDaniel, Melvyn W. Mosher, and Howard C. Price
Department of Chemistry, Marshall University
Huntington, West Virginia 25701

Abstract

The phytohemagglutinin was isolated from five different varieties of *Phaseolus* by the method of Sumner and Howells (13). These materials were compared as to their agglutination reactions on human erythrocytes. In all cases for detectable agglutination reaction, a concentration of about 10^{-4} grams per ml was required. A number of materials were tested to see if they would inhibit the agglutination reaction. Approximately a 20% inhibition of the lectin from navy and kidney beans was obtained with bovine brain ganglioside mixture and insitol. N-Acetylneuriminic acid, a component of many gangliosides showed about a 20% inhibition of the agglutination reaction of the lectin from kidney, navy, and marrow beans. The lectin from pinto beans showed approximately a 50% inhibition by arabinose.

Introduction

Materials of plant origin which possess the ability to aggregate red blood cells are called phytohemagglutinins. These macromolecules belong to a general class of compounds, lectins, which include plant or animal derived substances which can agglutinate erythrocytes. The first of these compounds were reported in the late 1880's and was detected in castor beans (1, 11). This compound had the ability to agglutinate red blood cells of humans and certain animals. Landsteiner established that the hemagglutinating ability of extracts of different seeds were different when tested against red blood cells. This difference was similar to that observed using the more conventional antibodies of animal blood serum (4).

Although the first lectin was isolated as a pure crystalline material from jack beans in 1919, it was not until 1936 that it was characterized. This phytohemagglutinin does not aggregate human erythrocytes, it does agglutinate horse ery-

throcytes at concentrations as low as 0.10 micrograms/milliliter (13). This material also precipitates glycogen in an antibody-antigen type reaction.

Some of the known lectins have very specific properties for blood cells of different species or blood groups within a species (3, 16, 17). Such a lectin is the one isolated from lima beans (*Phaseolus lunatus* L.) that is specific for human blood group A (3). A similar behavior is found for certain plants of the genus *Vicia* (15). Other blood groups have been shown to be selectively agglutinated by lectins from certain other legumes. For example, *Vicia granimea* is used mainly in Europe by blood banks to determine human blood group N. Plant extracts have been shown to be selective reagents for the species determination of certain salt water fish (15, 16).

In addition to these blood group specific phytohemagglutinins, other nonspecific compounds have been reported (1, 11, 15). Some lectins are inhibited in their agglutination reaction with blood cells by simple sugars. Mannose is an inhibitor to the aggreagation of horse erythrocytes by the jack beans lectin, Concanavalin A, while galactose is found to be an inhibitor to the reaction with human cells of the castor bean lectin (11).

No work has been done however on these compounds to determine the chemical and serological similarities and differences between those extracted from closely related plants. We would like to report our preliminary finding along these lines.

Results and Discussion

A number of dried beans and seed were extracted by blending the whole seed with 3 volumes of 1% saline. The blended materials were stored overnight in a refrigerator and then centrifuged. The clear extract was decanted and these extracts screened for lectin activity against human erythrocytes. The results of this set of studies is reported in Table 1.

Protein phytohemagglutinins from the dried beans of five different varieties of Phaseolus was obtained by either the method of Sumner and Howells (13), Figure 1, or Rigas and Osgood (10), Figure 2. The beans used for the isolation were pinto, kidney, navy, michigan pea, marrow, and great northern. In all cases the isolated materials were white powders. All of these compounds were found to cluster human red blood cells down to concentrations in the range of 0.1 mg/ml, see Table 2. The concentration range of these materials was about 100 times less sensitive than that reported for Con-A toward horse erythrocytes (13).

Having isolated* the lectins from pinto, kidney, navy, and marrow beans research was conducted to determine their serological characteristics. One important characteristic of many of the previously isolated lectins is that they may have a specific simple sugar that inhibits the clustering reaction. The isolated phytohemagglutinins were tested to determine if they in fact did have an inhibitor, and if the inhibitor was similar for all of the lectins from these closely related beans. In addition to the use of monosacchraides, a mixture of calf brain gangliosides was included. The ganglioside mixture was included in this work since a number of recent studies (2, 7, 12, 14, 18) have demonstrated their presence in bovine blood plasma, and also in erythrocytes. Mannose, galactose,

*The lectin from pinto, navy, and kidney was isolated by the method of Sumner and Howells, while the lectin from marrow and kidney beans was isolated by the method of Rigas and Osgood. The isolated kidney lectin showed no differences as a function of the isolation scheme, and no distinction has been made here between the two lectins.

Table 1. Screening Results of Seed Extracts* on Human Erythrocytes of Blood Groups Indicated. The Numerical Value Is the Average of at Least 5 Individuals in Each Blood Group.

lectin extract from:	*Blood Groups*			
	A	*B*	*AB*	*O*
avacado (Florida)	0	0	0	0
sweet corn	0	0	0	0
popcorn	2	2	2	2
garbannzo bean	0.5	0.5	0	0
lintels	0	0	0	0
great northern beans	4	4	4	4
kidney	3	3	3	3
black-eyed peas	0.5	0.5	0	0.5
michigan pea beans	2	4	2	3
mung bean	0	0	0	0
scarlet runner bean	4	4	4	4
navy	1	1	2	2
soybeans	0	0	0	0
marrow	3	4	3	3
pinto	0.5	0.5	0	2

*Extract prepared by grinding beans or seeds in 3 volumes of 1% saline and allowing to stand overnight. Extract separated by centrifuging mixture at 5000rpm for 15 minutes.

xylose, and glucose have been found previously to be specific inhibitors for various lectins. Mannose and galactosamine have also been shown to be components of bovine brain gangliosides and erythrocytes membranes. A secondary reason is the report that the lectin isolated from horseshoe crab (*Limulus polyphemus*) is inhibited by sialic acid (5), a further constitutent of gangliosides. The results of these inhibition tests on our phytohemagglutinins and their control reaction are reported in Tables 3 and 4.

Inhibition of the agglutination reaction of the lectin from pinto beans of 50% or more was obtained with both arabinose and fructose. A similar type of inhibition with kidney bean lectin was obtained with the calf brain ganglioside mixture and inistol. A 50% inhibition by the navy beans lectin was obtained with none of the materials tested. The lectin from marrow beans again showed no inhibition with the inhibitiors used. The lectin from lucust was inhibited by insitol. N-Acetylneurinimic showed about a 20-30% inhibition for the lectins from kidney, marrow, and navy beans. A similar range of inhibition was noted on the navy lectin by insitol and calf brain ganglioside.

The finding with the gangliosides and insitol are the first examples of an inhibiting effect of these materials. Insitol and gangliosides are materials found wide spread throughout the body, and on erythrocyte cell walls (2, 7, 12, 14, 18). Other material structurally similar to gangliosides (12) have been isolated from human blood group O and suggested to be a major H-active component. The major difference between this material and gangliosides isolated from the brain is the absence of a neuraminic acid, and the order of the first two sugars (12). The presence of these group specific materials and gangliosides on the cell walls might give rise to the active site where agglutination by the lectin takes

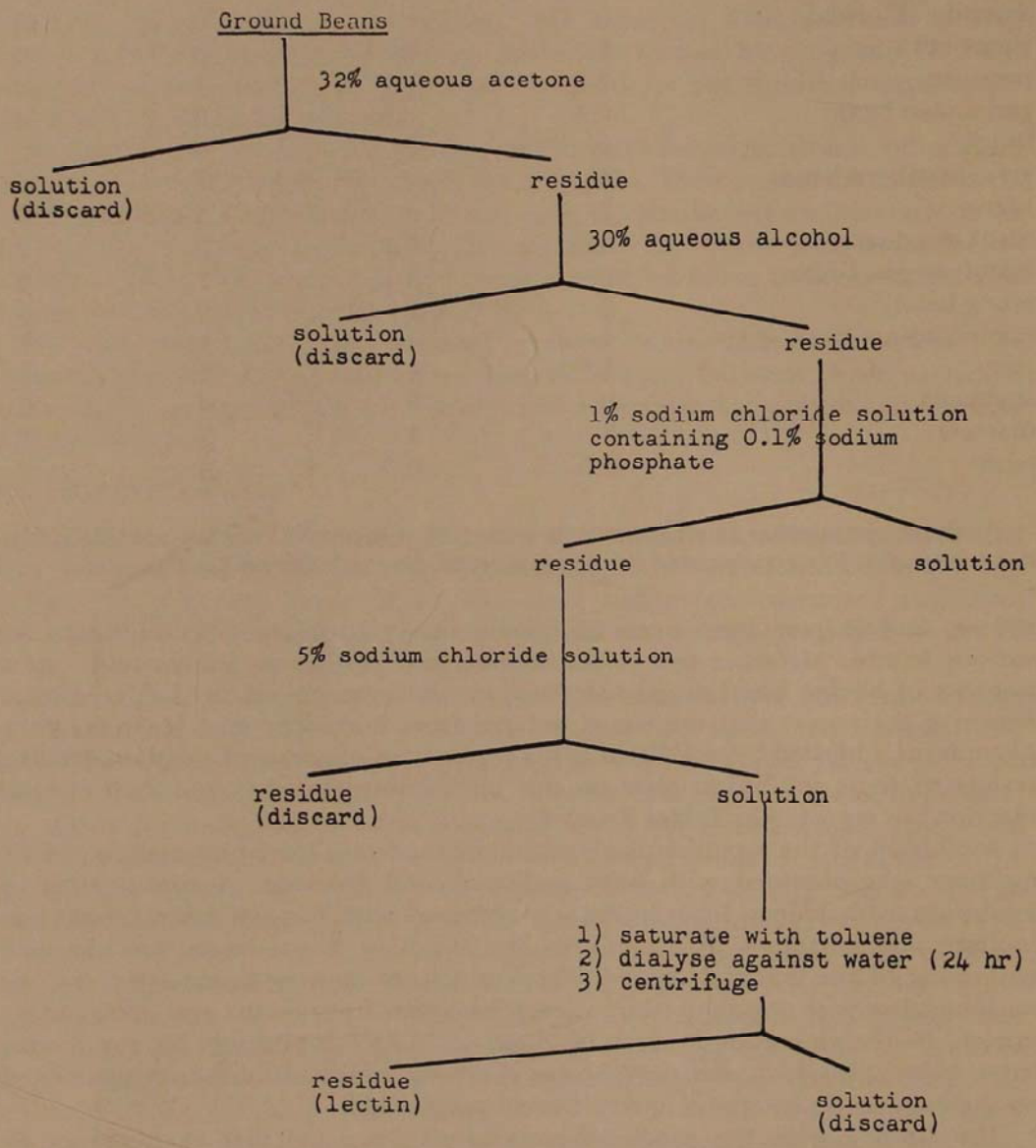

FIGURE 1. Isolation scheme used by Sumner and Howells (reference 13) to obtain crystalline Concanavalin A.

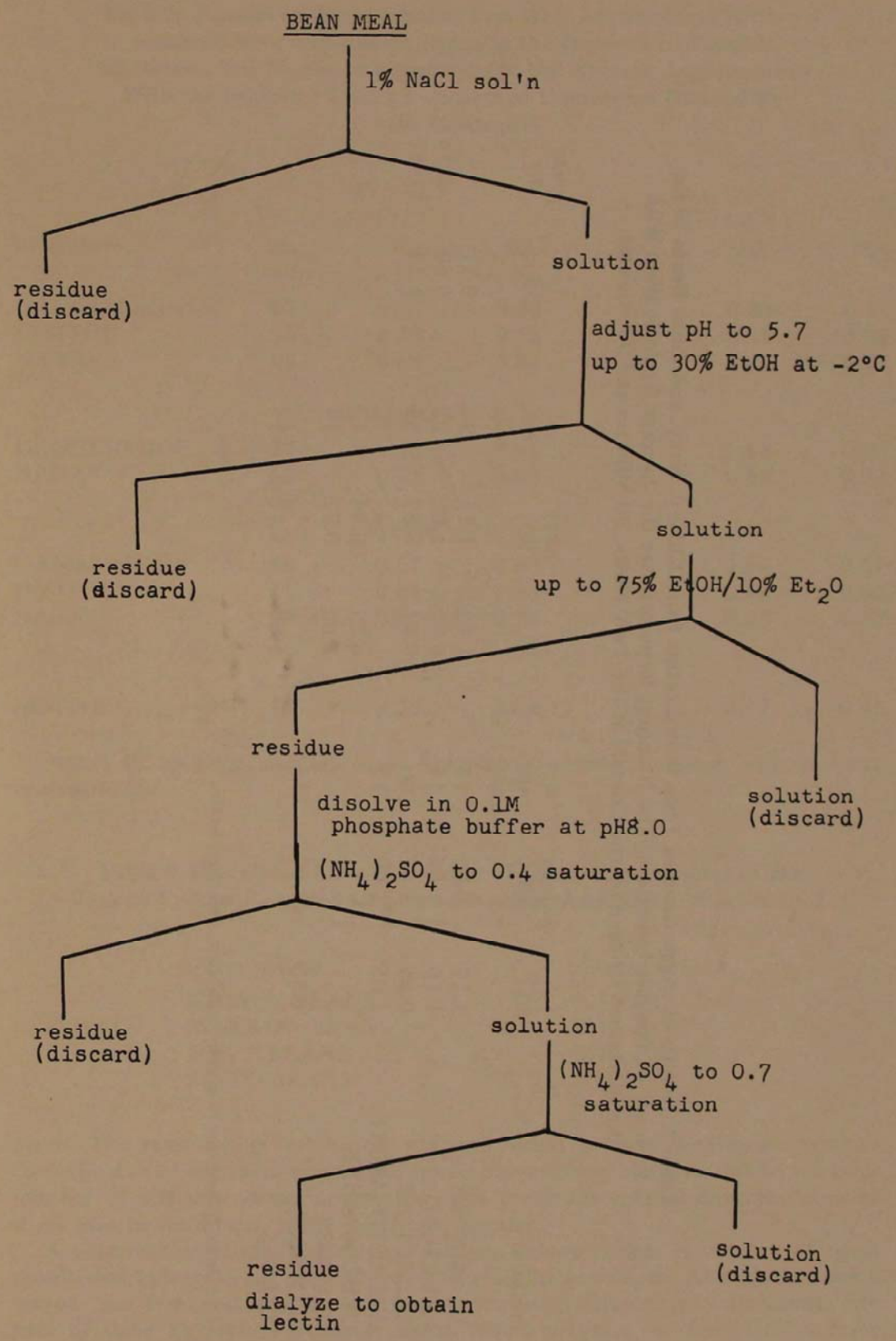

FIGURE 2. Isolation scheme of Rigas and Osgood.

Table 2. Results of Agglutination Tests With Lectins from Kidney, Navy, and Pinto Beans in the Presence of Possible Inhibitors. The Numbers Reported Are the Average Agglutination With the Inhibitor* Divided by the Control at the Two Times, 30 Minutes and 90 Minutes.

	kidney			*navy*			*pinto*		
inhibitor	*30*	*90*	*no. cells*	*30*	*90*	*no. cells*	*30*	*90*	*no. cells*
ARABINOSE	1.11	0.91	14	1.13	1.11	26	0.51		17
FRUCTOSE	1.16	1.00	14	0.92	1.00	21	0.60	1.14	17
GALACTOSE	0.85	1.07	20	0.81	0.87	35	1.14	0.38	17
GALACTOSAMINE	1.05	1.00	15						
GLUCOSAMINE				0.73	0.94	17			
GLUCOSE				1.00	0.77	14			
MANNOSE	1.36	1.02	14						
XYLOSE				1.00	1.12	13			

*Order of addition was cells, inhibitor, and then lectin.

Table 3. Results of Agglutination Test With Lectins from Kidney, Marrow, Navy and Lucust Beans in the Presence of Possible Inhibitors. The Numbers Reported Are the Average Agglutination With the Inhibitor Under Two Sets of Conditions Divided By the Control.

		KIDNEY				
		CIL[a]			*LIC*[b]	
inhibitor	*no. cells*	*30*	*90*	*no. cells*	*30*	*90*
GANGLIOSIDE	67	0.67	0.43	22	0.83	0.80
INSITOL	30	0.75	0.58	30	0.58	0.58
NANA[c]	68	0.89	0.81	51	1.14	0.87
		MARROW				
GANGLIOSIDE	32	1.38	1.01	32	1.18	0.95
NANA[c]	50	0.73	0.89	42	0.99	0.77
		NAVY				
GANGLIOSIDE	88	0.67	0.69	40	0.66	0.51
INSITOL	15	0.65	0.86	15	0.40	0.87
NANA[c]	29	0.67	0.78	22	0.62	0.77
		LUCUST				
INSITOL	16	0.36	0.68	16	0.77	0.45

[a]CIL=cells, inhibitor, and then lectin. [b]LIC=lectin, inhibitor, and then cells. [c]N-acetyl-neuraminic acid.

Table 4. Calculated Lowest Number of Grams Per Milliliter of the Various Lectins Required to Give an Average Agglutination Score of 2.

lectin source	*concentration**
KIDNEY BEANS	1.10×10^{-4}
MARROW BEANS	1.15×10^{-4}
NAVY BEANS	3.15×10^{-4}
PINTO BEANS	5.0×10^{-4}

place. The reason large inhibition was not found for our ganglioside mixture could be due to the small concentration employed, lmg/10ml, or due to the large number of different components present in the brain isolated mixture. Some of these may be inhibitors, while others are inactive.

A germination study was carried out on kidney beans. A number of equal samples of kidney beans were allowed to start to germinate. At various times a sample was removed and the crude phytohemagglutinin extract obtained. The titer of these extracts were determined. Many enzymes are found to increase upon germination. The results with kidney beans are exactly opposite. Similar

results have been found by Boyd during the germination of Lima beans (6). Many phytohemagglutinins have been found to have mitogenic properties. The decrease of the lectin upon germination might be explained along these lines.

The lectin from kidney and navy beans were also tested by the Ouchterlony technique (9) to determine if these materials contained precipitin activity. In both cases a number of precipitins were formed with human blood sera, though the titer of these reactions has not yet been determined. Other previous workers (8), have noted that concanavalin-A does in fact react with blood sera of various animals. Serum albumins of mammals and birds do not react with con-A and this has been ascribed to the absence of carbohydrate moiety on the protein. Con-A has been found to react, however, with glycoproteins, mainly the α, α_2, and β globulins (8).

Further work is in progress to characterize these five lectins as to their amino acid composition, molecular weight, iso-electric points, and iso-ionic points. These results of these studies will be presented at a later time.

Experimental

The phytohemagglutinins were isolated by either of two different methods (a) Sumner and Howells (13) or (b) Rigas and Osgood (10). The isolation schemes are represented in Figures 1 and 2 respectively. Once isolated the lectins were stored as dry powders at $^{-10}$°C.

Serological Tests

Human whole blood samples obtained from the Chemistry Laboratory at Cabell-Huntington Hospital were centrifuged down, the serum decanted and the erythrocytes washed with 1% saline solution two times, and then diluted to a 2% cell suspension. The accurately weighted purified lectin (approximately 50 mg) was dissolved in 1% saline to a total volume of 10 ml. A dilution of the sugar (100 mg per 10 ml of water) was prepared. All solutions were stored at near 0°C until the actual tests were to be run. To each tube of one set of 3-inch test tubes was added 2 drops of the individual 2% blood cell suspensions, 2 drops of distilled water (to prevent a difference in dilution) and two drops of the lectin solution. To another set of tubes was added 2 drops of each individual blood suspension, the sugar and the lectin. To a third set was added the lectin, inhibitor and then the cells in that order. The test tubes were shaken and then allowed to stand at room temperature. After 30 minutes, the tubes were lightly tapped to resuspend the clusters. Agglutination in each tube was rated on an arbitrary scale of 0 to 4, 0 being for no agglutination, 4 being a large cluster of clusters with no small units and a clear background. After scaling the agglutination, the tubes were allowed to stand an additional hour.

The inhibition test using the gangliosides were done similarily except that instead of the sugar dilution, the ganglioside dissolved in a minimual amount of 1% saline, and instead of adding distilled water to the control, 1% saline was used. N-Acetylneuraminic acid was dissolved in water and 1M sodium hydroxide was added to a pH of 7.

Germination Studies

A number of equal samples of kidney beans were allowed to germinate in sand. At various times a sample was removed and the crude lectin extract isolated. The extract was tested for lectin titer and the results showed a constant decrease in the amount of the phytohemagglutinin present.

Ouchterlony Tests

Double diffusion reactions were run after the method of Utter (16).

Acknowledgments

The authors wish to thank Marshall University and the Society of Sigma Xi through a Grant-in-Aid of Research for their support of this work. We also wish to thank International Nickel Corporation, Allied Chemical Corporation and other Huntington industries which supported DGC for the summer, 1972. Special thanks go to the Medical Technology Laboratories at Cabell-Huntington Hospital for furnishing blood samples.

Literature Cited

1. Boyd, W. C. 1963. Lectins, their present status. *Vox Sang.* 8:1-54.
2. Brady, R. O., C. Borek, and R. M. Bradly. 1969. Composition and synthesis of gangliosided in rat hepatocyte and hepatoma cell lines. *J. Biol. Chem.* 244:6552-54.
3. Galbraith, W., and L. J. Goldstein. 1972. Phytohemagglutinins of the lima bean (*Phaseolus lunatus*). Isolation, Characterization, and Interaction with type A blood group substance. *Biochem.* 11:3676-84.
4. Landsteinger, K. 1945. The specificity of serological reactions. K. Landsteiner Ed., Harvard University Press. p. 4-5.
5. Marchalonis, I. J., and G. M. Edelman. 1968. Isolation and Characterization of the hemagglutinin from *Limulus polyphemus. J. Mol. Chem.* 32:453-65.
6. Martin, F. W., E. Waszczenko-Zacharcyenko, W. C. Boyd, and K. F. Schertz. 1964. Lectin content of the lima bean during development of the seed and seedling. *Ann. Botany.* 28:319-24.
7. Max, S. R. 1970. The effect of denervation of the ganglioside composition of skeletal muscle. *Federation Proc.* 29:3740.
8. Nakamura, S., S. Tominaga, A. Katsunao, and S. Murakawa. 1965. Specific reaction of concanavalin-A with sera of various animals. *Comp. Biochem. Physiol.* 15:435-44.
9. Ouchterlony, O. 1958. Diffusion-in-gel methods for immunological analysis. In Progress in Allergy, P. Kallos Ed., vol. 5, p. 1-78. S. Karger, NY.
10. Rigas, D. A., and E. E. Osgood. 1955. Purigication and properties of the phytohemagglutinin *Phaseolus vulgaris. J. Biol. Chem.* 212:607-15.
11. Sharon, N., and H. Lis. 1972. Lectins: Cell agglutinating and sugar specific proteins. *Science.* 177:949-59.
12. Stellner, K., K. Watanbe, and S. Hakomori. 1973. Isolation and characterization of glycosphingolipids with blood group H specificity from membranes of human erythrocytes. *Biochem.* 12:656-61.
13. Sumner, J. B., and S. F. Howells. 1936. The identification of the hemagglutinin of the jack bean with concanavalin-A. *J. Bacteriol.* 32:227-37.
14. Tao, R. V. P., and C. C. Sweeley. 1970. Occurrence of hematosides in human plasma. *Biochem. Biophys, Acta.* 218:372-75.
15. Toms, G. C., and A. Western. 1971. Phytohemagglutinins. In Chemotaxonomy of the Leguninosea, J. Harborne, D. Boulter, and B. L. Turner Ed., Academic Press, New York.
16. Utter, F. M., G. J. Ridgway, and H. O. Hodgins. 1964. Use of plant extracts in serological studies of fish. U. S. Fish and Wildlife Service, Special Scientific Report-Fisheries N. 473, Washington, D.C., February.
17. Vann, D. C., and J. E. Cushing. 1966. Reaction of the lectin from Dolichos biflorus with erythrocytes from California bonito. *Federation Proc.* 25:1394.
18. Yamakawa, T., and S. Suzuki. 1951. Lipid of posthemolytic residue of stroma of sethrocytes (I) ether insoluble lipids of lyophilized horse blood stroma. *J. Biochem.* 38:199-212.

Rennin—The Milk-Clotting Enzyme
An Introductory Biochemistry Experiment

Howard C. Price
Department of Chemistry, Marshall University
Huntington, West Virginia 25701

Abstract

An introductory biochemistry experiment has been designed which permits the student to obtain quantitative kinetic data on an enzyme without the use of a spectrophotometer. Thus large classes, where the extensive use of instruments becomes costly and/or creates waiting lines, may be introduced to enzyme kinetics. Students follow the clotting action of rennin on milk and note the dependence of clotting reaction time on enzyme concentration, temperature, and pH. Quantitative information such as specific activity and an estimate of pH of maximum activity are obtained.

Introduction

If topics in biochemical research were ranked according to volume of published results, enzyme characterization studies would certainly score near the top. It is reasonable, therefore, that many instructors in biochemistry may wish to incorporate into their laboratories an experiment which demonstrates some of the important characteristics of enzyme catalyzed reactions. Published experiments on the nature of enzymes and the reactions they catalyze typically fall into two divergent categories: 1) simple, ("recipe"), experiments demanding little in terms of either technique or thought on the part of the student; 2) relatively sophisticated experiments employing spectrophotometers, well adapted for laboratories where the student/instrument ratio is low, but otherwise presenting serious bottlenecks or requiring students to work in groups. As an alternative to these extremes, we wish to describe an enzyme experiment we have incorporated into our introductory biochemistry laboratory. Requiring no instrumentation and utilizing only inexpensive, readily obtained materials it can be adopted by the most modestly endowed laboratory. While making moderate demands on the technique of the student, this experiment provides insight into the dependence of the rate of enzyme catalyzed reactions on the enzyme concentration, temperature, and pH, including the demonstration of half of the bell-shaped rate—pH profile typical of many proteolytic enzymes.

Rennin is an endopeptidase found in the digestive tract of certain newborn mammals. Several reviews on rennin biochemistry have been published. (5,6). It functions as a coagulative agent for milk by converting soluble casein into paracasein, which precipitates as the calcium salt. The mechanism of this conversion involves the cleavage of a specific methionylphenylalanine linkage in κ-casein. Rennin is obtained commercially from the fourth or "true" stomachs of calves and, as the crude extract "rennet", is used in the production of cheese.

In several respects rennin is similar to the more extensively studied digestive enzyme, pepsin. The two enzymes are comparable in the specificity of their catalytic activity (e.g., pepsin also clots milk and preferentially attacks peptide

linkages involving aromatic amino acids) and in their molecular weights (approximately 40,000 and 34,000 for rennin and pepsin, respectively). Both enzymes have maximum stability and catalytic activity in the acid pH range.

Rennin's catalysis of the milk clotting reaction is the basis for a convenient assay of the relative activity of rennin preparations. In general, the activity of an enzyme sample is reported in terms of units of activity or units of activity per quantity of enzyme sample. An activity unit is defined as the quantity required to produce a certain effect (e.g., liberate a specified amount of product) in a given length of time under specific assay conditions (temperature, pH, etc.). For rennin preparations a specific activity has been defined: (1,3,4) $\frac{1}{(CT/ml)\ (A_{280})}$, where CT/ml is the time in seconds required for one ml of enzyme solution to clot ten ml of a standard milk preparation and A_{280} is the net absorbance of the enzyme solution at 280 nm (assumed to be proportional to the enzyme concentration).

Experimental

Materials

Rennin is available from many biochemical suppliers. An inexpensive grade (such as ICN Nutritional Biochemicals Technical Grade) is sufficient for this experiment. The stock rennin solution is made with distilled water just prior to use. Its concentration is adjusted so that one ml clots ten ml of pH 5 buffered milk in approximately 40 seconds at ambient temperature.

Any locally available nonfat dry milk may be used. However, since clotting characteristics and pH vary slightly, the experiment should be conducted with a single lot of powdered milk.

Buffer solutions are prepared which, when mixed with an equal volume of stock milk (see procedure), yield pH values covering the range 5.0 to 6.2 in increments of 0.1-0.2 pH units. We used 0.1M potassium acid phthalate buffers, Clark and Lubs solutions (2), of the following pH values (pH when mixed with equal volume of our stock milk is listed in parentheses): 3.40 (5.05), 4.20 (5.30), 4.50 (5.40), 4.80 (5.55), 5.10 (5.70), 5.50 (5.95), 5.80 (6.15).

Push-button timers or stopwatches are desirable but watches with sweep second hands are acceptable substitutes.

Other reagents and equipment are commonly available in most laboratories.

Procedure

a. Preliminary

Make a stirrer by bending a loop at one end of a ten-inch section of glass rod. The loop should be small enough to slide freely inside the test tubes to be used for the clotting determinations. The clotting point is best detected by watching the stream of milk draining onto the inside of the test tube as the loop is repeatedly submerged and withdrawn from the milk solution. An increase in viscosity occurs just prior to the clotting point.

b. Dependence of the Clotting Reaction on Enzyme Concentration.

Prepare stock milk by mixing 6.0 g of powdered milk with 50 ml of 0.02 M calcium chloride.[1] With distilled water, make two-, three-, four-, six-, and eight-

[1]Students should be cautioned to mix all liquids in the experiment as gently as possible to reduce foaming which tends to denature proteins.

fold dilutions of one ml aliquots of the stock rennin solution. Measure the time required for one ml aliquots of the diluted solutions and the stock rennin solution to clot ten ml of pH 5 buffered milk (made by pipetting five ml of the stock milk and five ml of the appropriate buffer into a test tube).[2] Plot 1/(CT/ml) against enzyme concentration. Is clotting time inversely proportional to enzyme concentration over the entire range?[3] If not, can you suggest possible reason(s) for deviation from linearity? Obtain the net absorbance (A_{280}) of the stock rennin solution from the instructor[4] and calculate the specific activity of the rennin solution using the three- or four-fold dilution clotting time.

c. Ph Dependence of the Clotting Reaction

Prepare stock milk as before. Obtain the clotting times for one ml aliquots of the stock rennin solution on ten ml of buffered milk made by mixing five ml of the stock milk with five ml of each of the buffers. (The pH of the resultant buffered milk will be supplied by the instructor.) Plot 1/(CT/ml) against the milk pH and note the shape of the curve obtained. Could this curve be part of a bell-shaped rate-pH profile? If so, in what pH region would the enzyme exhibit maximum activity? Note the effect of one ml of 0.1 M hydrochloric acid and 0.4 M sodium hydroxide on separate ten ml samples of milk made by diluting five ml of stock milk with five ml of distilled water. Why would milk be an unsatisfactory "substrate" for a kinetic study on rennin under highly acidic or basic conditions?

d. Temperature Dependence of the Clotting Reaction

Using one ml aliquots of a four- or six-fold dilution of the stock rennin solution, measure the clotting times on ten ml samples of pH 5 buffered milk maintained at ambient temperature, at five and ten degrees above, and at five degrees below ambient. Plot 1/(CT/ml) against temperature. Does this system obey the common rule of thumb that a ten degree rise in temperature is accompanied by a two- or three-fold increase in reaction rate?

Literature Cited

1. Berridge, N. J. 1952. Some observations on the determination of the activity of rennet. *Analyst* (London) 77:57-62.
2. Bower, V. E., and R. G. Bates. 1955. The pH values of the Clark and Lubs buffer solutions at 25°. *J. Res. Nat. Bur. Stand.* 55:197-200.
3. Bundy, H. F., N. J. Westberg, B. M. Dummel, and C. A. Becker. 1964. Purification and partial characterization of prorennin. *Biochemistry*. 3:923-26.
4. Ege, R., and P. Menck-Thygesen. 1933. Uber die Aktivierung des Propepsins. *Biochem. z.* 264:13-23.
5. Foltmann, B. 1966. A review on prorennin and rennin. *Compt. Rend. Trav. Lab. Carlsberg.* 35:143-231.
6. ———. 1971. Biochemistry of prorennin (Prochymosin) and Rennin (Chymosin). *Milk Proteins* 2:217-54.

[2]It is best for the inexperienced student to begin clotting determinations with the more dilute solutions first.

[3]The questions included in the experiment assume only introductory level lecture background in enzyme-catalyzed reactions. A list of suggested answers may be obtained by sending a stamped, self-addressed envelope to the author.

[4]To calculate specific activity, students are given A_{280} of the stock rennin solution. When the instructor does not have access to a UV spectrophotometer, a "modified" specific activity expression may be used in which A_{280} is replaced by the enzyme concentration in g/ml.

Chlorination by Trichloromelamine A N-Chloroamine

Ronald L. Neal and Melvyn W. Mosher
Department of Chemistry, Marshall University
Huntington, West Virginia 25701

Abstract

The free radical reactions of trichloromelamine (TCM) with alkanes and substituted alkanes were studied under initiation with thermal free radical initiators, and under photolytic conditions. In these reactions when the solvent was the alkane or substituted alkane, the hydrogen abstracting species was chlorine atoms, as indicated by the tertiart to primary selectivity, the polar effects of the abstracting radical, and the relative rates of reactions of different substrates. In the reactions of TCM when trifluoroacetic acid was the solvent, the hydrogen abstracting species appears to be the protonated amino radical as indicated by the change in the polar effects of the abstracting radical, and the relative rates of reaction.

Introduction

In recent years, considerable attention has been given to the free radical reactions of organic positive halogen compounds. Of these, N-haloamines have been shown to form reactive free radical intermediates capable of hydrogen atom abstraction from alkanes (8,23). The abstraction reaction of these compounds fall into two classes; a) intramolecular and b) intermolecular. In both cases, these reactions are catalyzed by strong acid and are found to be free radical chain processes (4,8,23).

The intramolecular abstraction reaction of N-haloamines is usually referred to under the general heading of the Hofmann-Loeffler-Freytag-Reaction (4,8,22), see scheme I.

Scheme I:

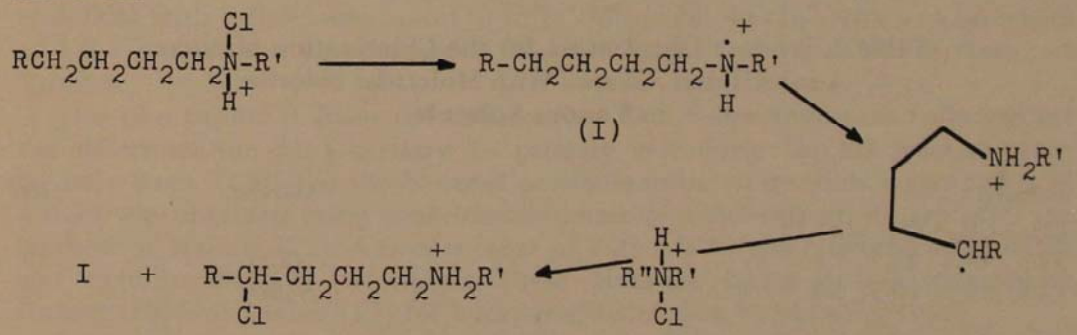

The intramolecular process of these compounds is similar to the well known reaction of long chain alkyl hypohalites that proceed under neutral conditions (20,21) where hydrogen atom abstraction takes place predominantly at the δ-carbon. The intermolecular hydrogen atom abstraction reaction of N-haloamines in strongly acid media has been shown to exhibit unusual free radical properties (2,6,10,11). The products of the reaction of N-chloroamines

with 1-substituted alkanes shows a high selectivity for attack at the ω-1-carbon. The yields of the chlorinated product approaches 90% for this one isomer, see table 1.

Table 1. Product Distribution for the Chlorination of Some 1-substituted Alkanes With Various N-chloroamines

Substrate	*N-chloroamine[a]/ solvent*	*Ref*
$CH_3-CH_2-CH_2-CH_2Cl$	CDM	
5.5 88.5 6 0	H_2SO_4/HOAc(85/15)	10,11
14 64 18 4	CDM 4M H_2SO_4/HOAc	14
$CH_3-CH_2-CH_2CH_2-CO_2CH_3$	CDM	
7.3 77 15.7 0 0	H_2SO_4/HOAc(85/15)	10
$CH_3-CH_2-CH_2-CH_2-CH_2-CH_2-CH_2-CO_2H$	CDP	
1 80 14 4 0 0 0	90% H_2SO_4	6
$CH_3-CH_2-CH_2-CH_2-CH_2-CH_2OH$	CDP	
6 90 2 2 0 0	72% H_2SO_4	6

*In percent.
[a]N-chlorodimethylamine=CDM; N-chlorodiisopropylamine=CDP.

The possibility that chlorine atoms are the radical chain carrying species for these reactions, and that the unusual product distributions arose through a solvent effect of the strong acid media has been ruled out, see table 2. As a result, to explain this high selectivity for attack at either the ω-1-carbon or the δ-carbon, the chain carrying radical for these abstraction reactions has been suggested to be the protonated amino radical, II.

Table 2. Product Distribution for the Chlorination of Some 1-substituted Alkanes With Molecular chlorine in Various Solvents

Substrate	*Solvent*	*Ref*
$CH_3-CH_2-CH_2-CH_2Cl$		
19.7 49.2 23.7 7.8	CCl_4	19
21.6 52 20.9 5.4	H_2SO_4	18
$CH_3-CH_2-CH_2-CH_2-CO_2CH_3$		
13.8 47.3 33.1 5.8 0	CCl_4	15
$CH_3-CH_2-CH_2-CH_2-CH_2-CH_2-CH_2-CO_2H$		
17 24 19 16 15 9 1.5	CCl_4	5
41 3 2 10 31 8 5	90% H_2SO_4	5

Table 2. *Continued*

$CH_3-CH_2-CH_2-CO_2H$				
42	53	5	CCl_4	5
79	21	0	90% H_2SO_4	5

*In percent.

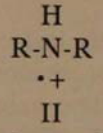

Although considerable work has been done on N-haloamines as a hydrogen abstracting species and considerable study of their synthetic usefulness in acidic media has been presented, little work has been done with this class of compounds in neutral media. In addition, no work has been presented to compare the hydrogen atom abstraction reactions of these compounds in protic and non-protic solvents. We would like to report the result of our finding here with the N-chloroamine, trichloromelamine (TCM).

Results and Discussion

The reaction of cyclohexane and TCM in the absence of acid to form chlorocyclohexane could be initiated by either light or benzoyl peroxide, a thermal free radical initiator. The chain length for the reaction was found to be 2.5 ± 1.0. In a number of free radical reactions with low chain lengths that use benzoyl peroxide as an initiator, the peroxide has been found to be required for the reaction and other thermal initiators will not cause the reaction to take place. Two other examples of reactions where benzoyl peroxide is one of the reactants are the free radical reaction of thionyl chloride with alkanes, where the peroxide first reacts with thionyl chloride to form benzoyl hypochlorite and benzoyl chlorosulfite, which then go on to the observed products (9); and the chlorination of alkanes by hydrogen chloride, where the first step in the reaction is the formation of benzoic acid and benzoyl hypochlorite (3).

To determine the role of benzoyl peroxide in this reaction, azo-(bis-isobutyronitrile) (AIBN) was used as an initiator. Reactions of cyclohexane and TCM with AIBN were found to form chlorocyclohexane with a chain length of 1.8 ± 0.2, a value comparable to that for the benzoyl peroxide reactions, see Table 3.

The two products from the chlorination of 2,3-dimethylbutane allowed for the determination of a tertiary to primary selectivity for the reactive intermediate from TCM. For the benzoyl peroxide initiated reaction, a value of 6.72 ± 0.65 was obtained using hexachloropropene as a chlorine atom trap after the method of Walling (22). A similar value of 7.25 ± 0.35 was observed using AIBN and trichloroethene as a scavenger. These values are similar to those reported by Russell (13) and Tanner (17) for hydrogen abstraction by chlorine atoms.

In the photochemical reaction of TCM with cyclohexane, chlorocyclohexane was formed, but with a very small quantum yield, in the visible region. The selectivity for the photochemical reaction was 6.02 ± 1.00 at 1.9% conversion. Irradiation by two 200-watt incandescent lamps required 20 days to produce this amount of product. At higher percent conversion, a comparable selectivity was found. The selectivity was also found not to change when the chlorine atom scavenger was omitted, see table 4. The lack of change in the selectivity with percent conversion indicates that there is no hydrogen atom abstraction by alkyl

radicals from hydrogen chloride. The low rate of reaction is possibly due to the very low solubility of TCM in the hydrocarbon solvent. Such a result has been found, coupled with reversible hydrogen abstraction, for the high selectivity of iodobenzenedichloride (IBD). When IBD is in solution, a selectivity of 1/15 is observed (16). Attempts to dissolve TCM in inert non-protic solvents were unsuccessful.

To further show that chlorine was indeed responsible for the hydrogen atom abstraction, the polar effects on 1-bromobutane and 1-chlorobutane were determined (see table 5). In all cases, the values determined were similar to that reported for elemental chlorine (17). The formation of 1-chlorobutane in the TCM chlorination of 1-bromobutane is of some interest and also suggests that elemental chlorine is being formed during these reactions. It has been shown earlier (1) that molecular chlorine will displace alkyl bound bromine to produce the chloroalkane in the absence of light and via an ionic reaction. Other positive chlorine compounds such as t-butyl hypochlorite or N-chlorosuccinimide do not produce this halogen exchange reaction.

Further evidence for the abstraction of hydrogen atom by chlorine atoms was obtained from the relative reactivity, of several compounds with TCM. These values are reported in Table 6. The thermal reactions are found to be considerably higher than those of the photochlorination reactions. This could be explained by the very low chain length and in these reactions, the importance of abstraction by the radical from the initiator.

Selected reactions were run in trifluoroacetic acid solutions, the selectivity of the abstracting radical was determined from the relative rates of reactions (Table 6). The selectivity was calculated to be 1/6/28 for primary/secondary/tertiary for the hydrogen abstracting radical. The polar effects on 1-bromobutane and 1-chlorobutane showed high selectivity for attack at the ω-1-carbon. The preference for the ω-1-carbon hydrogens was not as pronounced as was reported by Minisici (10,11) although similar to that reported by Ingold (14), Table 2. The acid catalysed reaction of TCM with 1-bromobutane did not produce any of the halogen exchange material, indicating the absence of chlorine in this reaction.

Conclusions

Evidence presented suggests that chlorine is the abstracting radical in the reactions of TCM in non-protic solvents. The chlorine atoms are either formed by heterolytic cleavage of the N-Cl bond, or by the well known reaction of hydrogen chloride with positive halogen compounds to produce molecular chlorine. In the case of the acid catalyzed reactions of TCM, the abstracting radical appears to be similar to that previously reported, that of structure II.

Experimental

All materials were commercially available and used without further purifica-

Table 3. Chain Length for the Chlorination of Cyclohexane and 2,3-dimethylbutane with TCM Initiated by Either Benzoyl Peroxide or AIBN.

Substrate	*Initiator*	*mole x 10^{-4}*	*moles products x 10^{-4}*	*Chainlength*
Cyclohexane	Bz_2O_2	1.21	chlorocyclohexane 1.72	1.42
Cyclohexane	Bz_2O_2	1.53	chlorocyclohexane 4.13	3.25
Cyclohexane	Bz_2O_2	1.70	chlorocyclohexane 3.42	2.00
Cyclohexane	AIBN	1.10	chlorocyclohexane 1.72	1.56
Cyclohexane	AIBN	1.33	chlorocyclohexane 2.61	1.96
2,3-dimethylbutane	Bz_2O_2	1.43	A 0.97 B 0.89	1.30
2,3-dimethylbutane	Bz_2O_2	1.21	A 1.19 B 1.06	1.86
2,3-dimethylbutane	AIBN	1.58	A 0.80 B 0.79	1.00
2,3-dimethylbutane	AIBN	1.86	A 0.97 B 0.89	1.56
2,3-dimethylbutane	AIBN	1.83	A 1.59 B 1.32	1.97

A=2-chloro-2,3-dimethylbutane B=1-chloro-2,3-dimethylbutane

Table 4. The Tertiary to Primary Selectivity for the Reactive Intermediate From TCM Upon 2,3-dimethylbutane

Initiator	*Selectivity*	*% Conversion*	*Remarks*
Bz_2O_2	7.44±0.13	73.	
Bz_2O_2	6.72±0.65	46.	hexachloropropene added
AIBN	7.25±0.35	—	trichloroethene added
AIBN	6.08±0.44	—	trichloroethene added
AIBN	8.28±0.65	70	
AIBN	6.83±0.98	81	
hν	9.28±0.37	0.7	
hν	6.30±0.17	8.9	
hν	9.9 ±3.5	0.1	trichloroethene added
hν	13.7 ±2.7	0.06	trichloroethene added
hν	11±1.7	0.8	
hν	12.7 ±0.9	5.1	
hν	6.02±1.00	1.9	

Table 5. Isomer Distribution in Percent for the Chlorination of 1-Bromobutane and 1-chlorobutane With TCM.

C———	*C*———	*C*———	*CCl*	*Solvent*	*Remarks*
16.2	47.5	24.2	11.9	neat	Bz_2O_2 initiated
16.3	46.2	22.2	13.9	neat	AIBN initiated
16.5	48.5	24.2	12.2	neat	AIBN initiated
15	60	18	7.7	TFA	$h\nu$ with $FeSO_4 \cdot 7H_2O$
C———	C———	C———	CBr		
23.5	50.2	16.8	7.3	neat	AIBN initiated 1-chlorobutane (16%)
23.0	49.0	16.2	8.1	neat	Bz_2O_2 initiated 1-chlorobutane (23%)
23.0	50.0	21.3	5.0	neat	$h\nu$; chlorobutane (47%)
25.9	73.1	11.0	tr	TFA	$h\nu$ with $FeSO_4 7H_2O$

Table 6. Relative Reactivities of Selected Hydrocarbons With TCM and Molecular Chlorine

Substrate	*TCM*				
	Bz_2O_2	AIBN	$h\nu$	$h\nu$[b]	Cl_2[c]
Cyclohexane[a]	1.00	1.00	1.00	1.00	1.00
Cyclopentane	1.12±0.06	1.55±0.06	0.63±0.07	—	0.82±0.09
2,3-dimethyl-butane	1.52±0.02	1.74±0.11	0.73±0.1	0.95±0.09	0.75±0.11
2,2,3,3-tetra-methylbutane	0.88±0.39	—	0.65±0.03	0.25±0.1	0.44±0.10

a) assigned a relative value of 1.00.
b) in TFA with added $FeSO_4 \cdot 7H_2O$.
c) all taken from reference 21 except last entry which is from reference 20.

tion. TCM was 95 ± 1% pure by iodometric titration. Recrystallization from boiling water did not change this value. Glpc analysis was performed via a Hewlett-Packard F and M Model 700 gc equipped with either a 6′ x 1/4″ 10% SE-30 on chromosorb W glpc column or a 10′ x 1/4″ 10% didecyl phthlate on chromosorb W glpc column. All reported numbers are the average of at least three independent determinations except for the photochemical reaction in hydrocarbon solvent reported in table 4.

Chlorination of Cyclohexane

Solutions were prepared containing cyclohexane as a solvent, 0.03-0.04 g of the thermal initiator, and 0.1 g of TCM. These solutions were placed in reaction tubes, degassed twice by the freeze-thaw-pump method, sealed, and placed in a water bath at approximately 95°C. After the reaction was completed, the reaction tubes were opened and to their contents an internal standard (chlorobenzene) was added. From the glpc traces on column A, the results reported in table 3 were obtained.

Chlorination of 2,3-dimethylbutane

Solutions were prepared containing 2,3-dimethylbutane as the solvent, 0.1 g TCM and 0.03-0.04 g of the initiator. These solutions were placed in reaction tubes, degassed twice by the freeze-thaw-pump method, sealed and placed in a water bath at approximately 95°C. After the reaction was completed, the tubes were then opened and to their contents an internal standard (chlorobenzene) was added. The two products, 2-chloro-2,3-dimethylbutane and 1-chlorobutane were detected. The yield of these materials is reported in table 3.

In a similar set of reactions, hexachloropropene, or trichloroethene was used as a chlorine atom scavenger. The amount of the scavenger was approximately 12M. The results of some representative determinations are illustrated in Table 3.

In a third set of reaction tubes (22), no initiator was used. The tubes were photolysed in a water constant temperature bath at 27 ± 3°C by two, 220-watt incandescent lamps placed 6 cm from the bath. At various times, tubes were removed, and the external standard added. Typical results are summarized in Table 3. A parallel set of tubes was prepared containing trichloroethene. No apparent difference was detected between the two sets.

Chlorination of 1-substituted butanes by TCM

Either 1-chlorobutane or 1-bromobutane was added to a reaction tube containing 0.1 g TCM, 0.03-0.04 g initiator, the tubes degassed by the freeze-thaw-pump method, sealed, and placed in a water bath, at approximately 90°C. After the reaction was complete, the tubes opened and 1-chloro-octane or isopropyl chloride was added as an external standard. The polar effects are reported in table 4. In the case of 1-bromobutane, the two additional peaks were identified

by comparison of their retention times with authentic samples of 1-chlorobutane or 1,2-dichlorobutane on two different glpc columns.

Another set of experiments was performed using no initiator. The results are reported in table 4.

In a third set of experiments, trifluoroacetic acid was used as the solvent and 0.05 g iron (II) sulfate heptahydrate added as a catalysis. The tubes degassed, sealed and irradiated with two, 200-watt incandescent lamps for 3 hours. In the case of 1-bromobutane, no additional products other than the 4-chloroinated 1-bromobutanes were detected.

Competitive Chlorinations

The competitive chlorinations using either TCM in chloroform, or TCM in trifluoroacetic acid were carried out by the method previously reported by Tanner (18) and Mosher (12). The relative reactivities were calculated by the method of Hutchinson (7). The values obtained are reported in table 5.

Acknowledgments

The authors wish to thank Marshall University and the Society of Sigma Xi through a Grant-in-aid of Research for their support of this work.

Literature Cited

1. Adkins, L. S., D. G. Childers, D. A. Hunt, M. J. Hutchinson, and M. W. Mosher. 1972. Halogen Exchange Reactions. II. *47th Annual Meeting, W. Va. Acad. Sci.*, Bluefield, April.
2. Bernardi, R., R. Galli, and F. Minisci. 1968. Polar and seteric effects in hydrogen abstraction by dialkylamine cation radicals. *J. Chem. Soc. B*, 324-25.
3. Bunce, N. J., and D. D. Tanner. 1969. Benzoyl hypochlorite, an intermediate in the oxidation of ionic chlorides and hydrogen chloride by benzoyl peroxide. *J. Amer. Chem. Soc.* 91:6096-102.
4. Corey, E. J., and W. R. Hertzler. 1960. A study of the formation of haloamines and cyclic amines by the free radical chain decomposition of N-haloammonium ions (Hofmann-Loeffler Reaction). *J. Amer. Chem. Soc.* 82:1657-68.
5. Deno, R. Fishbein, and J. C. Wyckoff. 1970. Cation Radicals. I. Chlorination of carboxylic acids *via* oxygen cation radicals. The McLafferty Rearrangement in Solution. *J. Amer. Chem. Soc.* 92:5274-75.
6. Deno, N. C., W. E. Billups, R. Fishbein, C. Pierson, R. Whalen, and J. C. Wyckoff. 1971. Cation Radicals. I. Selectivity (90%) for -1 Monochlorination of C_6 and C_8 Alcohols, Ethers, and Carboxylic Acids using Nitrogen Cation Radicals. *J. Amer. Chem. Soc.* 93:438-40.
7. Hutchinson, M. J., and M. W. Mosher. 1971. Relative reactivities in free radical systems: An organic chemistry experiment. *J. Chem. Ed.* 48:629-31.
8. Kovacic, P., M. K. Lowery, and K. W. Field. 1970. Chemistry of N-bromoamines and N-chloroamines. *Chem. Rev.* 70:639-65.
9. Krasniewski, J. M., Jr., and M. W. Mosher. 1972. Thionyl chloride chlorinations. *47th Proc. W. Va. Acad. Sci.*, Bluefield, April.
10. Minisci, F., R. Galli, and R. Bernardi. 1967. Polar effects in radical reactions: A new selective type of radical bromination. *Chem. Communic.* 903-4.
11. ———, ———, and ———. 1968. A new selective process of radical hydrogen abstraction from saturated hydrocarbon chains. I. Ether of C_4-C_7 carboxylic acids and alicylic chloro derivatives. *Chem. Ind.*, (Milan), 49:594-600. (1967). *Chem. Abst.* 68:28914d.

12. Mosher, M. W., and N. J. Bunce. 1971. The free radical photoximation of alkenes by Nitrosyl Chloride. *Can. J. Chem.* 49:28-34.
13. Russell, G. A. 1958. Solvent effects in the reaction of free radicals and atoms. IV. Effects of aromatic solvents in sulfuryl chloride chlorination. *J. Amer. Chem. Soc.* 80:5002-3.
14. Spanswick, J., and K. U. Ingold. 1970. Halogenation with N-haloamines in strong acid. I. The nature of the chain propagating radical. *Can. J. Chem.* 48:546-60.
15. Singh, H., and J. M. Tedder. 1966. Free radical substitution in aliphatic compounds. Part XII. The chlorination on n-hexane in the gas and liquid phases. *J. Chem. Soc., B,* 605-8.
16. Tanner, D. D., N. J. Bunce, and M. W. Mosher. Unpublished results, University of Alberta.
17. Tanner, D. D., and P. van Bostelen. 1967. Free radical chlorination reactions of iodobenzene. *J. Org. Chem.* 32:1517-21.
18. Tanner, D. D., and M. W. Mosher. 1969. Metal ion initiated halogenation reactions of N-haloamines. *Can. J. Chem.* 47:715-21.
19. Walling, C., and M. F. Maychi. 1959. Some solvent and structural effects in free radical chlorinations. *J. Amer. Chem. Soc.* 81:1485-89.
20. Walling, C., and A. Padwa. 1963. Positive Halogen Compounds. VII. Intramolecular chlorinations with long chain hypohalites. *J. Amer. Chem. Soc.* 85:1597-1601.
21. Walling, C., and D. Bristol. 1972. -Chloro alcohols and tetra-hydrofurans from primary and secondary alkyl hypochlorites. *J. Org. Chem.* 37:3514-16.
22. Walling, C., and J. A. McGuinness. 1969. Positive halogen compounds. XVI. Comparison of alkoxy radicals from different sources and the role of halogen atoms in hypohalite reactions. *J. Amer. Chem. Soc.* 91:2053-58.
23. Wolff, M. W. 1962. Cyclization of N-halogenated amines (The Hoffmann-Loeffler Reaction). *Chem. Rev.* 62:55-64.

Sulfur Dioxide Levels of the Middle Kanawha Valley

Donald L. Bloss and Herbert P. Kagen
Chemistry Department, West Virginia State College
Institute, West Virginia 25112

Abstract

A National Science Foundation sponsored SOS grant allowed a study of the sulfur dioxide air pollution levels of the middle Kanawha Valley to be made.

The studies indicated general compliance with the primary ambient SO_2 standards set by the EPA in 1971. The average SO_2 levels found were 0.009 ppm compared to the EPA primary requirement of 0.0275 ppm. However, the data showed a significant difference in results between samples taken during wet and dry spells with the latter results running 3.5 times greater than the former. Thus in dry periods, the EPA requirements were frequently exceeded.

Additionally, one site appeared to be consistantly high in SO_2 levels. This site was situated across from the John Amos Power Plant in Poca, West Virginia.

Introduction

A multidisciplinary study on sulfur dioxide was carried out during the summer of 1972. The study was supported by a National Science Foundation—Student Originated Studies grant (NSF-SOS) and involved sulfur dioxide studies in the areas of biology, psychology, and chemistry. This paper relates only to the work done by the chemistry group.

Some general studies of SO_2 levels in the Kanawha Valley had previously been reported (1). The original study was done by the Kettering Laboratory of Cincinnati in 1950-1951 and a follow-up study was made between 1964-1966. The data indicated some lowering of SO_2 concentration during this fifteen year span but nevertheless, the concentrations generally were above the primary ambient conditions set forth by the EPA effective as of the early part of 1971. Therefore, this study was to help determine whether the new standards were being effected in the Kanawha Valley.

Materials and Methods

The analytical procedure adopted to sample and determine the amount of sulfur dioxide in the atmosphere was the Scarengelli Modification of the West-Gaeke Method (2). This method is utilized by the United States Public Health Service, principally because sulfur trioxide, nitric oxides, chlorides, amines, and halogen acids do not interfere with the test.

Sulfur dioxide was collected by scrubbing air through a midget impinger containing 10 ml of .04 M potassium tetrachloromercurate reagent. Sampled air was drawn through the impinger by use of a sampling manifold containing a hypodermic needle. The needle acted as a limiting orifice as long as the collection pump maintained a minimum vacuum of 0.5 atmospheres. Thus a constant flow rate could be maintained. The SO_2 is fixed in solution as disulfitomercurate. Once the sample is collected, sulfamic acid is added to eliminate interference by normal, atmospheric nitrogen dioxide. The disulfitomercurate solution is then reacted with formaldehyde in the presence of bleached, specially purified, paraosaniline dye and the red-violet color formed is measured spectrophotometrically at a wavelength of 548 mu. Beer's Law is adhered to throughout the working range of the calibration curve.

The Scarengelli Modification of the West-Gaeke Method of analysis employs the following reagents, prepared as indicated:

1. Potassium tetrachloromercurate, .04 M: 10.0 g. of mercuric chloride and 5.9 g. of potassium chloride were dissolved in distilled water and then diluted to 1 liter.
2. Acetate buffer solution: 34.02 g. of sodium acetate trihydrate and 14.3 ml. of glacial acetic acid; bring to 250 ml. with water.
3. Purified pararosaniline, .2 per cent (nominal) stock solution—In a 500 ml separatory funnel, 125 ml each of 1-butanol and 1 N HCl were equilibrated. Into a 150 ml beaker was weighed .1 g. of pararosaniline hydrochloride (PRA or fuschin dye). To this was added 50 ml of the equilibrated HCl from the separatory funnel, and the solution was then allowed to stand for a few minutes. The pararosaniline dye solution in the beaker was added to a 125 ml separatory funnel containing 50 ml of 1-butanol and was extracted. Some of the violet impurity in the dye was transferred to the organic (top) layer. The bleached PRA was preferentially soluble in the aqueous (bottom) layer, which was then trans-

ferred into another 125 ml separatory funnel. To this aqueous layer was added 20 ml of the equilibrated 1-butanol, and an extraction was again performed. The extractions were repeated three additional times using 10 ml of the equilibrated 1-butanol in each extraction. After the final extraction, the lower phase was filtered through a 125 ml separatory funnel whose stem was loosely packed with a cotton plug. The solution was collected in a 50 ml volumetric flask and diluted to 50 ml with the equilibrated HC1. This process was repeated 11 times and the resulting yellowish-red stock solutions were combined in a 1000 ml volumetric flask.

4. Pararosaniline (PRA) reagent: 80 ml of the pararosaniline stock reagent and 100 ml of 3 M Phosphoric acid were diluted to 1000 ml with distilled water. The solution is stable for at least ten weeks.
5. Sulfamic acid, 0.6% aqueous.
6. Formaldehyde 0.2%: 0.5 ml of 37% formaldehyde diluted to 100 ml with distilled water. The solution must be prepared fresh each day.
7. Sodium sulfite solution, 0.08% aqueous.

Apparatus necessary to collect and analyze the SO_2 samples included a Bausch and Lomb Spectronic 20 Colorimeter, one centimeter spectrophotometric cells, and Bendix Midget Impingers.

To determine the amounts of SO_2 in the samples, it was necessary to compare each to a previously established calibration curve. This procedure was followed in preparing that curve:

Immediately after the sulfite solution was prepared, it was standardized by titrating it against 25 ml of a .01 N iodine solution to the starch end point. While this procedure was being performed, another portion of the sulfite solution was used to make up standards for the calibration curve. This kept the lapse time between standardization of the solution and calibration of the curve to a minimum, and error due to instability of the sulfite solution was reduced.

Into a 100 ml volumetric flask was pipetted 2 ml of the standardized sulfite solution. This was diluted to 100 ml with the .04 M potassium tetrachloromercurate reagent. Using a graduated pipette, 0.0, 0.5, 1.0, 2.0, 3.0, 4.0, and 4.5 ml portions of the sulfite-tetrachloromercurate solution were transferred into respective 150 ml beakers. These portions were diluted to 10 ml with potassium tetrachloromercurate reagent. An additional beaker containing 10 ml of potassium tetrachloromercurate was prepared and used as a blank.

To each of the standards and to the blank was added 1 ml of .6 per cent sulfamic acid. These were mixed and allowed to stand for 10 minutes, and then 2 ml of the .2 percent formaldehyde and 5 ml of the pararosaniline reagent were added. The solutions were mixed, allowed to stand for 30 minutes, and finally were adjusted to 20 ml, using 2.0 ml of distilled water.

The color intensity of the standards was measured spectrophotometrically in a one centimeter cell at a wavelength of 548 mu.

The sequence for sampling and analysis was as follows:

A 10 ml portion of potassium tetrachloromercurate was placed in each of the six midget impingers, and they were then sent out to the sampling sites. When the impingers were returned to the lab for analysis the volume of the potassium tetrachloromercurate solution in each was adjusted to 10 ml with additional potassium tetrachloromercurate solution. The sample was then transferred to 20

ml test tubes, stoppered, and stored in a refrigerator to prevent breakdown of the disulfitomercurate complexes.

The samples were analyzed in the same manner as the original standards using two blanks and eight samples for each analysis. All calibration and analytical procedures were conducted in an air-conditioned laboratory so that a constant room temperature would be maintained and the same rate of breakdown in each of the disulfitomercurate complexes would occur.

Experimental Results

Six sites covering a distance of some 25 miles in the middle Kanawha Valley were selected as sampling stations. The sites were metered continuously over a period of nine weeks. Nearly 1000 different samples were collected and analyzed. The results have been graphed in a variety of ways and show some interesting data. Table 1 shows the weekly SO_2 levels at each site.

Table 1. Weekly SO_2 Averages (ppb)

Impinger Site

	NITRO	*POCA*	*INSTITUTE*	*NORTH CHARLESTON*	*EAST CHARLESTON*	*BELLE*	*ALL SITES*
5/28-6/3	2.39	4.54	3.71	2.24	1.53	6.64	3.51
6/4-6/10	11.19	39.66	12.24	24.79	26.69	22.74	22.89
6/11-6/17	5.68	21.86	5.56	8.10	6.27	9.35	9.47
6/18-6/24	1.35	1.34	1.29	1.73	.30	1.03	1.17
6/25-7/1	1.81	4.08	4.18	7.71	2.01	2.76	7.10
7/2-7/8	5.44	8.03	4.18	6.67	6.97	5.09	6.07
7/9-7/15	1.84	5.81	3.37	7.02	15.64	9.79	7.24
7/16-7/22	11.98	28.41	7.65	16.28	13.06	11.64	14.84
7/23-7/29	8.25	8.98	15.59	30.12	18.83	12.82	15.76
Total Average/site							
5/28-7/29	5.30	13.64	6.09	11.63	10.14	9.09	9.32

Table 2 shows the data broken down by the day of the week. Some significant differences appear here and these will be detailed in the discussion section.

Table 2. Daily SO_2 Averages (ppb)

	NITRO	*POCA*	*INST.*	*NORTH CHAS.*	*EAST CHAS.*	*BELLE*	*AVE. FOR ALL SITES*
SUN.	4.12	9.81	9.51	9.01	10.39	7.16	7.14
MON.	4.91	26.78	7.93	17.09	10.66	10.71	13.01
TUES.	3.15	3.24	3.56	5.09	4.37	4.36	3.96
WED.	6.02	5.47	6.01	5.86	13.77	8.44	7.59
THUR.	5.20	19.39	7.20	14.58	9.87	11.12	11.22
FRI.	8.94	20.28	9.68	19.02	18.03	12.29	14.70
SAT.	4.31	7.85	3.77	6.90	7.66	9.09	6.59

Samples were collected at each site three times a day (about 6:00 a.m., noon, and 6:00 p.m.). Since monitoring was done continuously, data was not expected to be numerically equivalent since samples collected at 6:00 a.m. had been going for a 12-hour period rather than the 6-hour periods that were true of the morning and afternoon samples. Yet, the results shown in Table 3 indicate that the evening samples generally contained the lower amounts of SO_2.

Table 3. Comparison of SO_2 Concentrations According to Time of Day Collected (ppb)

	Morning	*Afternoon*	*Evening*
NITRO	6.69	5.12	3.56
POCA	20.56	13.60	13.44
INSTITUTE	9.22	6.27	3.18
NORTH CHARLESTON	16.92	12.83	4.07
EAST CHARLESTON	12.21	6.76	12.32
BELLE	13.23	4.91	9.09
AVERAGE	13.14	8.25	7.61

At the outset of the sampling experiment, it was speculated that rainfall would interfere with the concentrations of sulfur dioxide in the air. The magnitude of this interference was unexpected, however, and it became advantageous to collect meteorological data from U.S. National Weather Service.

When the SO_2 readings were compared to the rainfall data, it was apparent that precipitation not only immediately reduced the SO_2 content of the air, but that it took nearly a week for the SO_2 concentration to reach the "normal" levels ordinarily monitored at the sites.

During the period of June 18-24, for instance, 2.26 inches of rain fell, and the average SO_2 levels sank to .00117 ppm, the lowest average of the summer. From July 16-22, however, rainfall was only .03 inches, and the concentration had increased to .01484. Total samples collected during non-rainy weather had an overall average of .01068 ppm, while those collected during rainy weather had an overall average of .00301 ppm. Table 4 shows these results.

Table 4. Average SO_2 Levels Under Various Weather Conditions (ppb)

	RAINY WEATHER	*NON-RAINY WEATHER*	*ALL CONDITIONS*
NITRO	2.32	6.03	5.30
POCA	1.69	16.20	13.64
INSTITUTE	1.66	7.06	6.09
NORTH CHARLESTON	6.98	12.53	11.63
EAST CHARLESTON	2.79	11.65	10.14
BELLE	2.63	10.61	9.09
AVERAGE	3.01	10.68	9.32

Discussion of Results

Table 5 summarizes the data that has been obtained relating to sulfur dioxide levels in the middle Kanawha Valley since 1950.

Table 5. Comparison of Average SO_2 Levels Found in the Kanawha Valley (ppm)

Site	*NSF-SOS (Summer, 1972)*	*KVAPS (1964-1966)*	*Kettering Laboratory (1950-1951)*
Poca	0.014	—	—
Nitro	0.005	0.03	0.12
Institute	0.006	—	0.04
N. Charleston	0.012	0.07	0.03
E. Charleston	0.010	0.03	0.02
Belle	0.009	0.02	0.06

The NSF-SOS data leads to the conclusion that there has been a significant decrease in average SO_2 concentrations in the Kanawha Valley during the last six years. This undoubtedly reflects an effort by industry to alleviate SO_2 pollution, either by their own initiative, or to meet new Federal and State regulations.

In 1971, the Air Pollution Control Office of the Environmental Protection Agency issued two standards to govern the amount of SO_2 allowable in the atmosphere. The primary standard provided for an adequate margin of safety, and the maximum was set at .0275 ppm (80 ug/m^3). The secondary standard was to be reached within a "reasonable period of time," and provided for a maximum SO_2 level of .0206 ppm (60 ug/m^3). On the average, SO_2 pollution in the Kanawha Valley last summer was far below EPA's secondary standard.

Average SO_2 values, however, tended to camouflage several potentially dangerous situations, particularly in the Poca area, across the river from the Appalachian Power Company's new John Amos Power Plant. It was decided to monitor Poca after citizens complained that the new plant had drastically reduced the quality of their air. Data gathered at the Poca site strongly suggests that the citizens of Poca have a valid complaint, irrespective of the source of the pollution. Table 1 indicates that on a weekly average basis, more than 30 percent of the SO_2 levels monitored in Poca were in excess of the EPA's secondary stand-

ard of .0206 ppm. These averages occurred in the weeks of June 4-10 (.0397 ppm), June 11-17 (.0219 ppm), and July 16-22 (.0284 ppm). Examination of the analysis of the 152 samples collected at Poca showed that 17 percent were above .0206 ppm, and 13 percent were above .0275 ppm.

Significantly, nearly all high SO_2 averages followed periods in which rainfall was at a minimum. This led to the tentative conclusion that SO_2 concentrations in the Poca area would have been above EPA's standards for most of the summer, had not heavy rainfall during the middle weeks of the experiment effectively disguised the dimensions of the problem.

Another potential danger hidden by the summer average is illustrated by the week of June 4-10. At four of the six NSF-SOS sites that week, the average SO_2 concentration was above EPA's secondary standard. Little rainfall had preceded June 4 and the SO_2 concentration in the atmosphere appeared simply to accumulate. This condition suggests that residents of the valley, where air inversions frequently occur, are very dependent upon the whims of nature to provide the necessary amount of rainfall to keep sulfur dioxide levels within reason.

Analysis of the data shown in Table 2 indicated that the highest levels of SO_2 were collected on Thursdays, Fridays, and Mondays. These findings strongly support the hypothesis that local industry emits more pollution at the beginning of each work week and just before the slowdown of operations at the end of the "work week."

The authors were somewhat surprised at the results found in Table 3. They had expected the highest concentrations of SO_2 to be found in the evening sample. However, a knowledge of meteorology is important in air pollution studies. Apparently there is a shift in both wind direction and intensity as the evening hours approach. This probably helps to explain the lower evening readings. The significantly higher morning readings would seem to agree with this consensus. There is a diminishing of wind intensity coupled with the holding power of the heavier colder layer of air which rapidly builds up the SO_2 levels during the early daylight hours.

Overall, the study tended to indicate compliance with the sulfur dioxide emission levels of the EPA. Unfortunately, however, there is sufficient data to indicate that this might not be the case in any period of reasonably dry weather. A minimum of a one year study would be necessary to prove or disprove the argument as to whether there is a sulfur dioxide air pollution problem in the middle Kanawha Valley.

Acknowledgments

The authors would like to thank the National Science Foundation for its SOS grant. Further acknowledgments go to students A. Michael Adams, Donna J. Borkowski, Michael W. Lilly, Zachariah T. Phillips, and David L. Smith who participated in the work and to Esther Goodall and Shirley Finney for their assistance in the typing.

Literature Cited

1. National Air Pollution Control Administration and West Virginia Air Pollution Control Commission. 1970. Kanawha Valley Air Pollution Study. U.S. Department of Health, Education and Welfare, Raleigh, North Carolina.
2. Scarengelli, F. S., B. E. Saltzman, and S. A. Frey. 1967. Spectrophotometric determination of atmospheric sulfur dioxide. *Analytical Chemistry* 39:1709-19.

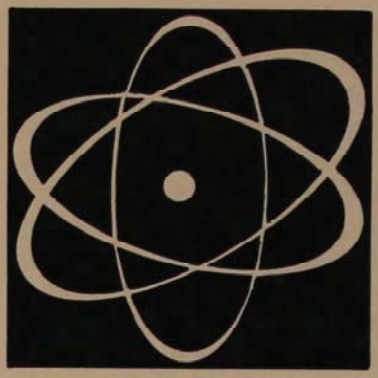

Physics

Ambiguities of the Principle of Relativity

John B. Kizer
Scioto Development Company
Route 3, Wheelersburg, Ohio 45694

Abstract

The problem of the clock paradox with three inertial observers is shown to lead to an ambiguity of interpretation because of the reciprocal nature of time dilatation. Irrespective of special relativity, the relativity principle alone leads to an ambiguity of interpretation when applied to electrodynamic phenomena. The relativity principle in concert with the principle of equivalence leads to an ambiguity of interpretation when applied to simple mechanical phenomena. These ambiguities cannot be resolved by any simple invocation of an ether hypothesis because any ether hypothesis which is consonant with experimental results also leads to the same ambiguities as those theories which involve a principle of relativity.

Although the clock paradox in the form of the twin paradox has probably been discussed more than any other facet of special relativity, because acceleration is required in an out-and-back journey, one cannot really observe the rigors demanded by the special theory by considering the paradox in this form, because the special theory is only strictly applicable to inertial motion. The failure to observe these rigors has led to much confused criticism of the principle of relativity. The principle of relativity is, however, open to some proper criticism in cases in which these rigors are observed.

One form of the clock paradox which can be formulated completely in terms of inertial motion was devised by Lord Halsbury (1957) who modified the twin problem so that it becomes a "problem of three brothers." Brother A is at rest in an inertial system and brother B travels directly away from him at a high constant speed V. B's clock agrees with A's at the instant the two separate. Later B passes brother C who is approaching earth at a constant speed V and B and C note that their two clocks agree as they pass each other. When C reaches earth, how does his clock reading compare with A's?

To answer this question one must realize that on B's outward flight both A and B read each other's clocks as being slow relative to his own. (All clock

readings in this discussion are corrected for time of signal transmission.) When B and C coincide and synchronize their clocks, both B and C will read A's clock as being slow relative to theirs because two coincident observers must agree on the simultaneity of any event, irrespective of their relative motion; and A will read C's clock, at the time of synchronization, as being slow relative to his, as it is synchronized with B's clock which A sees as running slow. A and C continue in uniform motion toward each other, each reading the other's clock as being slow relative to his own. When A and C are coincident no clock has left an inertial system, but A reads C's clock as being behind his own and C reads A's clock as being behind his own. As two coincident observers cannot disagree on the simultaneity of an event, i.e., the reading on one clock; this clearly implies a contradiction because coincidence, even in relativity, is absolute, and only the simultaneity of spatially or temporally separated events is in question.

Halsbury (1957) and Stephenson and Kilmister (1958) have tried to resolve this paradox by saying that B records the coincidence of B and C to be at an earlier time than that when A records this coincidence on their own respective clocks. This cannot be the case although A and B will both read each other's clock as slow. Each is at rest in his own inertial frame, thus, both A and B will record the coincidence of B and C as happening at the same time on his own clock. This then is an erroneous resolution of the paradox.

A well-known paradox of electrodynamics is that two charges at rest interact purely electrostatically; whereas, the same two charges considered from an inertial frame with respect to which they are in motion, will interact electromagnetically as well. Since the principle of relativity requires that all inertial frames be equivalent, there is an apparent ambiguity as to whether or not the magnetic field really exists as neither inertial frame can be preferred.

This paradox is usually considered readily resolvable in terms of special relativity by applying the Lorentz transformation and the special principle of relativity rather than the Galilean transformation and the classical principle of relativity to the above situation. That this resolution is not unambiguous can be seen by considering this electrodynamic paradox in the form of the following thought-experiment.

Assume that in the rest frame of the charges the observer (O') has two particle detectors which will record the electrons' impinging on them at time t if Coulomb's law is obeyed. O, who is in motion relative to the charges, also has particle detectors in his inertial frame so that when O' and O are coincident, their respective particle detectors on both sides will also be coincident, a fact which entails that at the time of the coincidence of the O' particle detectors and the electrons, the electrons will also be coincident with the O particle detectors. Simultaneity is assured because each observer can have a "clock" on his associated particle detector conventionally synchronized with his own clock. As this other clock is at rest relative to his own clock, he is assured that at the time of his own coincidence with the other observer, his particle detector is also coincident with the other observer's particle detector, as the two clocks are synchronized and the clock reading at a coincidence is absolute. O will observe, according to relativity, the electrons to be interacting in accordance with Coulomb's law multiplied by the relativistic force transformation.

Both O and O' observe his associated particle detectors as being the same distance from himself in his rest frame both before and at the time of coincidence as he observes his own detectors as being at rest relative to himself. Because the O detector and the O' detector are coincident, both O and O' must

agree that they are in the same place as this is the meaning of the absolute nature of coincidence. Because both observers observe the particle detectors and electron to be in the same place and as each observer is measuring the distance to his own particle detector (and hence the other detector and electron) in his rest frame, both observers must agree about the absolute distance to the electron and particle detectors (this applies equally well to both electrons) because absolute distance is measurable in one's own rest frame. The simultaneity of these position measurements is assured for the reasons mentioned above.

Although the above thought-experiment indicates that both O and O' must agree about the relative positions of the electrons at the observers' coincidence, the special theory of relativity demands that O' will observe the separating electrons as farther apart than O because O' will not observe the relativistic force transformation as applied to the electrons as will O.

As these are contradictory results, it can be seen that it is not unambiguously determinable what two presumably equivalent inertial observers will, in fact, observe in the above situation. Thus it can be seen that the special principle of relativity does not resolve the paradox any more than does the classical principle.

This same paradigm can be applied to a thought-experiment concerning uncharged masses. Uncharged masses in the same situation would lead to the same ambiguous situation. To the observer moving with the masses (O') the force of attraction would be observed to be less than to the observer to whom the masses are in motion (O). This is because relative to O the masses also have kinetic energy and, because of the equivalence of mass and energy, they are more massive than they appear to be to O'. As they are more massive relative to O the force of measured gravitational attraction between them would be greater and they would accelerate toward each other more rapidly for O than they would appear to for O'. This again, of course, leads to a contradiction as these observers are coincident and, therefore, *must* agree as to the relative positions of the masses.

It might be argued that any problem involving gravitation would have to be dealt with by using the full apparatus of general relativity. However, historically, problems of this type were dealt with before the development of general relativity. The reason that this thought-experiment is independent of general relativity is that as long as the principle of relativity and the principle of equivalence are accepted, the conclusion follows that coincident observers will make different and contradictory observations. It is certainly true that the magnitude of these differences will be different depending on whether one accepts the Einstein, the Brans-Dicke or some other gravitational theory; however, all gravitational theories not absolutely ruled out by observational evidence do, today, accept both the principles of relativity and equivalence, and this acceptance is all that is necessary to lead to ambiguous results.

It must not be thought that these ambiguities can be resolved by some simple invocation of an ether hypothesis because Gruenbaum (1963) has shown that the only ether theory known to be consistent with experimental results is the so-called doubly-amended Larmor-Lorentz theory, a theory with equations exactly the same as those of special relativity but with a different interpretation of those equations. This theory, which has been accepted by most of those British physicists who have opposed relativity, unfortunately because the equations are exactly the same as those of the special theory, involves precisely the same ambiguities as those theories which assume a principle of relativity.

Literature Cited

1. Gruenbaum, A. 1963. Philosophical Problems of Space and Time. Alfred A. Knopf. New York. See Chap. 12-15.
2. Halsbury, Lord. 1957. "Space Travel and Ageing." *Discovery* 18:174.
3. Stephenson, R., and Kilmister, C. 1957. Special Relativity for Physicists. Oxford University, London. pp. 42-44.

Cylindrical Electrets

Oleg Jefimenko

Department of Physics, West Virginia University

Morgantown, West Virginia 26506

Abstract

Cylindrical-shell electrets with radially-symmetric and axially-symmetric polarization are discussed. Theoretical expressions for the electric fields of such electrets are obtained. Possible applications of cylindrical electrets are indicated.

Introduction

Most published works on electrets deal with electrets in the shape of disks, plane-parallel slabs, and thin films. However, electrets of other shapes may be more appropriate for various experimental and theoretical studies. Spherical-shell electrets[1] were recently discussed and studied by Jefimenko and Sun (1972). The purpose of the present paper is to provide basic electric field data on cylindrical-shell electrets.

Theoretical

Consider a cylindrical-shell electret placed between two grounded conducting shields coaxial with the electret (Fig. 1). Let the electric field in the space between the inner shield and the electret be $\bar{E}_1$, the electric field in the electret be $\bar{E}_2$, and the electric field in the space between the electret and the outer shield be $\bar{E}_3$. We are interested in expressing $\bar{E}_1$, $\bar{E}_2$, and $\bar{E}_3$ as functions of characteristic geometrical and electrical parameters of the system. For a sufficiently long electret (such that the end effects of the system may be neglected) this can be done as follows.

Let the radii of the inner shield, inner electret surface, outer electret surface, and outer shield be a, b, c, and d, respectively. Since the shields are at the same potential, we have

$$\int_a^b \bar{E}_1 \cdot d\bar{r} + \int_b^c \bar{E}_2 \cdot d\bar{r} + \int_c^d \bar{E}_3 \cdot d\bar{r} = 0. \qquad (1)$$

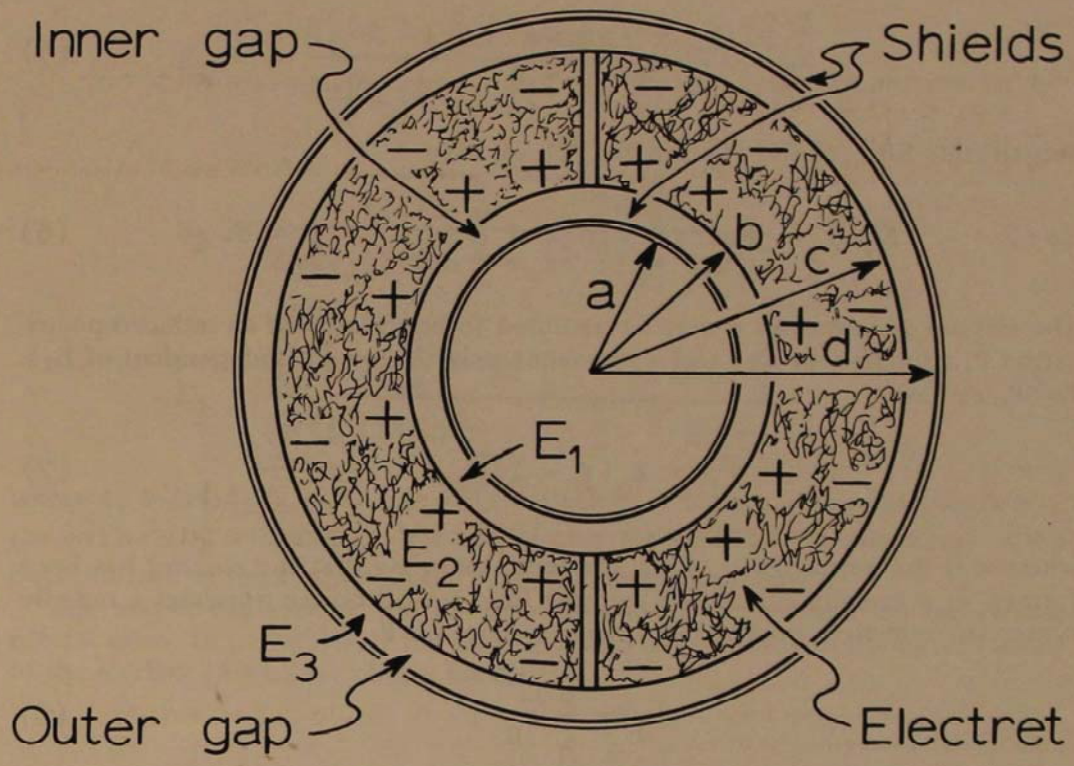

FIGURE 1. Radially-symmetric system.

At the surfaces of the electret the boundary conditions for the displacement vector $\bar{D}$ must be satisfied. Let the real surface charge densities on the inner and outer surfaces of the electret be σ_{12} and σ_{23}, respectively. At the outer surface we then have

$$(\bar{D}_3 - \bar{D}_2)\cdot\bar{r}_u = \sigma_{23}, \qquad r = c, \tag{2}$$

and at the inner surface we have

$$(\bar{D}_2 - \bar{D}_1)\cdot\bar{r}_u = \sigma_{12}, \qquad r = b, \tag{3}$$

where $\bar{r}_u$ is the radial unit vector, and the subscripts on the $\bar{D}$'s correspond to those on the $\bar{E}$'s.

The displacement vector inside the electret, $\bar{D}_2$, may be expressed in terms of the field vector $\bar{E}_2$ and the polarization vector $\bar{P}$ of the electret as

$$\bar{D}_2 = \epsilon_o\bar{E}_2 + \bar{P}\ , \tag{4}$$

where ϵ_o is the permittivity of space. Since there is no polarization outside the electret, $\bar{D}_3$ may be written as

$$\bar{D}_3 = \varepsilon_o \bar{E}_3. \tag{5}$$

Substituting Eqs. (4) and (5) into Eq. (2), we have

$$\varepsilon_o(\bar{E}_3 - \bar{E}_2)\cdot\bar{r}_u = \sigma_{23} + \bar{P}\cdot\bar{r}_u, \qquad r = c. \tag{6}$$

The electret polarization $\bar{P}$ may be assumed to be the sum of an induced polarization $\bar{P}_i$ (function of $\bar{E}_2$) and a remanent polarization $\bar{P}_r$ (independent of $\bar{E}_2$). For $\bar{P}_i$ we have

$$\bar{P}_i = \varepsilon_o(\varepsilon - 1)\bar{E}_2, \tag{7}$$

where ϵ is the permittivity of the electret. Assuming that the electret has been formed in a radially symmetric forming field (or otherwise possesses a radially symmetric remanent polarization), we can write for $\bar{P}_r$

$$\bar{P}_r = \frac{p}{r}\bar{r}_u , \tag{8}$$

where p is a constant. The total polarization in the electret is then

$$\bar{P} = \frac{p}{r}\bar{r}_u + \varepsilon_o(\varepsilon - 1)\bar{E}_2 , \tag{9}$$

which, with Eq. (6), yields

$$\varepsilon_o(E_3 - \varepsilon E_2) = \sigma_{23} + \frac{p}{c} , \qquad r = c, \tag{10}$$

where we took into account the assumed absence of edge effects and the radial symmetry of the system under consideration in eliminating r_u on the left side of the equation.

A similar calculation employing Eq. (3) yields for the inner surface of the electret

$$\varepsilon_o(\varepsilon E_2 - E_1) = \sigma_{12} - \frac{p}{b} , \qquad r = b. \tag{11}$$

Combining Eqs. (1), (10), and (11) and once again making use of the radial symmetry of the system, we obtain after some elementary transformations

$$\bar{E}_1 = \frac{K_1}{r}\bar{r}_u, \qquad \bar{E}_2 = \frac{K_2}{r}\bar{r}_u, \qquad \bar{E}_3 = \frac{K_3}{r}\bar{r}_u, \tag{12}$$

where the constants K_1, K_2, and K_3 are given by

$$K_1 = - \frac{q_i(\varepsilon \ln \frac{d}{c} + \ln \frac{c}{b}) + q_o \varepsilon \ln \frac{d}{c}}{2\pi \ell \varepsilon_o [\varepsilon(\ln \frac{b}{a} + \ln \frac{d}{c}) + \ln \frac{c}{b}]} , \qquad (13)$$

$$K_2 = \frac{q_i \ln \frac{b}{a} - q_o \ln \frac{d}{c}}{2\pi \ell \varepsilon_o [\varepsilon(\ln \frac{b}{a} + \ln \frac{d}{c}) + \ln \frac{c}{b}]} , \qquad (14)$$

$$K_3 = \frac{q_o(\varepsilon \ln \frac{b}{a} + \ln \frac{c}{b}) + q_i \varepsilon \ln \frac{b}{a}}{2\pi \ell \varepsilon_o [\varepsilon(\ln \frac{b}{a} + \ln \frac{d}{c}) + \ln \frac{c}{b}]} , \qquad (15)$$

where $q_i = 2\pi\ell(\sigma_{12}b - p)$ represents the effective charge of the inner surface of the electret, $q_o = 2\pi\ell(\sigma_{23}c + p)$ represents the effective surface charge of the outer surface of the electret, and ℓ is the length of the electret.

The above expressions for K's may be considerably simplified for various special cases. In particular, if the outer shield is in contact with the outer surface of the electret (d = c), we obtain for K_1

$$K_1 = - \frac{q_i \ln \frac{c}{b}}{2\pi \ell \varepsilon_o (\ln \frac{c}{b} + \varepsilon \ln \frac{b}{a})} . \qquad (16)$$

This expression can be further transformed into

$$K_1 = - \frac{q_i \ln (1 + \frac{L}{b})}{2\pi \ell \varepsilon_o [\ln (1 + \frac{L}{b}) + \varepsilon \ln (1 + \frac{d_i}{a})]} , \qquad (17)$$

or

$$K_1 = - \frac{q_i \ln \beta}{2\pi \ell \varepsilon_o [\ln \beta - \varepsilon \ln (1 + \alpha - \alpha\beta)]} , \qquad (18)$$

where $d_i = b - a$ is the width of the inner gap (space between the inner shield and the inner surface of the electret), $L = c - b$ is the thickness of the electret, $\alpha = d_i/L$, and $\beta = c/b$. Likewise, if the inner shield is in contact with the inner surface of the electret (a = b), we obtain for K_3

$$K_3 = \frac{q_o \ln \frac{c}{b}}{2\pi \ell \varepsilon_o (\ln \frac{c}{b} + \varepsilon \ln \frac{d}{c})} . \qquad (19)$$

This expression can be further transformed into

$$K_3 = \frac{q_o \ln (1 + \frac{L}{b})}{2\pi \ell \varepsilon_o [\ln (1 + \frac{L}{b}) + \varepsilon \ln (1 + \frac{d_o}{c})]} , \qquad (20)$$

or

$$K_3 = \frac{q_o \ln \beta}{2\pi \ell \varepsilon_o [\ln \beta + \varepsilon \ln (1 + \gamma - \gamma/\beta)]} , \qquad (21)$$

where $d_o = d - c$ is the width of the outer gap (space between the outer surface of the electret and the outer shield), L and β are as before, and $\gamma = d_o/L$.

For practical applications one usually wants to know the charges induced on the inner and outer shields by the electret. The density of the induced charge on the inner shield is $\sigma_i = \varepsilon_o E$ surface, or, according to Eqs. (12) and (18)

$$\sigma_i = \frac{q_i \ln \beta}{2\pi \ell a [\ln \beta - \varepsilon \ln (1 + \alpha - \alpha\beta)]} . \qquad (22)$$

The total induced charge on the inner shield is therefore

$$Q_i = \frac{q_i \ln \beta}{\ln \beta - \varepsilon \ln (1 + \alpha - \alpha\beta)} . \qquad (23)$$

This charge has its maximum value

$$Q_{i\,max} = q_i \qquad (24)$$

when the radius of the inner shield is equal to the radius of the inner surface of the electret ($d_i = 0$, and $\alpha = 0$ in this case). Let us define the "reduced charge" Q_i^* as

$$Q_i^* = \frac{Q_i}{Q_{i\,max}} . \qquad (25)$$

From Eqs. (23) and (24) we then have

$$Q_i^* = \frac{\ln \beta}{\ln \beta - \varepsilon \ln (1 + \alpha - \alpha\beta)} . \qquad (26)$$

Let now the inner shield, rather than the outer shield be in contact with the electret. As it follows from Eqs. (12) and (21) by a reasoning similar to that used in deriving Eq. (23), the charge induced on the outer shield is then

$$Q_o = \frac{q_o \ln \beta}{\ln \beta + \varepsilon \ln (1 + \gamma - \gamma/\beta)} , \qquad (27)$$

This charge has its maximum value

$$Q_{o\,max} = q_o \qquad (28)$$

when the radius of the outer shield is equal to the radius of the outer surface of the electret ($d_o = 0$, and $\gamma = 0$ in this case). Let us define the "reduced charge" Q_o^* as

$$Q_o^* = \frac{Q_o}{Q_{o\,max}} . \qquad (29)$$

From Eqs. (27) and (28) we then have

$$Q_o^* = \frac{\ln \beta}{\ln \beta + \varepsilon \ln (1 + \gamma - \gamma/\beta)} . \qquad (30)$$

In a similar manner one can define "reduced electric fields" E_i^* and E_o^* (for example, E_i^* is the field at the surface of the inner shield of a given radius a divided by the field at the surface of the inner shield of radius b). As can be easily seen

$$E_i^* = Q_i^* \frac{b}{a} , \qquad (31)$$

and

$$E_o^* = Q_o^* \frac{c}{d} . \qquad (32)$$

Theoretical curves for Q_i^* and E_i^* representing Eqs. (26) and (31) are shown in Fig. 2 for an electret of dielectric constant $\varepsilon = 2.5$, $b = 2.54$ cm, and $c = 3.81$ ($\beta = 1.5$), which are the parameters of the electrets normally used in our laboratory. Theoretical curves for Q_o^* and E_o^* representing Eqs. (30) and (32) for the same electret are shown in Fig. 3.

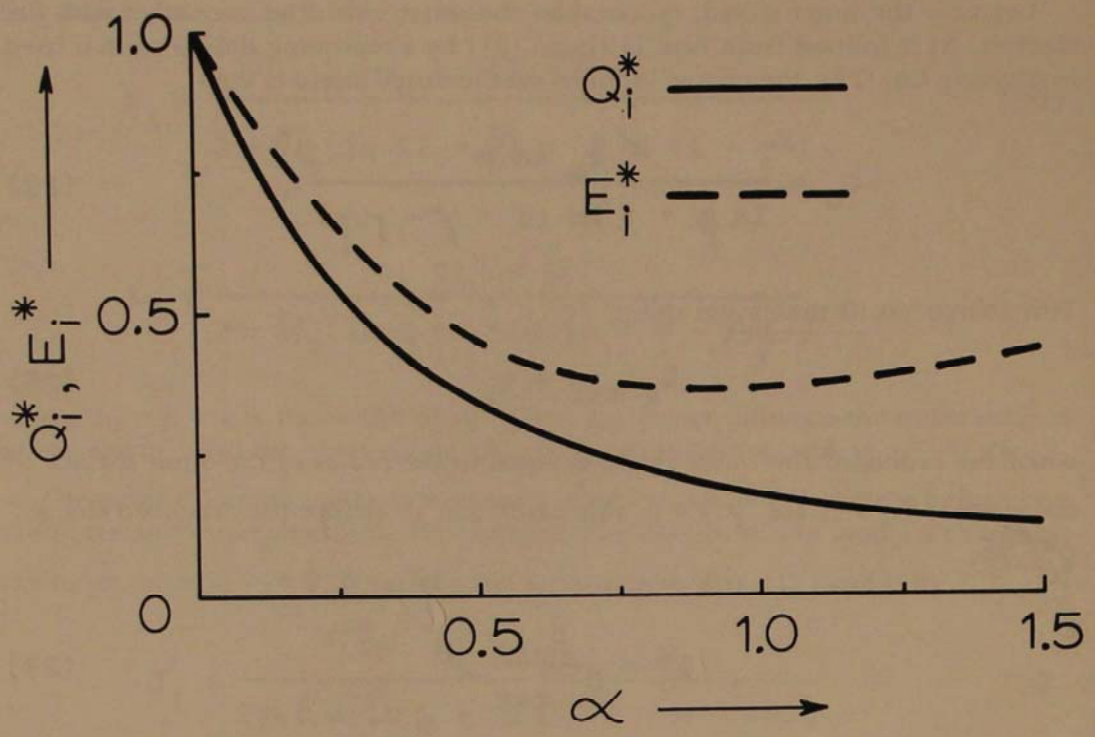

FIGURE 2. Reduced-charge and reduced-field curves for the inner shield.

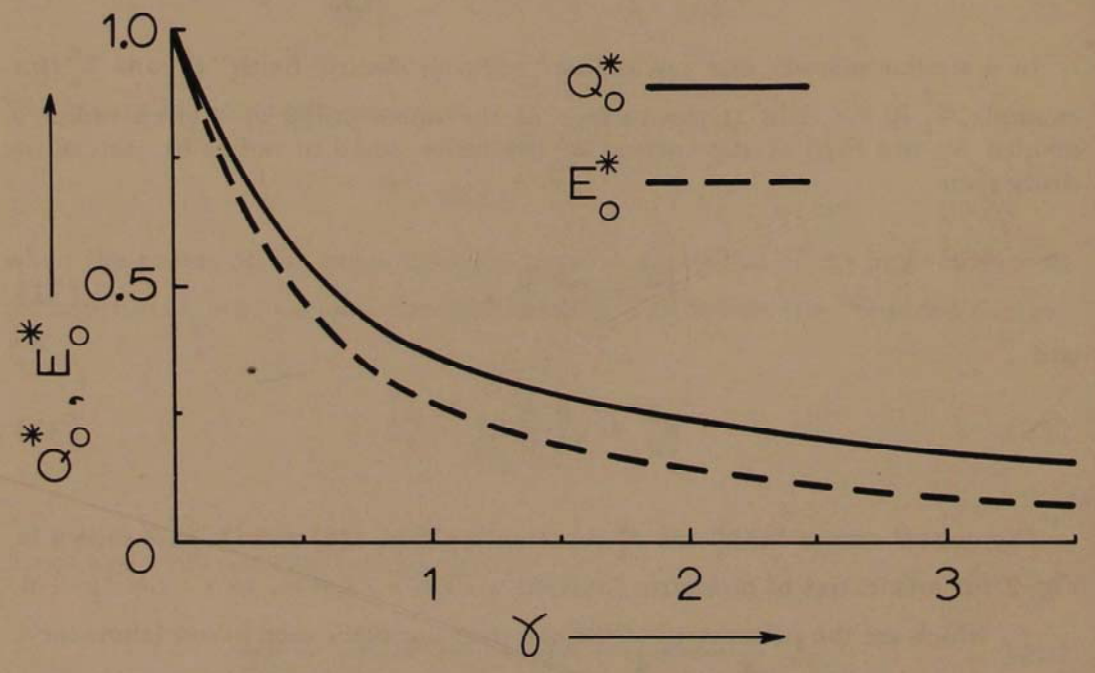

FIGURE 3. Reduced-charge and reduced-field curves for the outer shield.

The system shown in Fig. 1 was assumed to contain a radially-symmetric electret. Suppose now that this electret is replaced with an electret made of two halves of opposite polarity as shown in Fig. 4. The electric fields of such an axially-symmetric system can be found as follows.

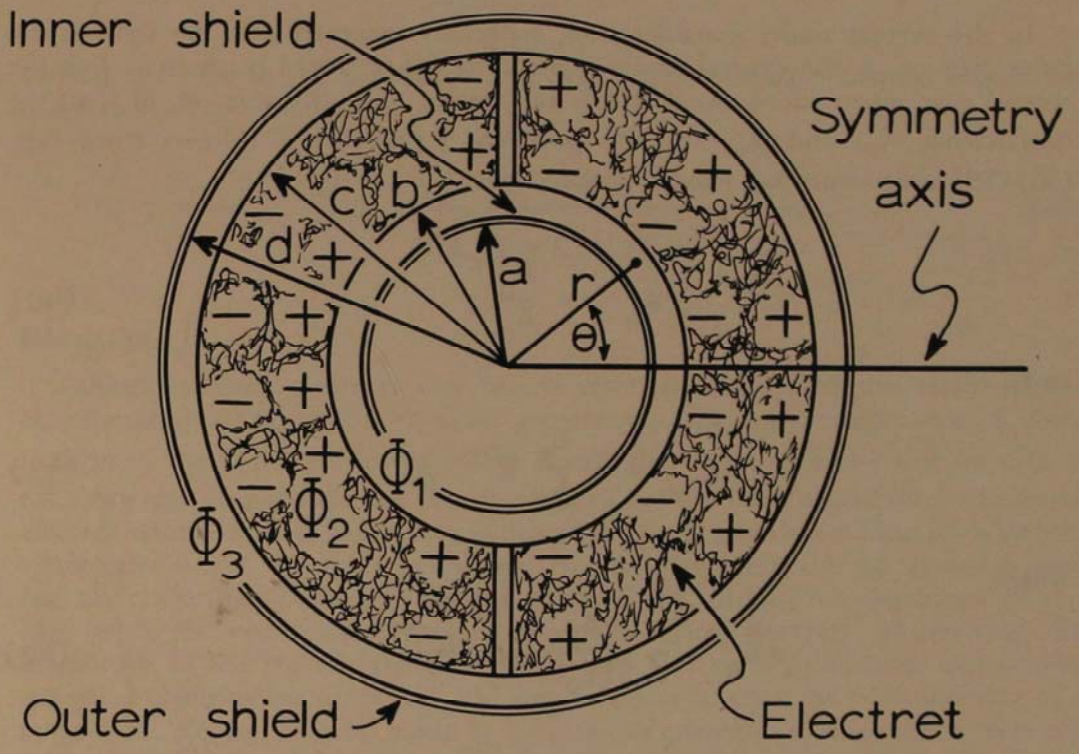

FIGURE 4. Axially-symmetric system.

Let the potentials in the inner gap, in the electret, and in the outer gap be φ_1, φ_2, and φ_3, respectively. From the symmetry of the system it follows that each of these potentials is of the form

$$\varphi = \sum_{n=1}^{\infty} (A_n r^n + B_n r^{-n}) \cos n\theta, \tag{33}$$

where A_n and B_n are constants, n is an integer, and r and θ are cylindrical coordinates as shown in Fig. 4. The constants A_n and B_n can be found with the aid of the following boundary conditions:

$$\varphi_1 = 0 \qquad \text{at} \quad r = a, \tag{34}$$

$$\varphi_3 = 0 \qquad \text{at} \quad r = d, \tag{35}$$

$$\varphi_1 = \varphi_2 \qquad \text{at} \quad r = b, \tag{36}$$

$$\varphi_2 = \varphi_3 \qquad \text{at} \quad r = c, \tag{37}$$

$$(\bar{D}_2 - \bar{D}_1) \cdot \bar{r}_u = \sigma_{12} \qquad \text{at} \quad r = b, \tag{38}$$

and

$$(\bar{D}_3 - \bar{D}_2)\cdot\bar{r}_u = \sigma_{23} \quad \text{at} \quad r = c. \tag{39}$$

In the system under consideration, especially interesting is the field in the inner gap or in the central cavity (when the inner shield is absent). For the special case when the outer shield is in contact with the electret (d = c) the coefficients A_{n1} and B_{n1} for the potential φ_1 are, as it follows from Eqs. (33)-(39) after somewhat lengthy calculations,

$$A_{n\,1} = \frac{L_n}{K_n}, \tag{40}$$

and

$$B_{n\,1} = -\frac{L_n}{K_n} a^{2n}, \tag{41}$$

where

$$L_n = -\frac{4\sigma_{ie}}{\pi\varepsilon_0 n} \sin\frac{n\pi}{2}, \tag{42}$$

$$K_n = nb^{n-1}\left[1 + \varepsilon - (\varepsilon - 1)\frac{a^{2n}}{b^{2n}} - 2\varepsilon\frac{b^{2n} - a^{2n}}{b^{2n} - c^{2n}}\right], \tag{43}$$

and $\sigma_{ie} = \sigma_{12} - p/b$ (the effective surface charge density of the inner surface of the electret). In the first approximation

$$\varphi_1 \approx (A_{11}r + B_{11}r^{-1})\cos\theta = \frac{L_1}{K_1}\left(1 - \frac{a^2}{r^2}\right) r\cos\theta, \tag{44}$$

where

$$L_1 = -\frac{4\sigma_{ie}}{\pi\varepsilon_0}, \tag{45}$$

and

$$K_1 = 1 + \varepsilon - (\varepsilon - 1)\frac{a^2}{b^2} - 2\varepsilon\frac{b^2 - a^2}{b^2 - c^2}. \tag{46}$$

It is interesting to note that for a = O (that is, when the inner shield is absent) Eq. (44) reduces to

$$\varphi \approx \frac{L_1}{K_1} r \cos \theta , \tag{47}$$

so that the field in the central cavity is then approximately homogeneous. The magnitude of this field is

$$E_1 \approx \frac{4\sigma_{1\theta}}{\pi\varepsilon_o\left(1 + \varepsilon - 2\varepsilon \frac{b^2}{b^2 - c^2}\right)} . \tag{48}$$

Discussion

Cylindrical-shell electrets can be conveniently used as active elements for electrostatic electrometers, motors, generators, and charge dispensers. A comparison of the Q_1^* curve shown in Fig. 2 with the corresponding curve for spherical electrets[1] shows that the charge induced on the inner shield of a cylindrical electret decreases with increasing width of the inner gap slower than for a similar spherical electret. Therefor cylindrical electrets are preferable to spherical ones for devices utilizing charges induced on the inner shields. A comparison of Eq. (48) with the corresponding equation for spherical electrets[1] shows that the magnitude of the electric fields in the central cavities of cylindrical and similar spherical electrets are practically the same. However, since the central cavity of a cylindrical electret can be made as long as one pleases, cylindrical electrets are also preferable to spherical ones for devices utilizing electric fields in the central cavities of the electrets. One may expect therefore that cylindrical electrets will be incorporated in many electret devices and will be at least as useful for practical applications as the plane and the spherical electrets.

Literature Cited

1. Jefimenko, Oleg, and Chang, N. Y. Sun. 1973. Spherical Carnauba Wax Electrets, in *Electrets, Charge Storage, and Transport in Dielectrics.* The Electrochemical Society, New York.

Electret Electrometers

Oleg Jefimenko and David K. Walker*
West Virginia University
Morgantown, West Virginia 26506

Abstract

Electrometers and voltmeters having electrets as active elements were built. They are well suited for measuring electric charges down to 10^{-13} coulomb and voltages down to 0.1 volt. The meters are inexpensive and of very simple construction.

The recently discussed electret slot effect[1,2,3] allows one to construct sensitive coulombmeters and voltmeters having electrets as active elements.

We have built and studied two types of meters of this kind: pointer-type meters and mirror-type meters.

A schematic diagram of the pointer-type meter is shown in Fig. 1. Actual photographs of such a meter are shown in Figs. 2 and 3. The two semi-circular electrets are supported by two Plexiglas plates which can be inserted between the electrodes by means of guides mounted on the base of the instrument. This allows one to interchange electrets of different polarization (strength), thus changing the sensitivity of the instrument. The electrodes are "painted" onto two mica disks with conducting paint and are "cross connected" internally (electrode 1 is connected to electrode 3, and electrode 2 is connected with electrode 4). The axle of the electrode assembly is made of a dielectric material (Plexiglas). The electrodes are connected with external (input) contacts of the instrument either with the aid of two spiral springs (not shown) providing the restoring torque, or with the aid of conducting strips on the axle if the restoring torque is provided by gravity.

With a carnauba wax electret of 7 cm diameter and 1 cm thickness the capacitance of the instrument is $\approx 10\ \mu\mu F$, and the sensitivity is ≈ 100 V or 10^{-9} coulombs for a full scale deflection. We have found this instrument especially useful as a coulombmeter. But since it has an input impedance in excess of 10^{17} ohm, it also serves very well as an electrostatic voltmeter (electrometer). The stability curve of the meter is shown in Fig. 4.

A schematic diagram of the mirror-type meter is shown in Fig. 5. Actual photographs of the mirror-type meter are shown in Figs. 6 and 7. Since the electrode assembly is now suspended from a torsion ribbon (standard 0.003 Au suspension from a torsion galvanometer), the sensitivity of this instrument is much greater than that of the one described above. Thus, with a carnauba wax electret 3.5 cm in diameter and 1 cm thick, the deflection observed on a screen 1 m from the reflecting mirror is 20 mm/volt or $\simeq 10^{12}$ mm/coulomb.

We believe that these types of simply constructed meters will soon become standard tools for electrostatic and other electrical measurements.

*Present address: Waynesburg College, Waynesburg, Pa. 15370.

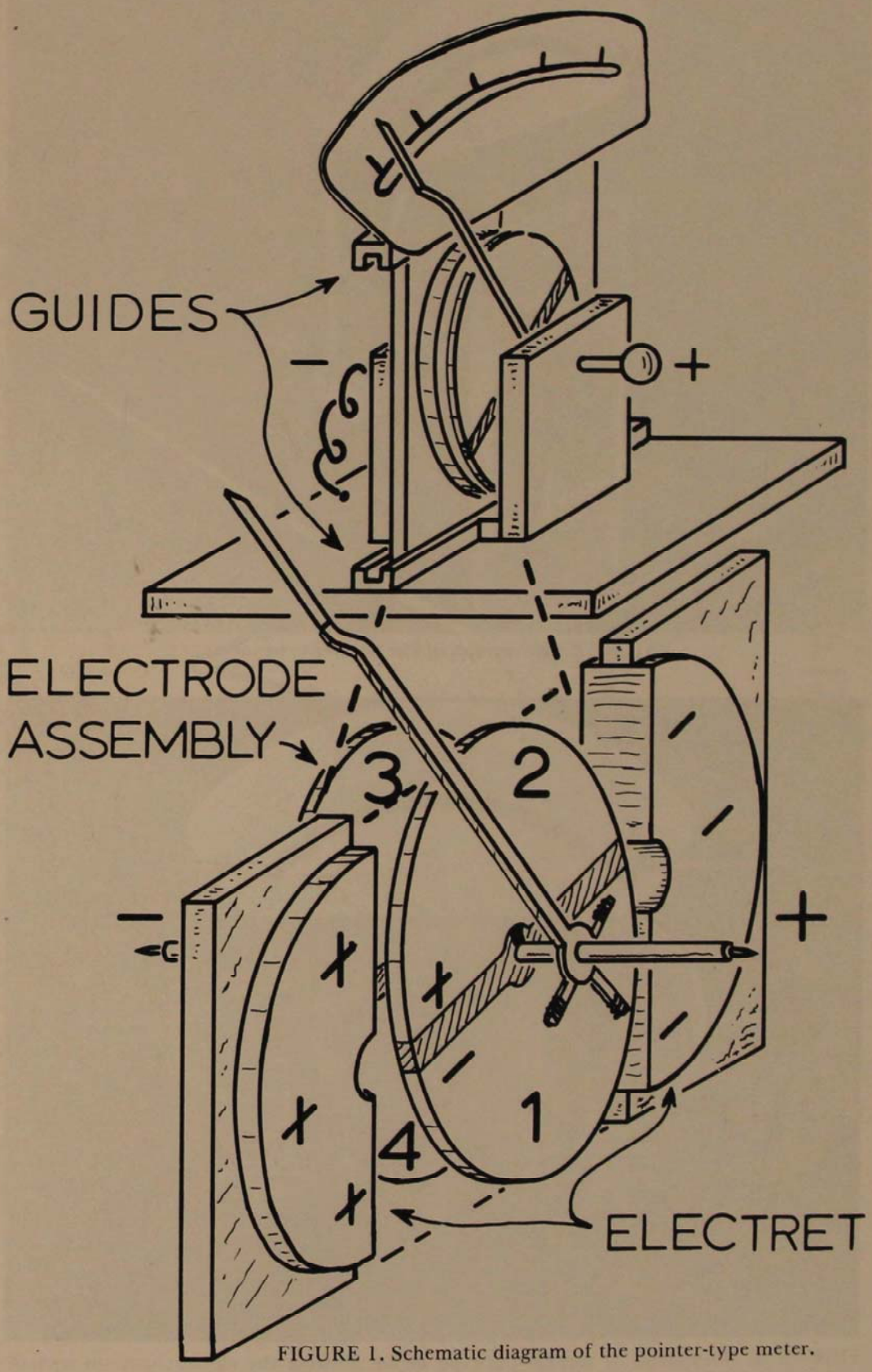

FIGURE 1. Schematic diagram of the pointer-type meter.

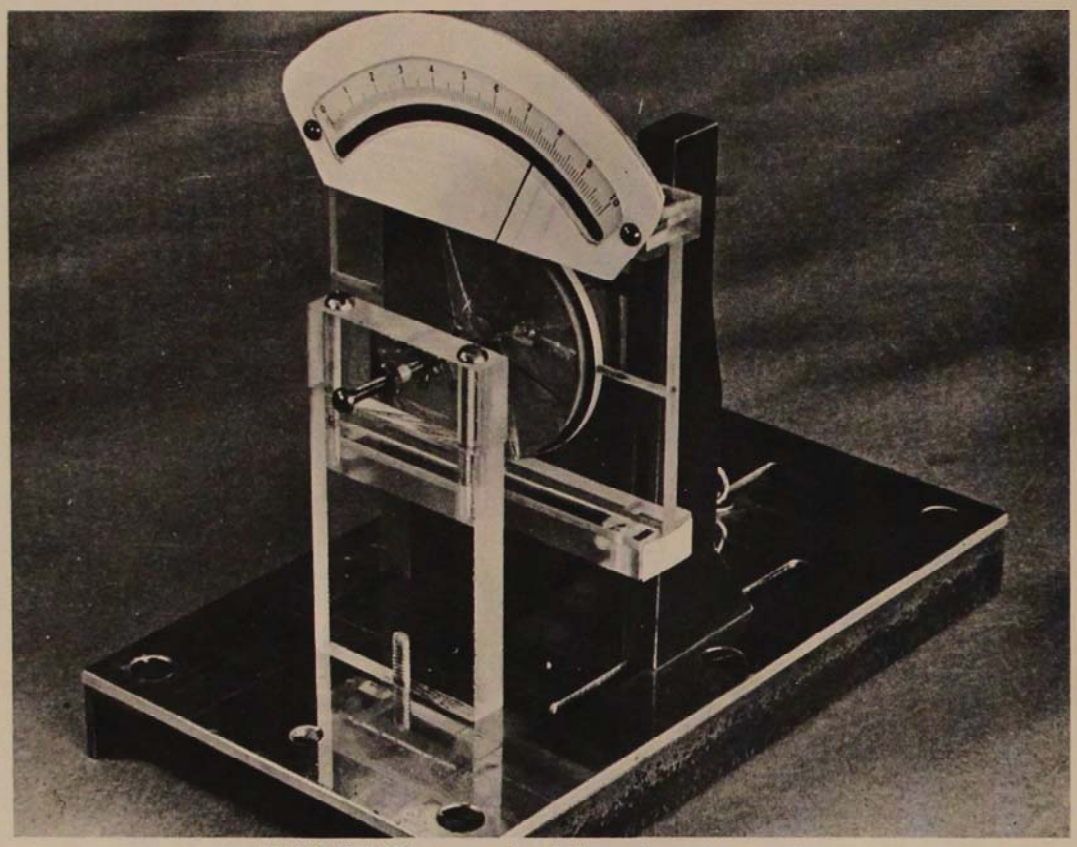

FIGURE 2. Photograph of the pointer-type meter.

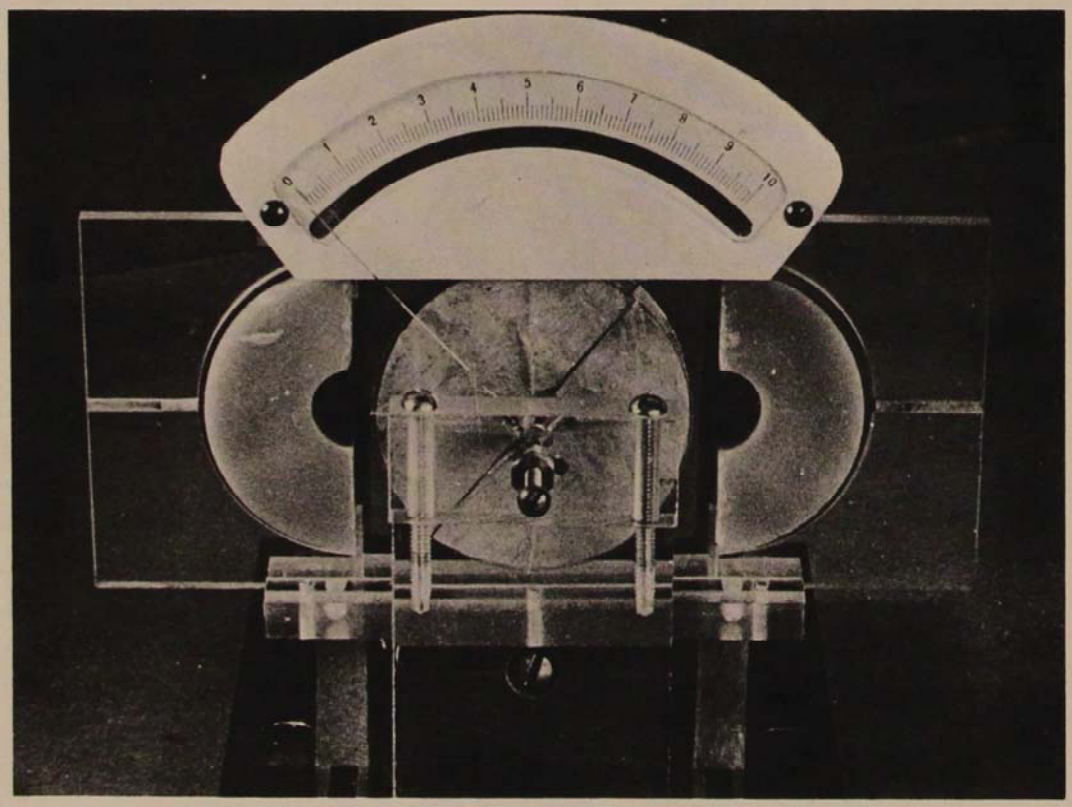

FIGURE 3. Photograph of the pointer-type meter showing the electret sections partially removed.

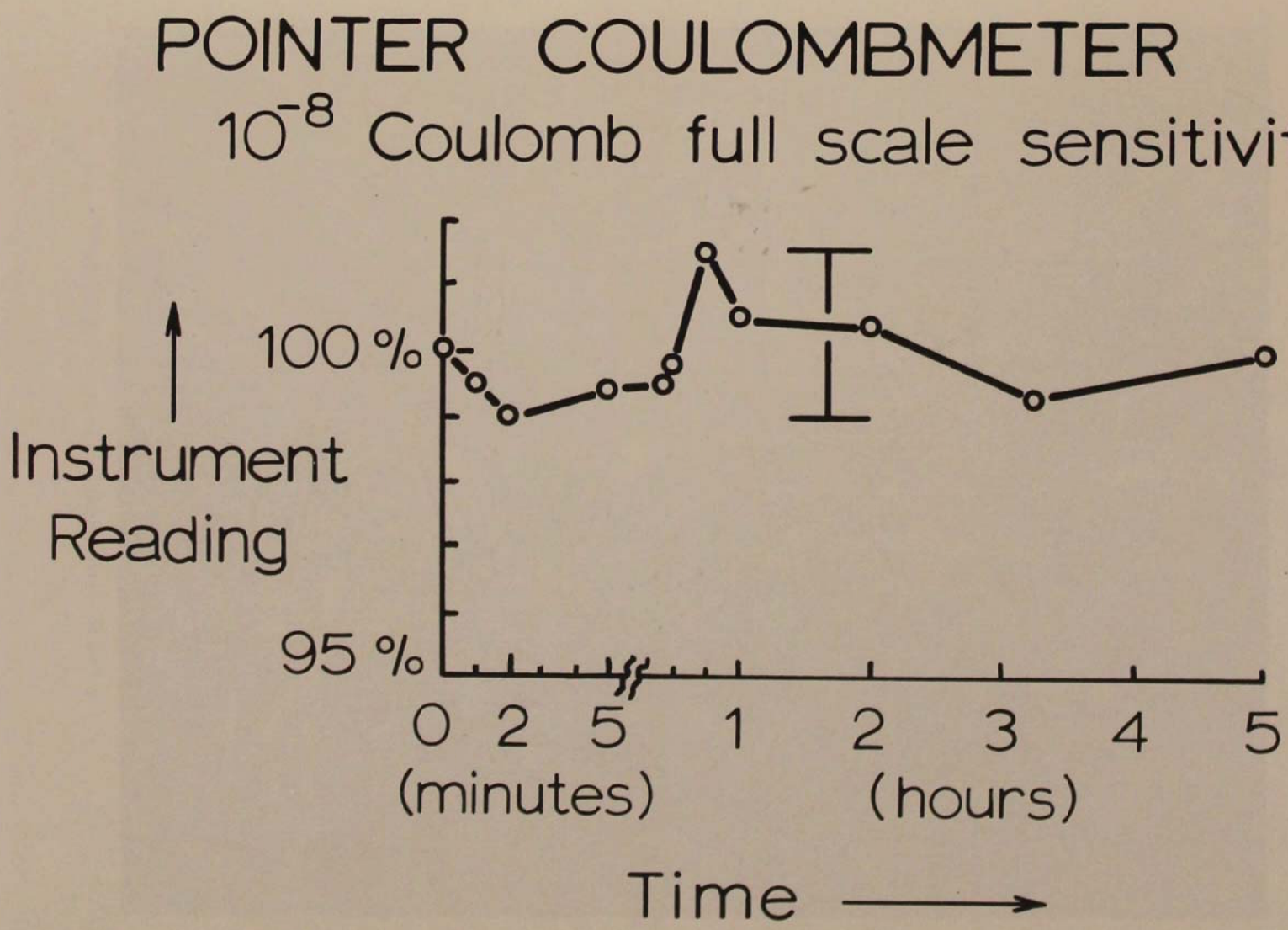

FIGURE 4. Stability curve of the pointer-type meter showing the reading over a five-hour period during which the meter was in continuous use.

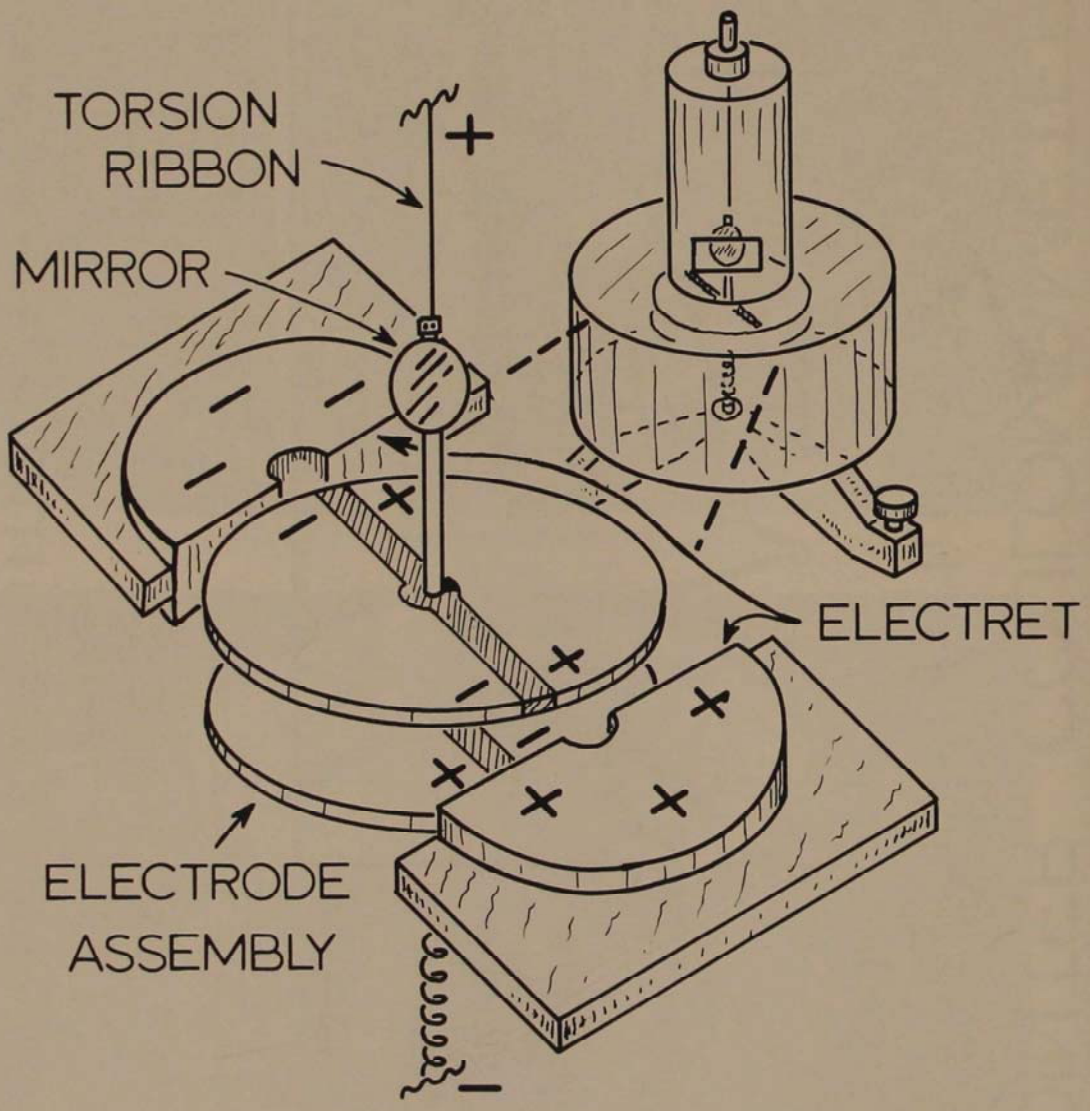

FIGURE 5. Schematic diagram of the mirror-type meter.

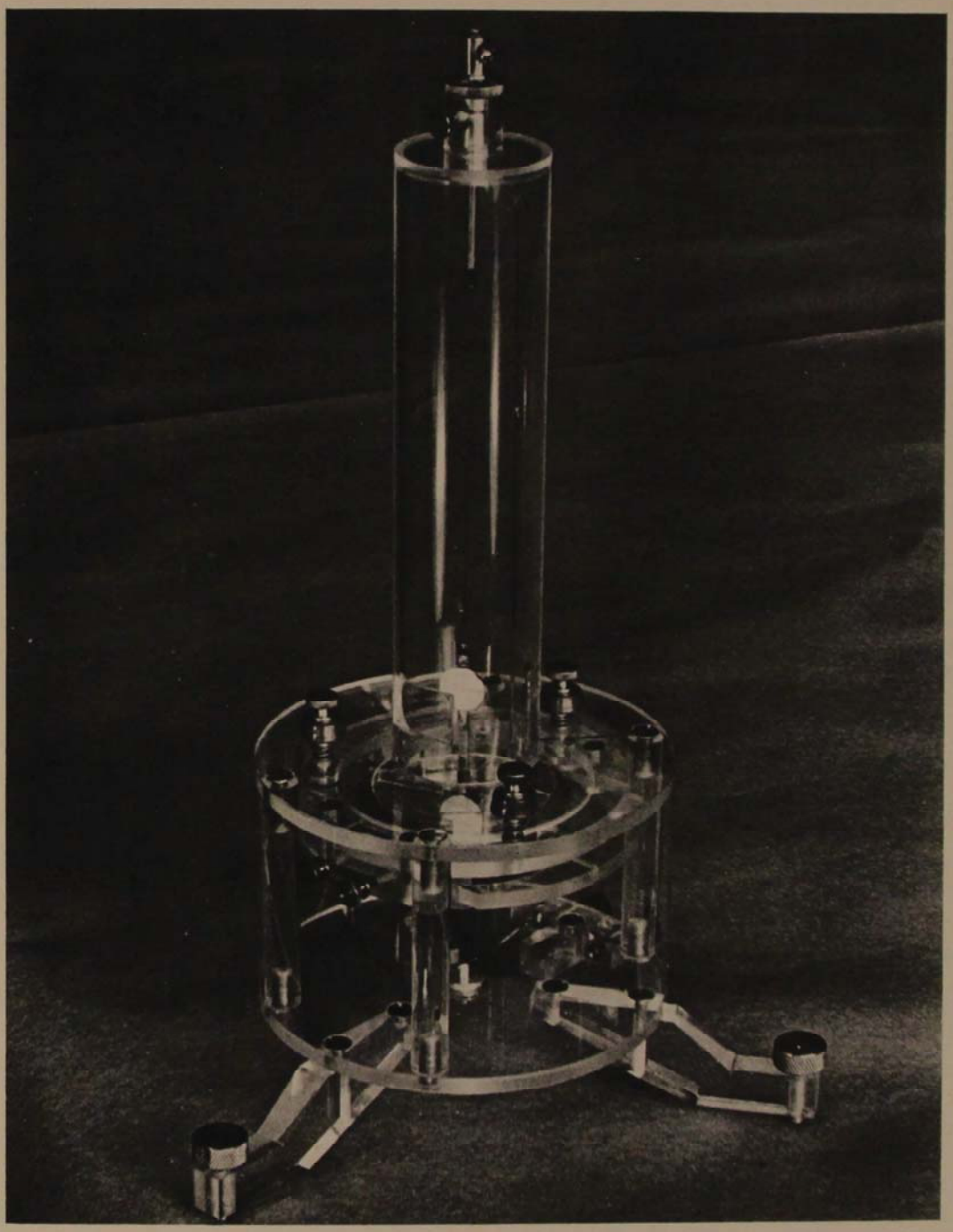

FIGURE 6. Photograph of the mirror-type meter.

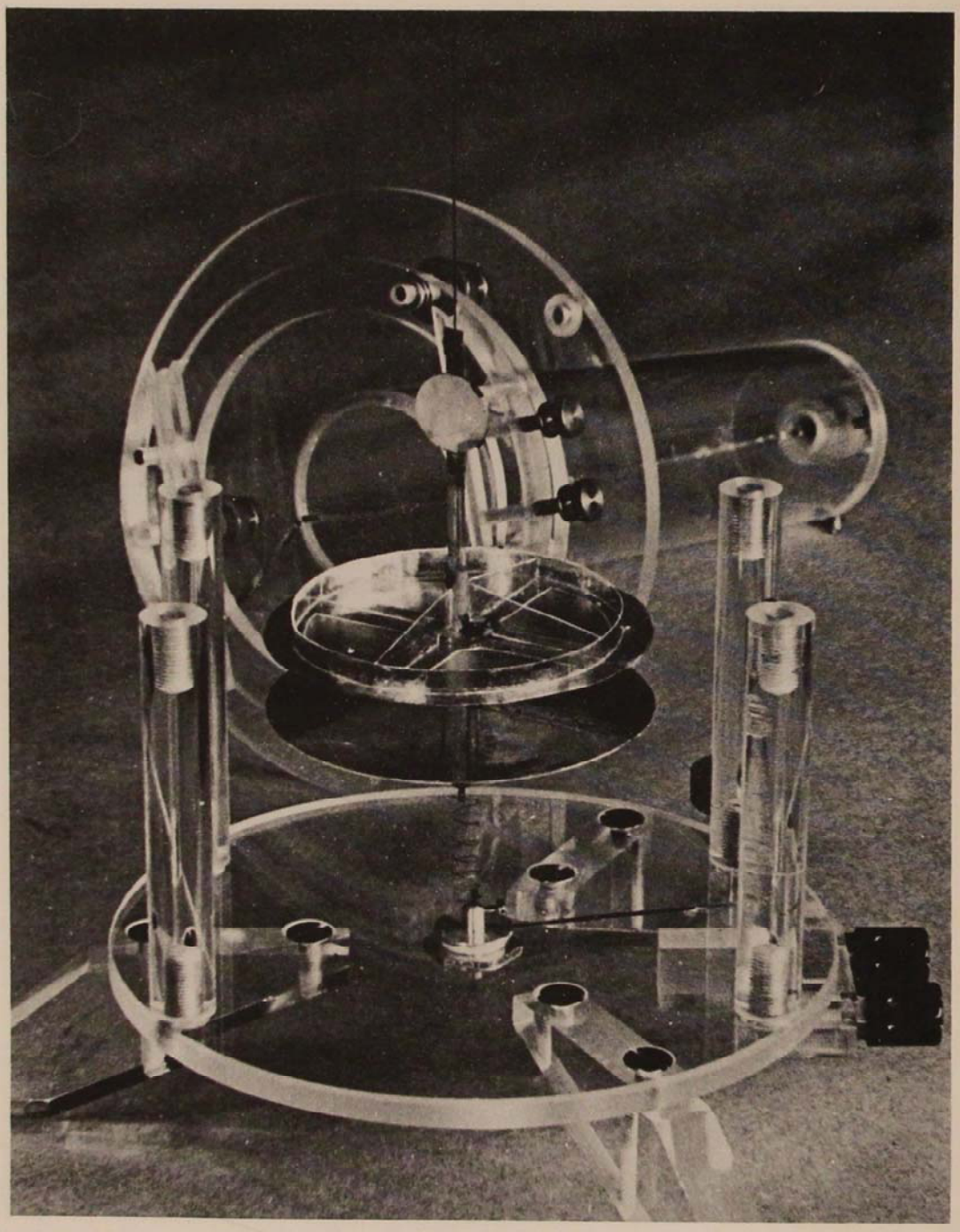

FIGURE 7. Photograph of the mirror-type meter partially disassembled to show the suspension and electrode assembly.

Acknowledgments

The authors would like to thank Mr. Jack Johnson, machinist, for his assistance in constructing the electrometers described in this paper.

Literature Cited

1. Jefimenko, Oleg. 1968. Slot effect in electret devices. *Proc. W. Va. Acad. Sci.* 40:345.
2. Jefimenko, Oleg, and David K. Walker. 1968. Force measurements on electrets. *Proc. W. Va. Acad. Sci.* 40:338.
3. Walker, David K., and Oleg Jefimenko. 1968. Electrostatic force in electret devices. *Bull. Am. Phys. Soc.* 13:618.

Gamma Photon Absorption in Natural Fibers

Richard E. McCoy, Jr., and T. J. Manakkil
Department of Physics, Marshall University
Huntington, West Virginia 25701

Abstract

Interaction of gamma photons of energies of 1.17 and 1.33 Mev from a cobalt source in a narrow-beam geometry with coir, jute, fowl feathers and cattle hair fibers has been investigated. Experimental measurements indicate that the mass absorption coefficients for the fibers are 12 to 18 percent larger than for lead at the same photon energies. The measurements seem to indicate that conventional shielding materials may not be the most economical shielding materials where space is not a constricting factor.

Introduction

The literature dealing with the characteristics of gamma-ray absorption is voluminous and covers a broad spectrum of photon energies and materials. (1) The materials for which the characteristics of gamma-ray absorption have been determined have been either the chemical elements, salts, or other inorganic materials. A search of the literature concerning the absorption of gamma-rays by organic materials reveals that the absorption characteristics of fibers from plants and animals has never been explored. Co^{60} has come into common use in both the pure and applied sciences, and is the by-product of certain nuclear devices and the interest in finding effective shielding against Co^{60} gamma-rays has increased accordingly. Gamma-rays of two energies (1.17 Mev and 1.33 Mev) are produced by this radioisotope (5).

Absorption of gamma-ray is attributed principally to a combination of four mechanisms: The photoelectric effect, Compton effect, pair production, and photonuclear reactions. Photonuclear reaction below 6 Mev are very unlikely, therefore, the latter is improbable at the lower photon energies of Co^{60} (5) and need not be considered here.

The present work was undertaken in order to determine the absorption characteristics of two animal fibers (cattle hair and fowl feathers) and two vegetable

fibers (coir and jute) for the gamma-rays given off by Co^{60}. These characteristics are compared to the three common materials used for shielding (iron, lead, and concrete).

Apparatus

In this investigation a 5 millicurie, Co^{60} source was used. The source was obtained through a commercial supplier and mounted on the end of a threaded steel pin which was screwed into the end of a ½" steel bolt. The design of the collimator incorporated the ½" steel bolt.

The source and collimator mounting was fabricated from a steel block (7.6cm x 7.6cm x 20.0cm) with a 1.27cm (½") diameter hole drilled axially through the block and was designed for easy mounting of the source.

The exit gamma-ray beam was collimated into various geometries by using different collimators made of ½" bolts which were axially drilled with holes of several diameters. These bolts were inserted in the ½" hole through the steel block mounting in the end opposite to that into which the source was mounted. A bolt with a 0.32cm (1/8") diameter hole, when selected for this experimental apparatus set up, would provide a narrow-beam geometry of 0.0004 steradian. The solid angles of the beam can be varied from 0.0004 to 0.0016 steradians.

The steel block in which the source and the collimator were mounted were completely encased in lead bricks during the experiment to prevent radiation from exiting except through the path provided by the hole drilled in the bolt.

The transmitted gamma radiation from the absorbing medium was measured by a gamma scintillation detector consisting of a 5.0cm diameter thallium—activated NaI crystal, photomultiplier and associated electronic equipment. The entire detector was encased in lead bricks to minimize the detection of background radiation by the counter.

The fibers for which the absorption characteristics were being determined were fabricated in two basic ways. The loose fibers (fowl feathers and jute) were packed in cylindrical containers of an inside diameter of 10.2cm and were carefully weighed to insure uniformity of density.

The coir (coconut fibers) and cattle hair were obtained in woven mats and sheet felt, respectively. Each fiber was cut into 10cm x 10cm squares. The squares were stacked to provide various thicknesses. These samples were easily mountable on a beam on a wooden railing.

The apparatus was carefully arranged and aligned after the manner of Bashandy (1) who used this narrow beam geometry to obtain the absorption coefficient of several of the metals. The alignment was obtained by sighting through the hole in the steel block and centering on the center of the NaI crystal. The absorbing material was aligned in a similar manner with the cylinders being mounted between two wooden rails at the appropriate height.

Experimental Procedure

The apparatus was set up as in Figure 1 and allowed sufficient time to stabilize. The background radiation was monitored before the source was removed from its storage area and set in place. The background radiation was again monitored after the measurements were completed. First, the photon intensity was measured as seen by the detector with no absorbers. Then fiber samples of definite thickness and density were interposed between the source and the detector and the transmitted photons were counted. Counts of transmitted radiation

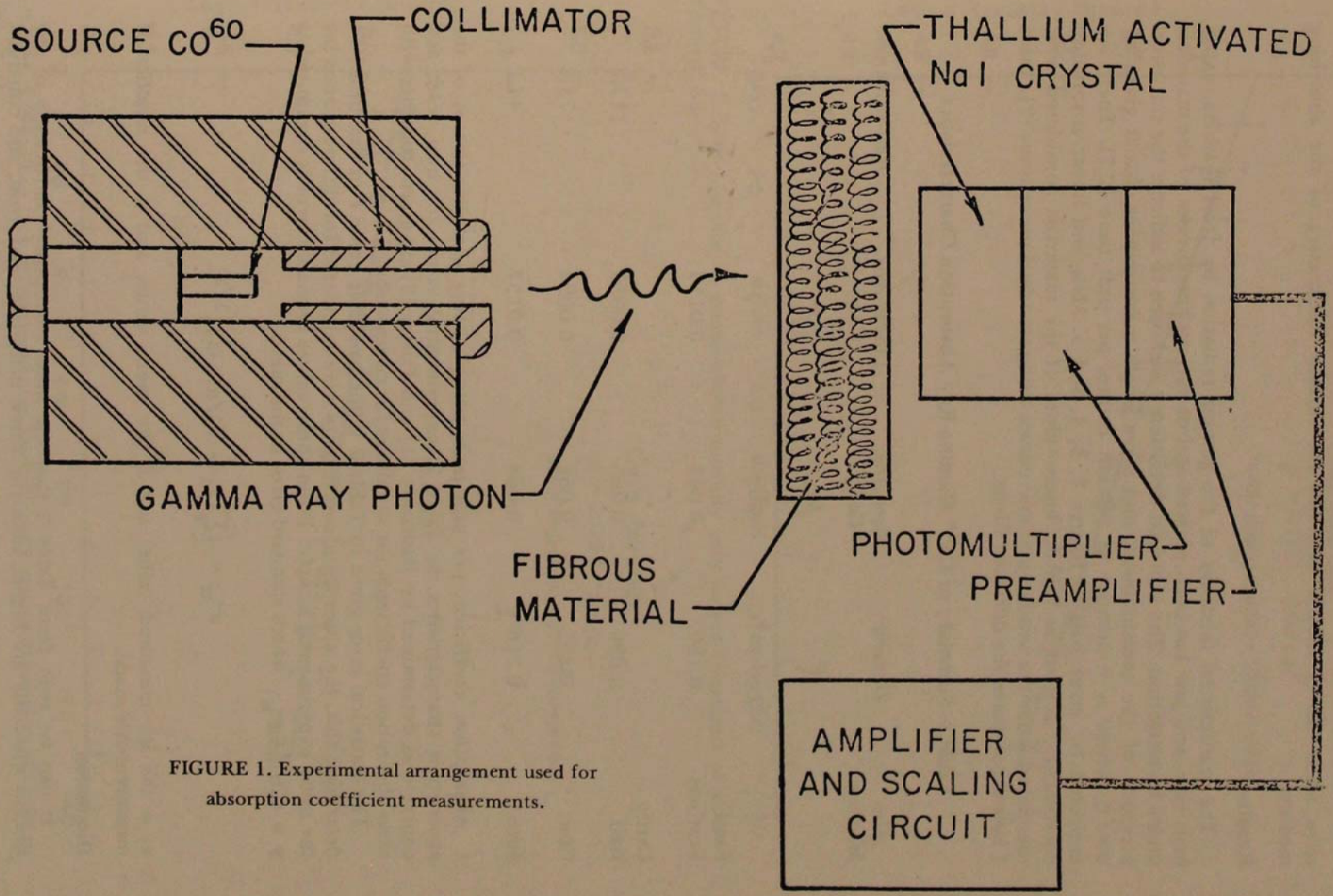

FIGURE 1. Experimental arrangement used for absorption coefficient measurements.

were made for 5 minute intervals for various thicknesses of the absorbing medium.

Results

The transmitted intensity of the gamma radiation by fowl feathers, cattle hair, coir, and jute has been plotted against various thicknesses of the materials under investigation. The standard deviation σ is chosen to indicate the statistical accuracy of the measurement, and for a single measurement this is given by $\sigma \simeq \sqrt{\eta}$, where n = number of photon counts per unit time (2,7). These are indicated by error bars in figures 2, 3, 4, and 5. Mass and linear absorption coefficients, as well as half-thickness values of the materials considered were calculated from the semilogarithmic curves using standard procedures (2). Table 1 below compares the different fibers.

Table 1. Summary of Co^{60} Gamma-Ray Absorption Characteristics

Abs. Medium	*Density* ρ	*Mass Abs. Coeff.* μ_m	*Linear Abs. Coeff.* μ	*Half-thickness* $X_{1/2}$
	gm/cm^3	cm^2/gm	cm^{-1}	cm
Fowl Feathers	0.190	0.063	0.0119	58.2
Cattle Hair	0.090	0.065	0.0059	117.5
Coir	0.152	0.062	0.0094	73.8
Jute	0.246	0.064	0.0157	44.2

Absorption coefficient per unit mass being a more useful indicator of the absorption characteristics, in Table 2, experimental values for iron, lead, and concrete as determined by Bashandy (1) and Foster (3) are given, together with mass absorption coefficients for the fibers for comparison.

The statistical error given in Table 2 is the probable error P of the mean. To determine this, the absorption coefficients were calculated for different runs for the same experimental sample. From these values probable error is computed as $P = 0.6745\sigma_m$, where standard error in the mean

$$\sigma_m = \left[\sum_i (x_1 - \bar{x})/n(n-1)\right]^{1/2}$$

x_i is the *ith* measured value, and $\bar{x}$ the mean value, and n the number of measurements made.

Discussion

It can be seen from Table 2 that the mass absorption coefficients of the fibrous materials are higher than the three materials, lead, iron, and concrete,

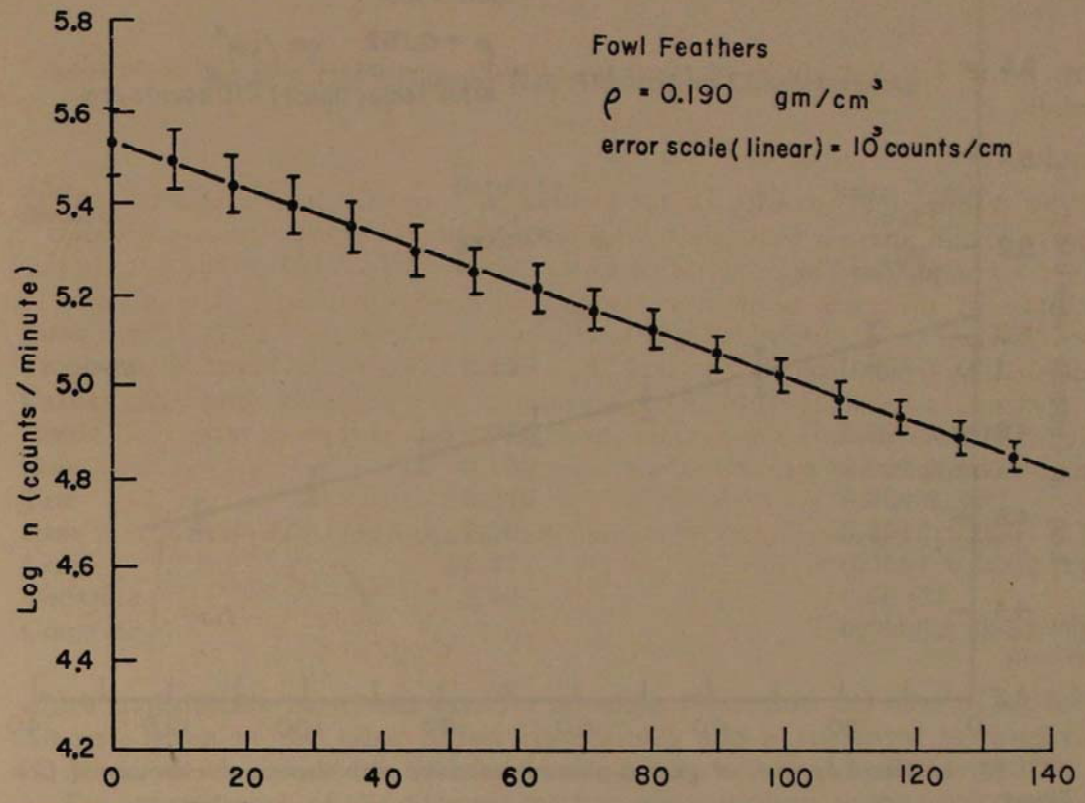

FIGURE 2. Semi-Log plot of gamma-photon intensity with various thicknesses of Fowl Feathers.

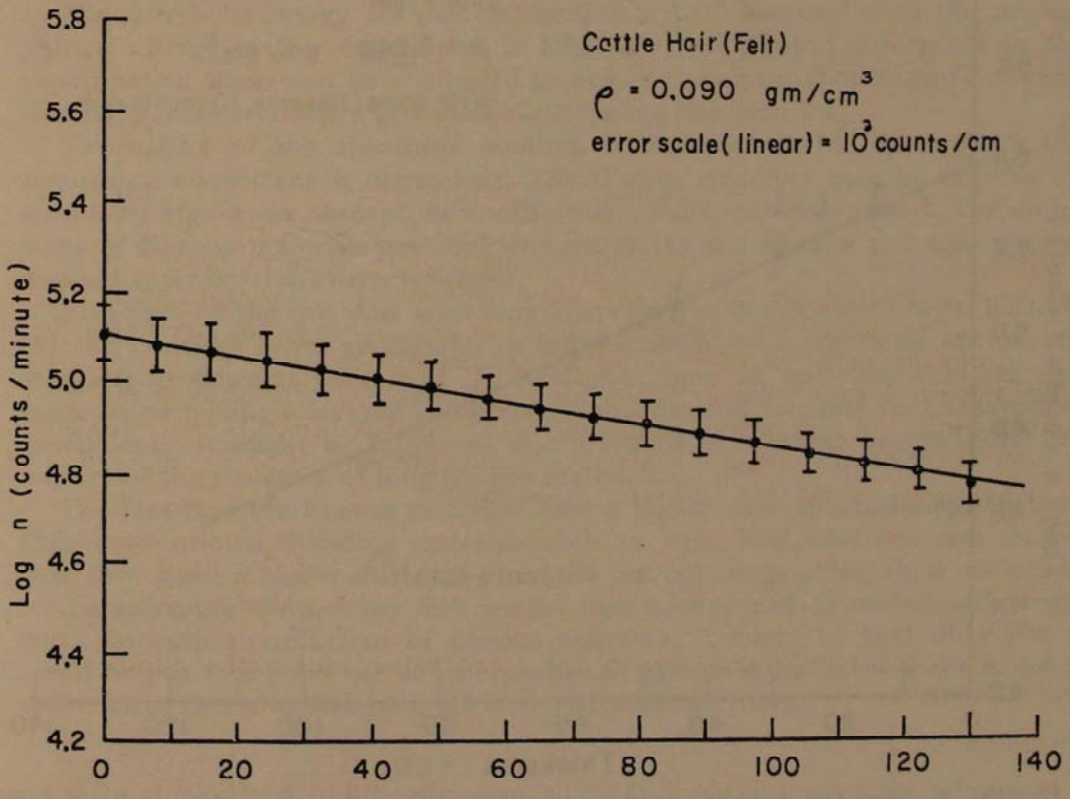

FIGURE 3. Semi-Log plot of gamma-photon intensity with various thicknesses of Cattle Hair (Felt).

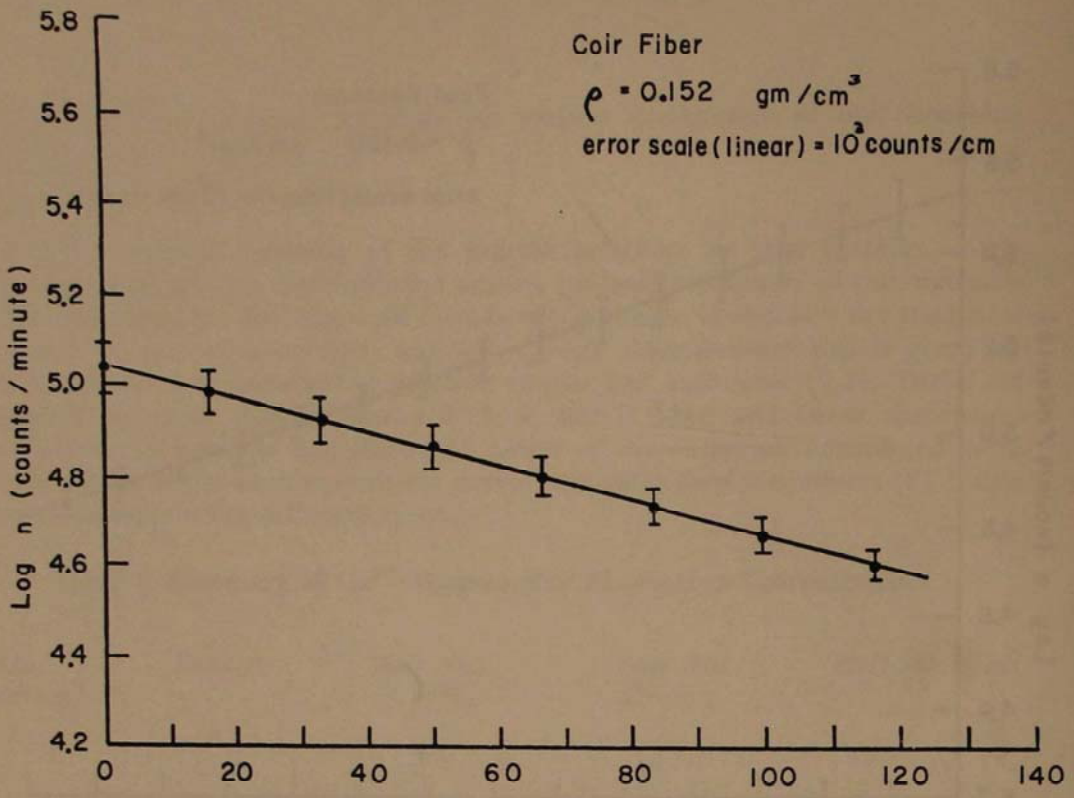

FIGURE 4. Semi-Log plot of gamma-photon intensity with various thicknesses of Coir Fibers.

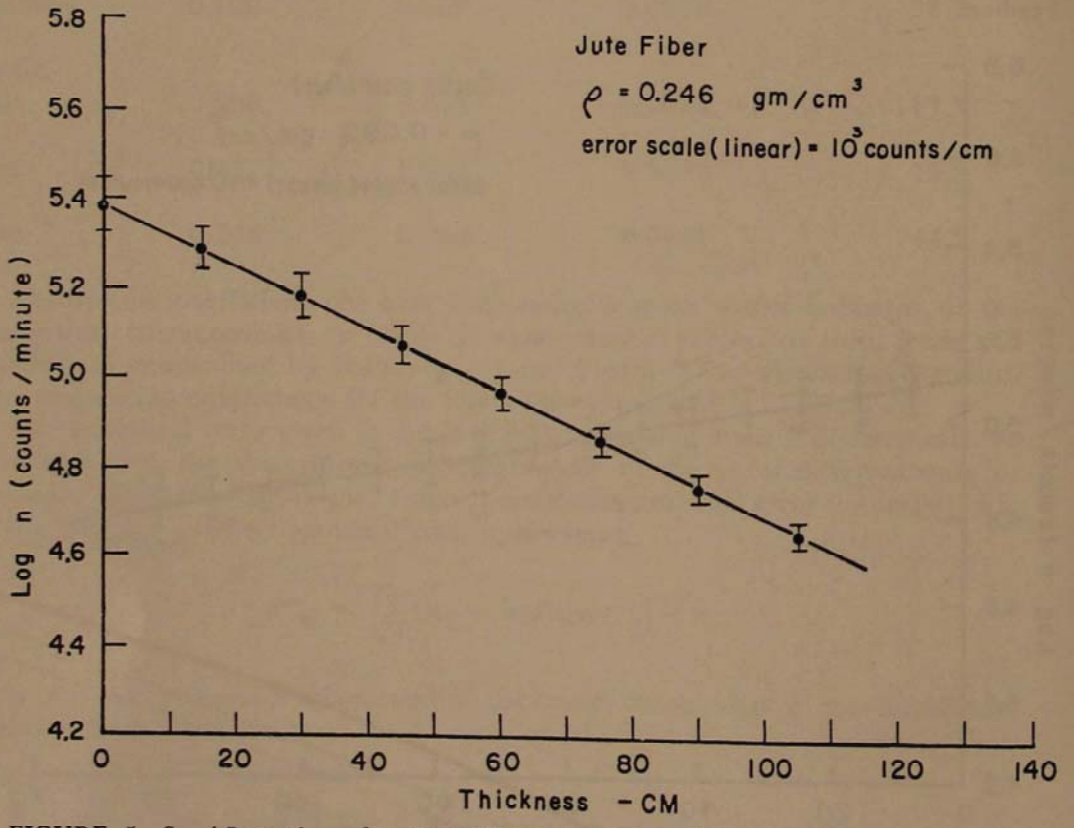

FIGURE 5. Semi-Log plot of gamma-photon intensity with various thicknesses of Jute Fiber.

Table 2. Co^{60} Gamma-Ray Absorption Characteristics

Abs. Medium	Density ρ gm/cm^3	Mass = Abs. Coeff. μ_m cm^2/gm
Fowl		
Feathers	0.190	0.063 ± .001
Cattle		
Hair	0.090	0.065 ± .003
Coir	0.152	0.062 ± .002
Jute	0.246	0.064 ± .002
Iron	7.20	0.0513 ± .0001 (1)
Lead	11.37	0.0554 ± .0002 (1)
Concrete	2.40	0.06 (3)
Concrete	?	0.0508 ± .0051 (1)

which traditionally have been used for shielding. Please note the value of μ_m for concrete given in the table differs considerably and is attributed to density. However, we were unable to find the density of concrete used by Bashandy.

The amount each of the different mechanisms contribute to the total absorption cross-section depends upon the energy of the gamma-ray photon and the nature of the absorber.

The threshold energy for pair production is 1.02 Mev and since the average photon energy in this experiment is 1.33 Mev, the photon absorption in the experimental fibers can be attributed primarily to pair production and compton scattering, with secondary processes contributing less than 2%.

The nature of the absorbing medium is the other factor upon which the absorption coefficient is dependent. The fibrous structure may be the clue to unusually high mass absorption coefficients of the materials tested. The molecules of fibrous materials are long structures (6) and layered and may possess unusual antennuation characteristics.

Although he did not deal with long fibers such as in this experiment, Rohach (4) did consider other geometries in his discussion of methods of optimizing shielding in shipping containers. In Rohach's paper an optimum absorber was made by providing a layered geometry of absorbers of two different absorption coefficients. It might be suggested that a similar phenomena occurs in the geometry of the structure of long fibered materials.

The fact that the fibrous materials have a higher mass absorption coefficient than conventional shielding materials such as, iron, lead, and concrete means that they have a higher shielding potential per unit mass. Also, these materials are considerably cheaper per unit weight than iron or lead. Considering the high mass absorption coefficient of fibrous materials, it might be that these fibers could be put to a good use as an absorber of gamma radiation if space is not a constricting factor in designing effective radiation shielding.

Acknowledgments

This work was partially supported by the Marshall University Research Board through a grant from the National Science Foundation. The authors also wish to thank Dr. Donald C. Martin, Marshall University, for his invaluable assistance during the course of this investigation.

Literature Cited

1. Bashandy, E. 1962. Experimental Determination of the Absorption Coefficients of Gamma-Rays through Different Barriers. *International Journal of Applied Radiation and Isotopes.* 13:173-78.
2. Chase, G. D., and J. L. Rabimourity. 1968. Principles of Radioisotope Methodology. Burgess Publishing Co., Minneapolis, Minn. pp. 75-108 and pp. 215-33.
3. Foster, Bruce E. March, 1968. Attenuation of X-Rays and Gamma-Rays in Concrete. *Materials Research and Standards.* 8:19-24.
4. Rohach, Alfred E. 1967. Weight Optimization of Gamma-Ray Shields Using Layered Media and Spherical Geometry. *Nuclear Science and Engineering.* 27:464-67.
5. Sakae, Shimizu, Tetsuya Hanai, and Sunao Okamoto. 1952. The Absorption of Gamma-Rays from Co^{60}. *Physical Review.* 85:290-94.
6. Sproull, Wayne T. 1946. X-Rays in Practice. McGraw-Hill Book Co., New York. pp. 530-34.
7. Squares, G. L. 1968. Practical Physics. McGraw-Hill Book Co., New York. pp 7-56.

Geology and Mining Section

Appalachian Energy Resources for the Future*

John M. Dennison
Geology Department
University of North Carolina
Chapel Hill, North Carolina 27514

Abstract

The first major American production of coal, natural gas and oil was from the Appalachian structural basin, but just the coal reserves will be spared depletion before 2000 A.D. Only in southern West Virginia and Virginia are there large quantities of low-sulfur coal. Probably no important oil fields will be discovered, because the carbon ratio decreases both with depth and eastward. Best hopes for new gas are in the area from Kentucky northward to New York, in potential reefs of the Silurian and lower Devonian Systems, Silurian sandstones, Cambrian and Lower Ordovician dolomites, and in the basal clastics of the Cambrian System, plus the Paleozoic rocks of the Warrior basin of Alabama. Nearly all the potential major hydroelectric sites have been developed which will not be faced with serious problems of flooding of towns or destroying recreational wilderness. Uranium resources will most likely be found in Paleozoic fluvial strata. The most favorable stratigraphic units for uranium prospecting are the Devonian Hampshire and Catskill Formations from New York to Virginia, the Mississippian Mauch Chunk and Pennington Group from Pennsylvania to Tennessee, the Pennsylvanian Pottsville Group, especially in Alabama Virginia and southern West Virginia, and the Pennsylvanian-Permian Dunkard Group in West Virginia. The best potential geothermal power area east of the Mississippi River is associated with Eocene igneous intrusions and thermal spring activity near Hot Springs, Virginia.

The Federal government should develop a firm policy of energy priorities, and Appalachian resources should be utilized in a manner consistent with these national goals.

Introduction

The Appalachian region was the birthplace of the energy industry in America. The first American coal production (1761) was at Pittsburgh, followed soon by Pennsylvania anthracite fields. Fortunately the most urbanized areas of the

*Opening address, Geology and Mining Section of West Virginia Academy of Science, Fairmont, West Virginia, April 6, 1973.

country were near the anthracite mines, relatively sparing those cities of an early pollution problem. Coal fueled the rail transportation industry, and the coal fields of southern West Virginia and adjacent Virginia and Kentucky became the basis of a large export business centered at Norfolk. Today this Norfolk complex forms the only significant export of American energy on the overseas market. Natural gas was known in pioneer times (Burning Springs discovered in 1773 near Belle, Kanawha County, West Virginia) and early gave rise to commercial gas production (Ruffner well drilled 59 feet in 1808) to fuel the salt works at Malden, near Charleston. This technology was hired by Pennsylvania interests to drill the Drake well in 1859 at the oil springs near Titusville. Folk stories have reached almost legendary proportions concerning the rapid expansion of the industry, with the birth of many major petroleum companies in the Appalachians, the great Bradford field, the Burning Springs field, and the practical application of the gravitational (anticlinal) theory of petroleum accumulation in the 1880's by I. C. White. Water power was early developed to aid transportation and operate pioneer grain mills. Hydropower use grew in the Appalachians until the Tennessee Valley Authority region became the most intensively developed water-management domain in the world.

The present paper assesses the Appalachian region's future in helping meet the energy needs of eastern United States.

Petroleum

Depletion of shallow oil and gas has made production more costly, but soaring fuel prices have brought resurging interest to drill deeper and to accept smaller gas pools for commercial development as population increases and need for pollution control raises the demand for clean heating fuel. Drilling will begin to test the deepest parts of the basin. The 19,537-feet depth achieved by December, 1972, in a Columbia Gas Transmission Corporation well in Mingo County, West Virginia, is the greatest depth ever drilled in northeastern United States. The Appalachian basin is not bottomless, however, and fuel needs will continue to rise.

Oil

The carbon ratio of the Appalachian region argues against significant new oil finds. This concept, developed in 1915 by David White, predicts that oil almost never occurs in strata near localities where the percantage of fixed carbon in coaly strata exceeds about 60-65 percent. The increase of carbon ratio beyond this critical value eastward in the Appalachian basin, along with the increase of carbon ratio with depth (Hilts law), suggests that all except the shallow oil has been destroyed by incipient metamorphism, which cracked the oil into smaller hydrocarbon molecules to form methane gas. The hundreds of thousands of wells drilled in the Appalachians have probably chanced upon all of the large oil pools originally there.

The value of Bradford-quality crude oil rose to $5.48 per barrel by the end of 1972, the highest price since 1920.

Natural Gas

Methane may occur associated with oil, either dissolved in it or as a gas cap in the pools, or it may occur free from oil and float directly on the water column in reservoir rocks. This gas itself seems to be decomposed by deep burial and metamorphism, perhaps breaking down into carbon dioxide and water as rocks

tend to become deoxygenated and lose their hydroxyl ions with increasing metamorphism. When the carbon ratio reaches 70 percent the rocks no longer generally contain commercial methane production. The Rockingham County, Virginia, Oriskany gas field was from an area with a carbon ratio of 85 percent; at about this degree of metamorphism rocks begin to show fracture cleavage in shaly beds. The eastern and deeper Appalachian wells yield gas discouragingly low in BTU content, although this lower quality gas can be blended with better gas from Louisiana and Texas to make a fuel of consistent and useful quality. The famous Oriskany Sandstone gas fields are now nearly all discovered and essentially depleted; these sufficed for two or three decades as the principal gas supplier of the Appalachians.

The best hopes for new Appalachian gas fields include the following: 1) the Devonian delta beds of the western Catskill region of northeastern Pennsylvania and New York in marine sandstone horizons older than the production from the same facies farther west; 2) scattered reefs in the Onondaga Limestone, extending production from a reef situation discovered in 1967 in south-central New York; 3) hoping to find favorable reefs in the Helderberg and Niagaran strata, especially on the north and west slope of the sedimentary basin located under the Appalachian Plateau in New York, Pennsylvania, Ohio, West Virginia and Kentucky; 4) Silurian sandstones, notably the Tuscarora-Clinch-Medina Sandstone (and equivalent Clinton sands of Ohio) at the base of the Silurian, as well as the younger Keefer (Big Six), Williamsport (Newburg), and associated sandstones that probably came mostly from a southern source located in southwest Virginia and possibly Tennessee, depositing marine sands concentrated in southern West Virginia; 5) Cambrian and Lower Ordovician dolomites, especially seeking traps at the unconformable top of or within the Knox-Beekmantown strata; and 6) in the basal clastics (Weverton-Unicoi, Antietam-Erwin, and Rome Formations) of late Precambrian and Lower Cambrian age. Categories 2, 3, and all but the basal Clinch-Tuscarora Sandstone in 4 can be developed only in the Appalachian basin from New York south to West Virginia and Kentucky, because farther south the unconformities associated with the Middle Devonian Wallbridge discontinuity stripped off nearly all beds of Middle Silurian through Lower Devonian age. Additional consideration of many of these possibilities is presented by Dennison (1970, 1971) and by Weaver, Calvert, and McGuire (1972). Deep drilling in the "Rome troughs" of Kentucky and West Virginia and possible troughs northward to Pennsylvania may well find that the basal Cambrian strata in these troughs are not all marine sandstones, but instead are partly non-marine beds accumulated in fault-bounded basins as the Proto-Atlantic Ocean opened in Late Precambrian time, analogous to the Triassic basins formed in eastern North America as the continental drift mechanism began to open up the present Atlantic Ocean basin. The Warrior Basin of Alabama has at least 25,000 feet of strata with largely unexplored reservoir possibilities for gas and possibly some oil ranging in age from Cambrian through Pennsylvanian (Pottsville). The Warrior Basin extends southward tens of miles beneath the Coastal Plain and it is probably deformed by both the southwesterly trending Alleghany orogeny fold trend and by the easterly trending and slightly earlier Ouachita fold trend recently identified in southeastern Alabama mapping by Thomas Carrington (1972).

Appalachian gas has been usually associated with anticlinal folds or updip pinchout at unconformities or facies change. Some geologists have pointed out that the structural patterns in carbonates of the Valley and Ridge Province are

very similar to the geology associated with the Foothills gas production in thrust-faulted structural traps in Alberta, except that erosion has exposed the structural patterns at relatively greater depths in the Appalachian structural sections. If the Valley and Ridge structures are stacked by imbricate faulting there is possibility of gas traps in folds beneath faults.

By the end of 1972 the price of new gas rose to 50 cents per thousand cubic feet, nearly double the value of 30 cents which had remained fairly steady during the period 1955-1970. Further rise in price will occur as the fuel shortage worsens, and renewed drilling will develop small fields which were previously not economically profitable.

Coal

Coal reserves are sufficient to meet the demand for at least a couple centuries, considering population projections, changing technology of production and consumption, and anticipating more stringent regulations on environmental protection during the mining operations. Coal may be the key to furnishing the bulk of our energy needs for electric power until the technology and reactor site litigation is settled to supply adequate nuclear power production by perhaps 1990. The major factor with coal is pollution—both at the mine and at the power plant. Modern laws concerning mine sealing and strip mining should adequately control the sulfuric acid and limonite stain stream pollution from new mining. Geologic factors are being considered more in mine safety, such as prediction of rock-fall danger sites near sandstone channel margins in the roof beds. Procedures can be developed at moderate cost for safer disposal of shale wastes, avoiding the hazard of dam bursts like at Buffalo Creek, West Virginia, in 1972.

Coal will meet a higher proportion of our energy needs, provided pollution can be controlled at the power plant. Fly ash can be collected by electrostatic precipitators, but I have seen a number of instances in West Virginia and elsewhere where this debris is then thrown into streams or in unmanaged and unsightly dumps along the highways.

Sulfur emission control is a different matter. The wet scrubbing methods of cleaning stack gases are too costly and inefficient to meet the impending legal regulations on air pollution. There is serious engineering talk now of abandoning stack scrubbing as the usual method, and instead to clean the coal by chemical treatment of a slurry before combustion. Technology apparently branched in the wrong direction in its haste to develop sulfur emission control. The coal technology industry says it cannot clean up the sulfur pollution to meet the 1975 deadline in the energy crisis if air pollution control laws are rigidly enforced.

Another way to cope with sulfur emission is to mine only low sulfur coal. Here the Appalachian coal fields are very important. The Pocahontas coal fields of southern West Virginia and adjacent Virginia and a bit of Kentucky are the largest reserve of low-sulfur bituminous coal in the nation. The southern West Virginia coal fields boast 43 minable seams and had 65 billion tons of coal containing less than 1.5 percent sulfur at the inception of mining operations (Barlow, 1971, p. 7). Quality of the Virginia coals is described by Brown and others (1952). One problem of national priorities should be noted. These very coals which can do the most to aid air quality in the eastern part of the country are also our principal export coals. We need the coal here, yet to stop export would hurt our balance-of-trade deficit on the international money market, since this is about our only remaining source of energy export. In 1971 over 57 million tons of coal were shipped from the U.S.; worth over $900 million, most

of this left via Norfolk and represents Appalachian low-sulfur coal. There are smaller low-sulfur reserves in Alabama, but these are too remote from the major markets, because coal cost roughly doubles with every 400 miles of rail transportation. Another low-pollution type is anthracite, but its future is grim. The limited quantities of anthracite remaining in the Virginias, Maryland, and Rhode Island are all in too thin beds, too structurally deformed, or are too high ash to be mined economically. The great anthracite fields of eastern Pennsylvania are already approaching depletion, so they are of trivial consequence in our total energy needs.

Developments in improved electrical insulation and higher voltage transmission capability has enabled industry to build power plants in the coal fields and ship the electricity by wire rather than the coal by train. Doubling the voltage roughly doubles the distance electricity can be transported economically. This helps avoid pollution in urban areas, but it also tends to add more pollution to the already blighted Appalachian area.

Hydroelectric Power

Total hydroelectric power in the Appalachians is only about one-third developed, but it will probably never be more than half developed. Hydroelectric generation produces only 4 percent of our present national energy budget, and will decrease in the future as nuclear power plants are built. Thirty-seven large sites already developed in the Appalachian region with individual capacities exceeding 50,000 kw are producing over 6 times the energy of 33 other smaller hydroelectric sites. Large hydroelectric projects are the obvious way to develop this energy resource with economic efficiency, and some 60 sites of over 50,000 kw remain undeveloped in the Appalachians (Johnson, 1968). Total hydroelectric energy potential of the Appalachians is nearly 16 million kilowatt hours.

The extent of development varies throughout the region, and for several reasons. Tennessee has the largest hydroelectric complex in the Appalachian states with over 71 percent of its total potential developed, largely as a consequence of the Tennessee Valley Authority. This strong government agency had broad authority for a vast program of land condemnation in an area where the economic worth of the displaced people was small and where history has now clearly demonstrated that introduction of widespread electrical energy greatly stimulated the economy of an underdeveloped region. Without TVA we probably could not have attained our nuclear capability during World War II, since Oak Ridge uses far more power than many large cities in America. The power needs of the TVA region have grown so much that only a fourth of the total TVA electricity is produced by hydropower. Most of the remainder is manufactured in coal-fired generating stations, making the TVA arm of the government the largest consumer of strip-mine coal in the nation. Two nuclear power plants are in operation and TVA has now entered into construction agreement with the AEC to build the first commercial-scale breeder reactor in the United States.

In the central Appalachians there is only modest hydroelectric development. West Virginia hydroelectric development has been handicapped by cheap coal, by a more pressing need for flood control (which means that the reservoirs should be kept nearly empty, for catching capacity, rather than nearly full for optimum hydroelectric generation), and by a desire to keep the mountain beauty unspoiled.

Every major Appalachian power site in Pennsylvania remains undeveloped. The reason is chiefly cost-benefit ratio: that is, it would be prohibitively expen-

sive to buy the land for flooding. Most of the really big power sites are in the water gaps of the Susquehanna River drainage system, and the resulting furor of displacing cities along that river system or the upper Ohio River drainage system would wisely prohibit the construction of dams. The floods of 1972 make clear another need in Pennsylvania. If dams are built, there will now be a public demand for flood control dams (which are more readily financed through federal taxation support of the Corps of Engineers). Flood control dams are inefficient for electrical power production. Small flood control dams can be built in the upper tributaries where there are fewer people, but even there the conservationists may have a valid case for preserving wilderness areas for the total public good. Nearly all major dam projects in the Appalachians, whether for flood control or hydro-electric power, are tied up in environmental litigation, and there is every indication that this factor will prohibit development of most of the remaining power sites.

Hydroelectric power has one very important function which cannot be readily duplicated. It is the one energy source which can be instantly started to shave peak electrical loads; indeed the turbines of TVA are computer operated. Nuclear and steam plants are most efficient for steady loads and lack instant response to emergency needs. Most new hydroelectric plants have associated pumped storage capacity to improve their efficiency. While total electrical needs are adequately met by other sources, like in the late night, the electricity from turbine generators can be used to pump water to high storage reservoirs for use later in the day to shave off peak electrical loads. This amounts to a sort of "battery" for mechanically storing electrical energy for alternating current distribution. A given amount of electricity can be generated from a large water volume with a low hydrostatic pressure head, or from a small volume at high pressure from a pump-storage reservoir. Raccoon Mountain in the TVA system and the proposed Rowlesburg project in West Virginia are pump-storage energy systems.

Some advanced planners are extending this concept even further. They envision shafts up to a mile deep, with water falling down them turning small turbines at very high pressure, with an underground catch basin at the bottom. This would be a peak-load device of huge proportions using nuclear power to pump the water back up to ground level at hours when electrical needs would be more than adequately met by nuclear generators. Schemes such as this are off into the next century, but when they happen stratigraphic and engineering geology will be important considerations in these power plant developments. The relatively simple geology of the Appalachian Plateau will favor location of such developments there.

Nuclear Fuel

The Appalachian region has never produced commercial uranium for nuclear power, but there is renewed interest in the possibility. During World War II and shortly thereafter a detailed search was made for commercial quantities of uranium in the Chattanooga Shale. In terms of total tonnage of uranium this is our largest national reserve, but the concentration is at best only about a hundreth of that necessary for present economic development. The best concentrations are in the upper five feet of the Chattanooga Shale in the Highland Rim area of the Appalachian Plateau in Tennessee (Conant and Swanson, 1961).

Other uranium shows have been reported in Pennsylvania in the Devonian Catskill Formation and at Jim Thorp in the Mauch Chunk Formation

(McCauley, 1961; Klemic, 1962). A serious test adit has been made near Jim Thorpe, where the uranium is a roll-type occurrence probably formed by a geochemical cell in a fluvial sandstone channel. Some 300 tons of ore were mined in this only commercial uranium attempt in the Appalachians.

Most large commercial uranium deposits in the United States are the Colorado Plateau and Rocky Mountain roll-type deposits formed in geochemical cells acting on a protore of arkosic, carbonaceous or pyritic, fluvial sandstone. Only exceptional deposits exceed 1 percent uranium content even in the orebody.

The Atomic Energy Commission is summarizing existing knowledge of the stratigraphy, sedimentology and mineralogy of fluvial sandstones in eastern United States. As part of this study I considered 22 fluvial or possibly fluvial stratigraphic units for uranium protore potential (Dennison and Wheeler, 1972). The most favorable stratigraphic units for Appalachian uranium exploration are the Devonian Hampshire and Catskill Formations from New York to Virginia, the Mississippian Mauch Chunk and Pennington Group from Pennsylvania to Tennessee, the Pennsylvanian Pottsville Group (especially in Alabama, Virginia, and southern West Virginia), the Pennsylvanian-Permian Dunkard Group in West Virginia, and the Triassic basins of the eastern Appalachians.

We are all counting on nuclear energy to bail us out of the energy debtor's prison, but at present the United States has only half the high-quality uranium ore potential reserves to meet our needs until early in the next century, by which time breeder reactors hopefully will be developed sufficiently to permit using lower grade ores and diverting some of this breeder reactor energy to mine and refine low-grade uranium bodies.

Geothermal Power

Geothermal power generation depends on finding a large temperature difference between the ground depths or hot springs and the cooler temperature at the ground surface. This energy potential is most frequently mentioned in connection with hot springs and geysers associated with volcanic activity in the Rocky Mountain and Pacific Coast states. The only significant geothermal potential site east of the Mississippi River is in the Appalachians, marked by a cluster of thermal springs centered at Hot Springs, Virginia, with a maximum temperature of 106°F. They are thought by some to arise from ground water circulating upward along faults. Fault patterns are not clearly developed, however, and indeed the structure does not differ greatly in those counties with thermal springs from other areas of the Valley and Ridge Province. Work done largely at the University of North Carolina has related this bull's-eye cluster of thermal distribution to possible residual heat from a swarm of Eocene andesitic dikes (Fullagar and Bottino, 1969) cropping out in nearby Highland County, Virginia. We think the major pluton, solidified but still cooling, may lie farther south with residual heat warming ground waters in Bath and Alleghany counties, Virginia, and parts of Monroe, Greenbrier, and Pocahontas counties, West Virginia (Dennison and Johnson, 1971). Hopefully, industrial interests will investigate this more thoroughly. Steam is not absolutely necessary to generate geothermal power, since mere hot water passed through a heat exchanger can convert a fluid like Freon to gas to run a turbine and then be condensed for recirculation. This geothermal potential in Virginia and West Virginia is perhaps small, but it is the best we have, and it certainly deserves closer study as part of our national inventory of energy resources.

The Hot Springs, North Carolina, and Warm Springs, Georgia, sites lack so

large a cluster of springs, but they too should be investigated more thoroughly to establish the heating mechanisms and evaluate their potential for geothermal electricity production.

Solar Energy

With standards of technology now achieved or likely to be reached in the next decade, solar energy will certainly have less than 1 percent input into the Appalachian energy system. Solar panels for electrical production are suitable only for specialized needs backed by high capital investment, such as space stations, microwave relay towers, and weather stations at sea. The most promising use is for direct solar radiation absorption by appropriate fluids to supplement home heating. This is not economical now, but is worthy of consideration as natural gas reserves become depleted as the best source of clean heating fuel. The high investment cost of a second home heating system will discourage its installation, even if long range savings can be demonstrated.

The Appalachians have an unusually high percentage of cloud cover, simply because they are mountains impeding the passage of prevailing westerly winds. We should wait until the clear Southwest has more successful solar electricity and heating experience before building up our hopes in the Appalachians. The heavy industrial development of the most densely populated parts of the Appalachian region blots out effective solar input by a too common smog cover. Uncontrolled stack emissions from electric power plants in the coal fields have the same effect in certain less densely populated areas.

Underground Fuel Storage

Natural gas is the ideal home heating fuel, but gas is not responsive to peak loads resulting from cold snaps because it cannot be transported fast enough from the major production areas of Texas and Louisiana. The northeastern states produce only a tenth enough gas for their own consumption, but these earliest developed, and now depleted reservoirs of the Appalachians are used to store gas brought in from the Gulf Coast during the summer and pumped underground into Appalachian reservoirs near to the urban centers of consumption. Underground reservoir capacity is now developed to store about 40 percent of a year's supply, a major factor in smoothing out peak loads in gas consumption.

Very little of the projected imports of liquified natural gas (LNG) from the Middle East or Africa will be stored in these reservoirs; rather it will probably be mostly used for direct consumption as the cryogenic tankers are unloaded near the eastern megalopolis.

Underground storage reservoirs may be specially developed in the future in the Appalachians to rebuild a large national stockpile of imported oil for national energy and defense emergencies. Such a scheme is, of course, dependent on the willingness of foreign interests to sell us the crude and will be a costly drain on the national economy. Underground oil storage near the eastern ports could best be developed by modifying depleted oil or gas reservoirs, or in geologically tight structural traps which were for some reason barren of combustible hydrocarbons. Large-capacity storage facilities are probably cheapest underground, and they certainly are much safer from potential enemy attack.

Need for National Policy

The United States is engaged in a real struggle for energy and economic vitality. We here in 1973 may well have the highest energy standard of living the

world will ever know in its entire history. Our economy could become bankrupt as our energy supply dwindles internally and we depend more on imports. This matter is of highest national emergency concern, and the Federal government needs to develop a strong management planning policy to establish and implement goals for the total good of the nation. This does not mean government operation of the energy industry, but it does mean government direction of national consumption patterns for the long-range total good. Full utilization of the Appalachian energy resources for the future should be developed as an integral part of national policy and not just haphazardly come about by supply and demand economics of local and regional needs.

Literature Cited

1. Barlow, J. A. 1971. Coal in West Virginia. W. Va. Geol. Survey Newsletter: 3-10.
2. Brown, A., H. L. Berryhill, Jr., D. A. Taylor, and J. V. A. Trumbull. 1952. Coal resources of Virginia. U.S. Geol. Survey Circ. 171. 57 p.
3. Carrington, T. J. 1972. Meta-Paleozoic rocks, Chilton County, Alabama. Alabama Geol. Soc., Guidebook for Field Trips, 21st annual meeting of Geol. Soc. America: 1-29.
4. Conant, L. C., and V. E. Swanson. 1961. Chattanooga Shale and related rocks of central Tennessee and nearby areas. U.S. Geol. Survey Prof. Paper 357. 91 p.
5. Dennison, J. M. 1970. Silurian stratigraphy and sedimentary tectonics of southern West Virginia and adjacent Virginia. Appalachian Geol. Soc., Field Conference Guidebook (1970): 2-33.
6. ———. 1971. Petroleum related to Middle and Upper Devonian deltaic facies in central Appalachians. *Amer. Assoc. Petroleum Geologists Bull.* 82:1179-93.
7. Dennison, J. M., and R. W. Johnson, Jr. 1971. Tertiary intrusions and associated phenomena near the Thirty-eight Parallel Fracture Zone in Virginia and West Virginia. *Geol. Soc. America Bull.* 82:501-8.
8. Dennison, J. M., and W. H. Wheeler. 1972. Precambrian through Cretaceous strata of probable fluvial origin in southeastern United States and their potential as uranium host rocks. U.S. Atomic Energy Commission open-file report GJO-4168-1, 211 p.
9. Fullagar, P. D., and M. L. Bottino. 1969. Tertiary felsite intrusions in the Valley and Ridge Province, Virginia. *Geol. Soc. America Bull.* 80:1853-58.
10. Johnson, A. 1968. Waterpower resources. U.S. Geol. Survey Prof. Paper 580: 48-51.
11. Klemic, H. 1962. Uranium occurrences in sedimentary rocks of Pennsylvania. *U.S. Geol. Survey Bull.* 1107-D:243-88.
12. McCauley, J. F. 1961. Uranium in Pennsylvania. Pennsylvania Topo. and Geol. Survey Bull. M43. 71 p.
13. Weaver, O. D., W. L. Calvert, and W. H. McGuire. 1972. A new look at the oil and gas potential of the Appalachian basin. *Oil and Gas Jour.* Jan. 17:126-30; Jan. 24:100-104.

The Migrational History of Barrier Islands at Wachapreague, Virginia

Thomas Floyd Kemerer
Department of Geology, West Virginia University
Morgantown, West Virginia 26506

Abstract

Historical records show that the sea is advancing in the Wachapreague Virginia area pushing the barrier islands lagoonward. The southern ends of the islands are migrating landward at an average rate of 15 feet per year during the past century. The migration of the northern ends of the islands is slightly different due to the influences of tidal inlets and sediment supply to the area. North Parramore Island prograded 15 feet per year whereas North Cedar and Metomkin Islands have retrograded 13 feet per year in the past century. The tidal inlets of this area migrate to the south at a rate of 7 feet per year being influenced by the predominantly southerly longshore currents.

Cores taken across the barrier island complex show a basal peat bed at depth, indicating an initial flooding of a beach on a Pleistocene surface to form barrier islands. Continued sea level rise in the Holocene terminated the growth of the basal peat bed, and lagoonal sediments have filled this area to the present level. Certain areas of the lagoon have filled so completely that new marsh is presently forming behind the islands. Future trends for this area seem to indicate that the lagoon will continue to fill, while the barrier islands are pushed landward. The retrograding nature of these barrier islands may cause the stratigraphic record of the lagoonal sediments to be partially or completely destroyed as the islands are pushed landward.

Introduction

The eastern shore of Virginia is bounded by a series of barrier islands which protect the lagoonal areas from the high energy of ocean waves and longshore currents. Analysis of topographic maps and core data describing the stratigraphy of the islands records the migrational trends of the entire barrier island complex. This paper shows the past and current migrational trends of the barrier islands by two methods:

1. Comparison of maps representing different times in the historic record to show changes in the position of the barrier islands.
2. Analysis of stratigraphic data to show barrier island migration during the Holocene.

Description of the Area

Wachapreague, Virginia, is situated on the eastern shore of the Delmarva Peninsula (fig. 1, insets). The study area is divided into three physiographic subdivisions: the barrier islands facing the Atlantic Ocean on the east; the lagoon in an intermediate position that is subdivided into marshes, tidal flats, tidal channels, and shallow bays; and the mainland, which is developed on Pleistocene sediments.

The barrier islands in this area all trend north-northeast and are separated from one another by tidal inlets. The northern ends of the islands exhibit well

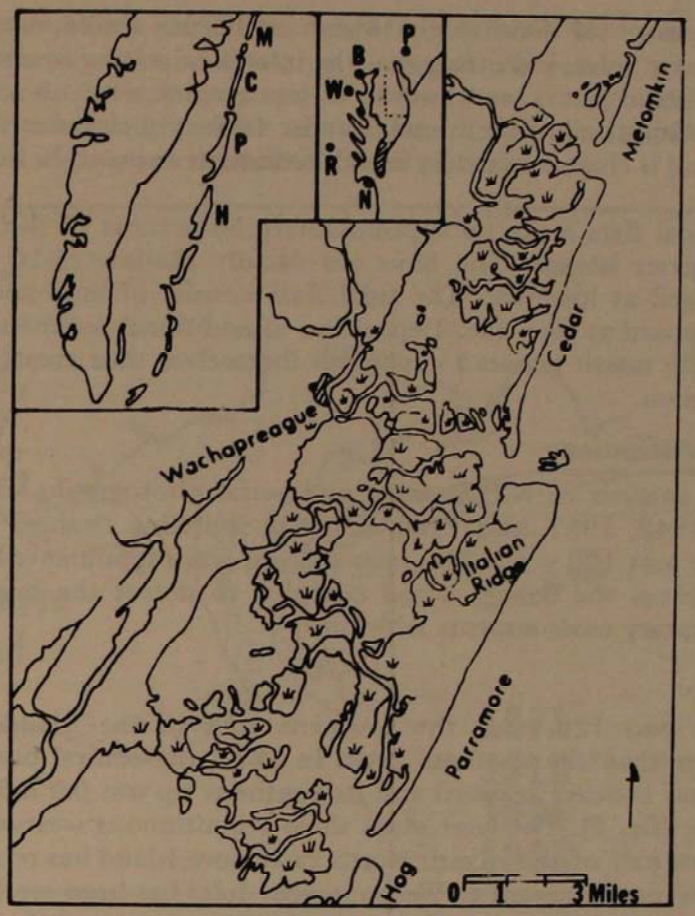

FIGURE 1. Area of investigation along the Virginia coast.

developed dune fields in contrast to the southern portions of the islands. The islands are wider to the north than they are to the south, and are situated in an en echelon arrangement.

Parramore Island exhibits the highest elevations of all the barrier islands along the southern coastline of the Delmarva Peninsula with the exception of Chincoteague Island to the north. Its topography ranges from shoal areas on its southern end to elevations of 30 feet or more along Italian Ridge, a northeast trending dune ridge, located in the northern part of the island. On the central part of the island, numerous stumps of oak (*Quercus virginiana*) are found in the backshore in front of the dune ridges thus indicating a retrograding shoreline. The dune ridges at the northern end of the island are truncated by the ocean indicating that the shoreline has shifted with time.

Cedar Island displays a very subdued topography, most of which is under 10 feet in elevation, except in the northern end where elevations may reach 20 feet. The southern end of the island is characterized by spit formation from the interaction of the southerly longshore drift and the inlet mouth. A small healed inlet located 1.5 miles north of Wachapreague Inlet is periodically opened during storms such as the March 7-8, 1962 "Ash Wednesday" storm. In the central part of the island, many outcrops of the marsh grass, *Spartina sp.*, are found just below the high tide line on the foreshore. The northern end of the island has the

highest development of dune ridges. Marsh sediments are exposed in the foreshore at Metomkin Inlet, indicating that the inlet is migrating southward.

Metomkin Island has a very subdued topography with no extensive dune development. Almost all of the island is under 10 feet in elevation. The southern end of the island is characterized by marsh sediments exposed in the surf zone at low tide.

Bays and tidal flats make up approximately 50 percent of the lagoonal area behind the barrier islands. The bays are usually shallow (5-10 feet) and are barely submerged at low tide. The tidal flats consist of mud and silt, and are extensively exposed at low tide. Deposition of additional sediments on the tidal flats enables the marsh grasses to establish themselves thus creating new marsh areas in the lagoon.

Methods of Investigation

A detailed analysis of N.O.S. maps and aerial photographs of 1851, 1871, 1910, 1935, 1942, 1957, and 1966 delineate shoreline changes of the barrier islands for the past 120 years. This map analysis was supplimented by a series of cores taken across the barrier island complex to detect the migration of the various sedimentary environments with time.

Results

During the past 120 years the southern ends of the islands have moved landward faster than the northern ends. In 1871, the central portion of Parramore Island was concave seaward and its southern tip was 0.9 mile north of the 1910 shoreline (fig. 2). The later maps show a continuous westward movement of the southern half of the island. North Parramore Island has retrograded at its tip whereas the part adjacent to Wachapreague Inlet has been eroded at a rate of 6.5 feet per year in the past century by the interaction of the inlet and the southerly longshore currents.

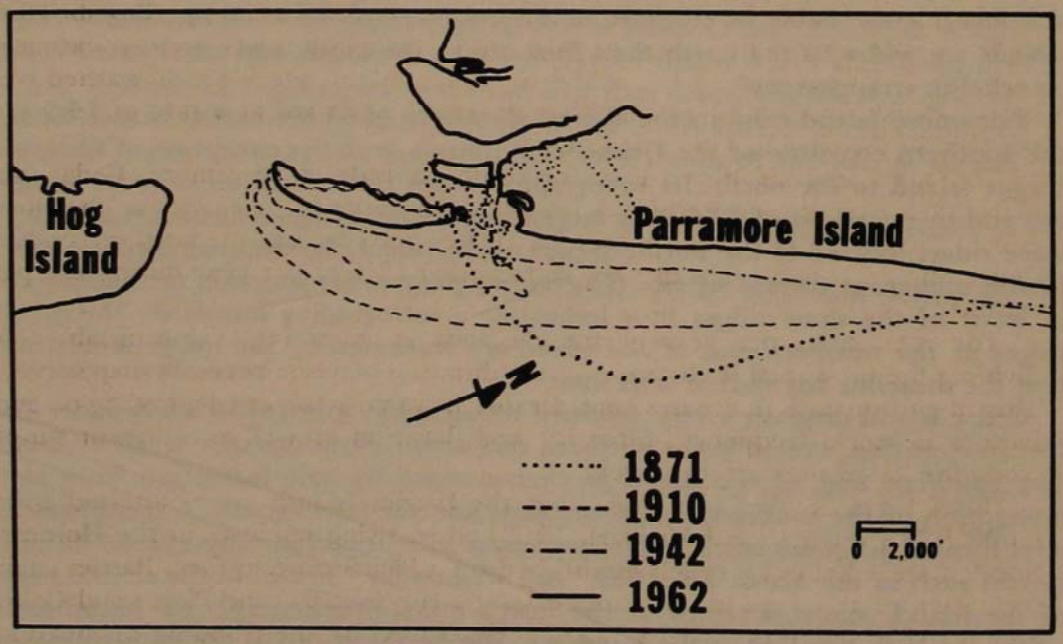

FIGURE 2. Shoreline changes of South Parramore Island from 1871 to 1962, taken from N.O.S. charts.

South Cedar Island (fig. 3) has migrated 16.5 feet per year westward during the past century and the southern tip of the island moved at a rate of 10 feet per year southward. The northern end of Cedar Island retrograded at a rate of 13.3 feet per year westward, and the northern tip of the island adjacent to Metomkin Inlet migrated slightly northward at several places.

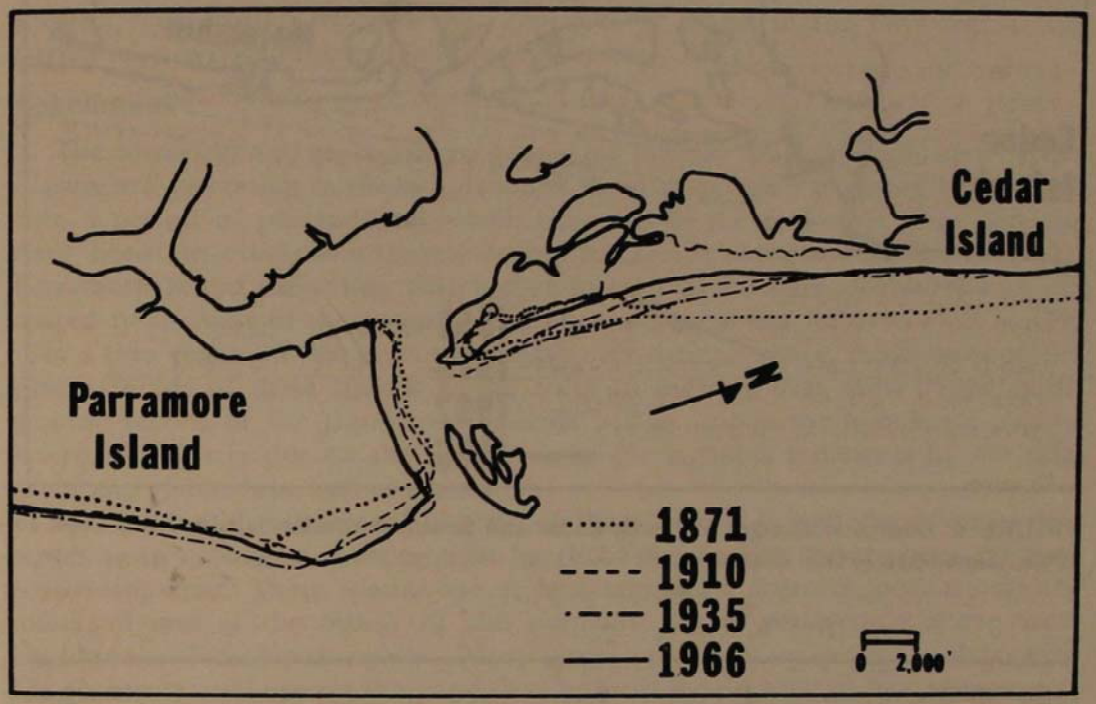

FIGURE 3. Shoreline changes of North Parramore and South Cedar Island from 1871 to 1966, taken from N.O.S. charts.

Metomkin Island shows perhaps the best example of a retrograding shoreline in the entire area. The landward migration of the island has been so extensive that the southern end of the island is composed of beach sands washed over recent marsh deposits. The island has retreated westward at a rate of 14.5 feet per year in the past 120 years (fig. 4).

The map analysis shows that the southern ends of Parramore, Cedar, and Metomkin Islands have retreated landward 15 feet per year whereas the north end of Parramore Island has prograded 15 feet per year and the northern ends of Cedar and Metomkin Islands have retrograded 13 feet per year during the past century.

The rate shifts per year of these islands is an average value obtained by dividing the total shift in distance by the duration of years between map surveys. This migration rate fluctuates considerably from year to year depending on such factors as storm frequency, intensity and duration as well as sediment supply along the longshore-current system.

Cores taken in this area show that the barrier islands were initiated about 5,000 B.P. (Newman and Munsart, 1968) when rising sea level in the Holocene flooded areas behind a beach established on a Pleistocene surface. Barrier island formation of this type has been discussed by Hoyt (1967) and Pierce and Colquhoun (1970) where the barrier island is developed by the flooding of low-lying areas behind a mainland beach during a slight rise in sea level. Continued sea

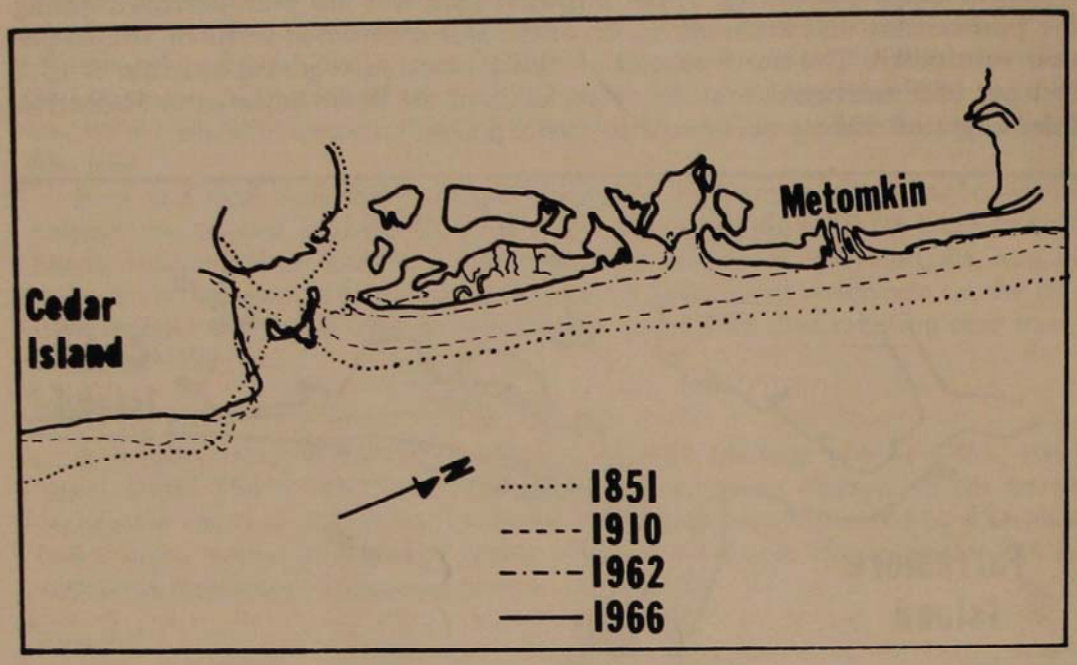

FIGURE 4. Shoreline changes of North Cedar and South Metomkin Islands from 1851 to 1966, taken from N.O.S. charts.

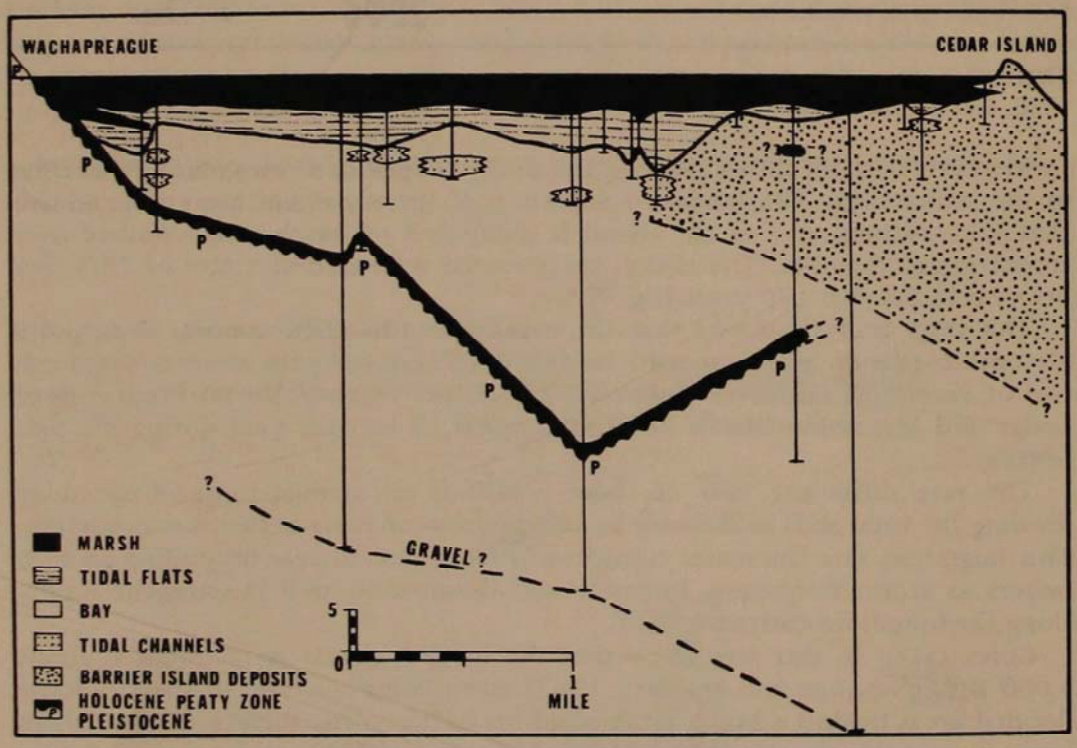

FIGURE 5. Cross-section from Wachapreague to Cedar Island.

level rise terminated the basal peat (marsh) that was deposited at the onset of flooding, and lagoonal sediments were deposited behind the barrier islands (fig 5). The numerous dune ridges on Parramore Island indicate a progradational stage of island development. At the present time, sediment upbuilding has filled the lagoon in many places so that extensive marshy (peat) areas now exist. The shallow bays are filling and shrinking as new tidal flats and marsh form. The present retrograding shoreline has exposed the marsh in the foreshore as the barrier islands have migrated landward (Kemerer, 1971).

Conclusions

The historical and geological records show that the Wachapreague area barrier islands are retreating landward although dune ridges on Parramore Island indicate a period of progradation which occurred in the Holocene. Peat deposits have been recorded immediately below the beach along the southern end of Parramore Island indicating that earlier formed dune ridges also must have occurred to the east of these marsh deposits but erosion has removed them leaving only a thin veneer of marine sand to mask over their presence. Projections on the future trends of these islands would seem to indicate that most of the stratigraphic record of the lagoonal sediments will be lost as the islands are pushed landward. This is due to the reworking of the lagoonal sediments by the tidal inlets and channels as well as the sea.

The landward migrational history of these islands is well documented and serves as an ecological warning light for those people who wish to open this area to development. These islands are at best temporary features located near the mainland and at the mercy of the elements, which persistently shove them landward with each passing year. Many intensive studies are needed to determine the environmental impact that land development would have on this area.

Acknowledgments

Logistical support for the field work was obtained from the Virginia Institute of Marine Science—Eastern Shore Branch, Wachapreague, Virginia. I would like to thank Mike Castagna and the staff at V.I.M.S.-E. for the information and help on the barrier island complexes in that area.

Literature Cited

1. Hoyt, John H. 1967. Barrier island formation: *Geol. Soc. America Bull.* no. 9. 78:1125-36.
2. Kemerer, T. F. 1971. Barrier island origin and migration near Wachapreague, Virginia: Unpubl. M.S. Thesis, West Virginia Univ., 154 pp.
3. Newman, W. S., and C. A. Munsart. 1968. Holocene geology of the Wachapreague lagoon, eastern shore peninsula, Virginia: *Marine Geol.* 5:81-105.
4. Pierce, J. W., and D. J. Colquhoun. 1970. Holocene evolution of a portion of the North Carolina coast: *Geol. Soc. America Bull.* 81:3697-3714.

Stratigraphy and Petrography of the Upper Silurian Williamsport Sandstone, West Virginia

Douglas G. Patchen
West Virginia Geological Survey
Morgantown, West Virginia 26505

Abstract

The Upper Silurian Williamsport Sandstone at the type section in Grant County, West Virginia, is typically composed of green and brown, very fine-grained sandstone, with some siltstone and shale. A local carbonate member, the Cedar Cliff Limestone, is present in the middle of the formation in nearby outcrops in western Maryland. To the north in Pennsylvania, the Williamsport can be traced into the Moyer Ridge Sandstone, which is a member of the Bloomsburg Formation. Eastward, in the eastern panhandle of West Virginia and Maryland, the Williamsport pinches out in the middle of the red, nonmarine Bloomsburg facies. Farther south the Williamsport undergoes a facies change into clean, well-sorted, mature sandstone. The subsurface continuation of this sandstone extends to the Ohio border where it has recently been found to be an important reservoir for natural gas.

Sandstones of the Williamsport in the subsurface are very fine to fine grained, subrounded to rounded, well sorted, and texturally mature and supermature. In general, sandstone is most abundant in the upper half of the unit, whereas carbonates become interbedded with sandstone layers in the lower half. Syntaxial quartz overgrowths serve as the primary cement in the upper part of the formation, but dolomite becomes important lower in the section. Gypsum, anhydrite, and barite are minor cements. Intergranular porosity is greatest near the top of the formation.

The immature sandstones and siltstones of the Williamsport in northeastern West Virginia probably were deposited on low-energy mud flats in front of the Bloomsburg Delta. Sediments were supplied by rivers from source lands farther east in Pennsylvania. The limestones and hematitic beds of the Cedar Cliff Limestone are interpreted as having been deposited in a lagoon associated with this tidal flat. Farther south, the cleaner, coarser, more mature sandstones were deposited in a barrier island-coastal complex. Regression of the shoreline spread a blanket of sand over the underlying subtidal to intertidal McKenzie Formation. As the shoreline and barrier island complex regressed westward the lagoonal sediments of the Wills Creek Formation were superposed on the clean sand of the Williamsport.

Gas accumulation in the Williamsport is due to a combination of stratigraphic and structural trapping. Salt water is present downdip in all fields, and updip porosity and permeability decrease where the sandstone thins westward. Gas flows in this formation are the greatest recorded in the Appalachian Basin making the Williamsport the most important deep target for drillers in West Virginia. Future exploration should examine the possibility that combination stratigraphic and structural traps exist near the eastern edge of the sand body in central West Virginia, and near the southwestern sandstone pinchout in south-central West Virginia.

Introduction

During the past nine years the subsurface Newburg sand has become known to be an important reservoir for natural gas in western West Virginia. At present six gas fields have been developed, in addition to a one-well oil field (Figure 1). Gas from this sandstone has also been produced from several wells in the Sanoma area.

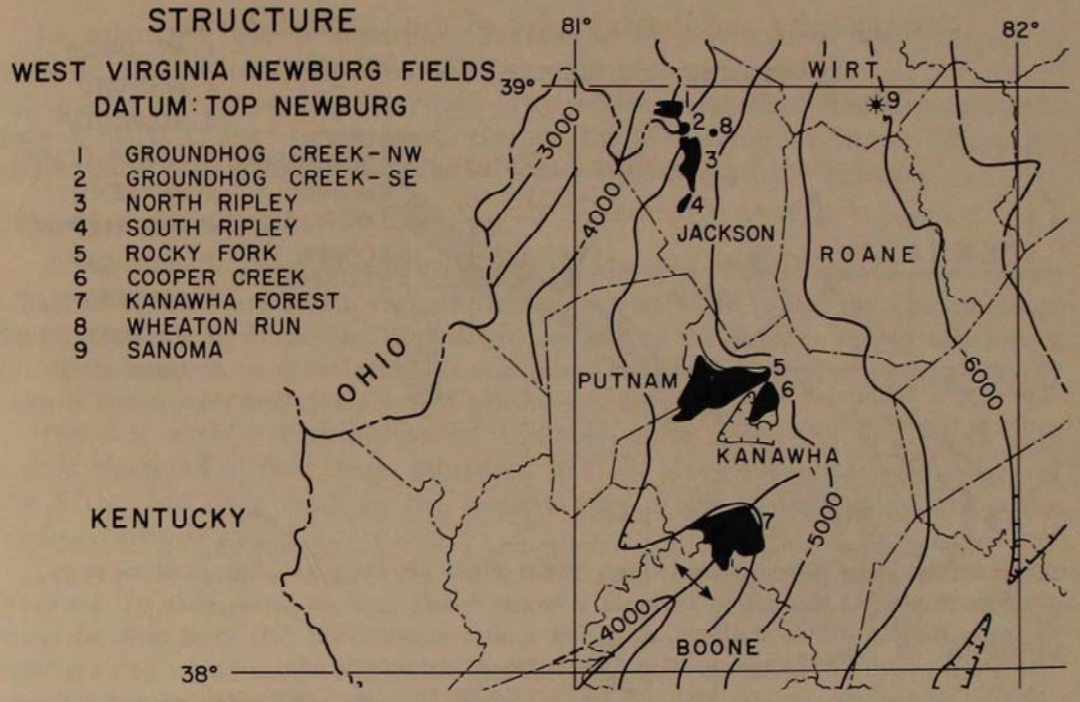

FIGURE 1. Structure on top of the Williamsport (Newburg) Sandstone in western West Virginia.

By the end of 1971, the cumulative delivery from the Newburg was 210 Bcf. However, remaining reserves were down to an estimated 50 Bcf. Therefore, more than 80 percent of the known Newburg gas has been produced. Wildcat wells are being drilled throughout western West Virginia, which hopefully will increase these reserves.

Due to the importance of the Newburg as a gas reservoir, and because of the large amount of interest in it, the West Virginia Geological Survey sponsored a detailed study of the unit that included: (1) a stratigraphic study to demonstrate the correlation of the subsurface Newburg and the surface Williamsport Sandstone of West Virginia's eastern panhandle; (2) a petrographic study to determine the textural and mineralogic properties of the subsurface Newburg sand and the surface Williamsport Sandstone; and (3) a paleoenvironmental study to determine the origins of different rock types observed in outcrop sections and in subsurface cores. The following paper is a summary of this over-all study (Patchen, 1971).

Surface Stratigraphy

The Williamsport Sandstone was originally named by Reger (1924) for a greenish-brown, very fine-grained sandstone between the McKenzie Limestone and Wills Creek Shale at Williamsport, Grant County, West Virginia (Figure 2). This formation was later correlated by other workers in the northeastern counties with an arenaceous, silty facies present between limestones and shales of the McKenzie and Wills Creek.

Eastward from the Grant County type section the greenish-brown sandstones can be traced into the middle of the red Bloomsburg facies, and eventually are

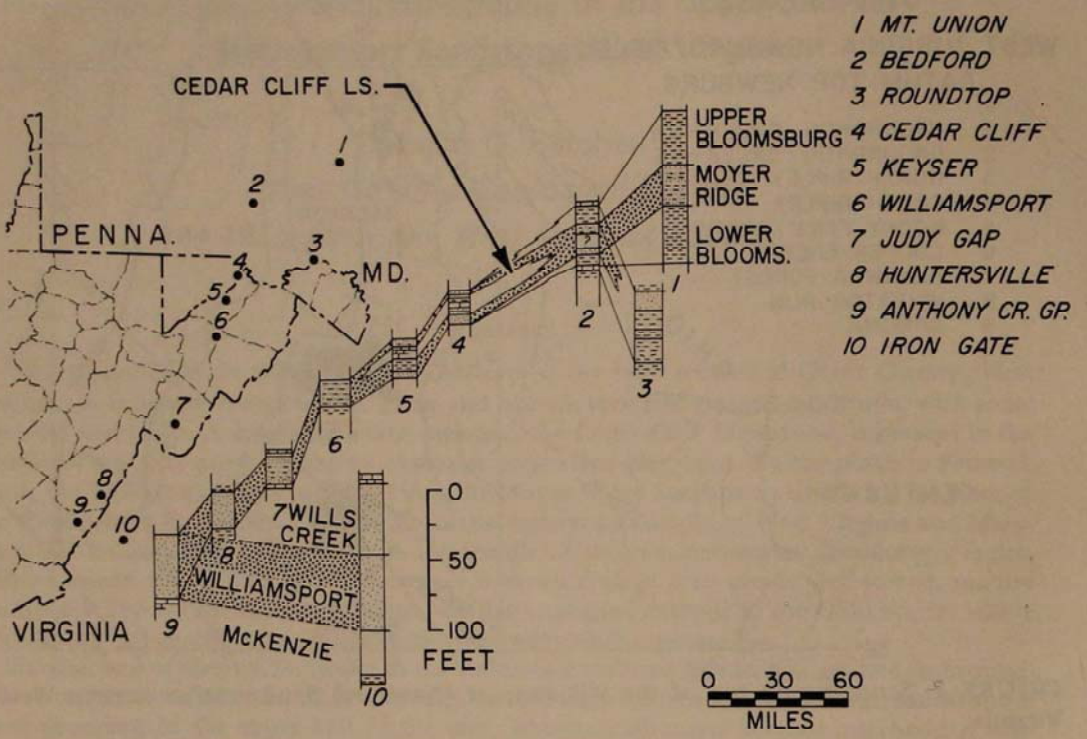

FIGURE 2. Regional stratigraphic relations of the Williamsport Sandstone.

totally replaced by red beds. To the north the Williamsport is probably laterally equivalent with the Moyer Ridge Sandstone (Hoskins, 1961).

A locally occurring carbonate facies, the Cedar Cliff Limestone is present in the middle of the Williamsport in several outcrop sections, whereas in other northeastern outcrops dark shale beds are present between upper and lower sandstone beds (Woodward, 1941).

In general, throughout this northeastern area the Williamsport is a very fine-grained, greenish, reddish, or brown sandstone, interbedded with dark siltstone and shale. Therefore, it is primarily a dark, very fine arenaceous facies present between carbonates and shales of the overlying Wills Creek and underlying McKenzie. Fossils are rare, but the large ostracode *Leperditia alta* has been found in the Williamsport, Moyer Ridge, Cedar Cliff, and even in red beds of the Bloomsburg. This ostracode first occurs near the base of the Williamsport-Moyer Ridge and continues to be present in the Upper Silurian rocks up to the Helderberg.

The Williamsport correlation was carried farther south by Price (1929) who correlated a brown sandstone between the McKenzie and Wills Creek near Huntersville, Pocahontas County, with the Bloomsburg of northeastern West Virginia. Later Woodward (1941) noted the presence of *Leperditia alta* in this sandstone and in a light gray to white sandstone in a similar stratigraphic position at Anthony Creek Gap, Greenbrier County, and called both sandstones Williamsport. Southeast of these southern outcrops in Virginia a thick sandstone section is present above the Rose Hill Shale that is probably equivalent to the Keefer, McKenzie, Williamsport, and perhaps Wills Creek Formations (Woodward, 1941). This is the "Keefer" Sandstone of Dennison (1970).

In summary, the Williamsport Formation of northeastern West Virginia is laterally equivalent to the middle of the red Bloomsburg facies and is replaced by this facies eastward in Maryland. Toward the south the Williamsport undergoes a facies change to a coarser, cleaner, lighter-colored sandstone. This sandstone passes into a thick sandstone section southeastward in Virginia.

Subsurface Stratigraphy

As part of the stratigraphic study 12 stratigraphic cross-sections were drawn between surface and subsurface control points with the top of the Onesquethaw Stage (Onondaga, Huntersville, and Needmore) as the datum. The correlation of the Williamsport on these sections was based only on physical criteria; primarily sample lithologies and character of gamma-ray logs.

There is a poor distribution of control points across the State with data points clustered in two areas: measured sections along the eastern boundary of the State; and deep wells in the western part of the State, particularly in the outlined area of Figure 3.

Cross-section AA' (Figure 4) runs from northwest to southeast across West Virginia. In this cross-section the Kanawha County well is in the main drilling area. In this area the Williamsport is a medium- to thin-bedded, fine-grained, light gray to white sandstone, with interbedded carbonates in the lower half. The upper contact with fine-grained, pyritic, anhydrite-bearing, argillaceous carbonate beds of the Wills Creek (Salina) is sharp, whereas the lower contact with coarser, cleaner carbonates of the McKenzie is gradational. At the northwest end of the cross-section the Williamsport undergoes a facies change to a green shale in the Mason County well. Toward the southeast, however, the sandstone facies thickens and becomes coarser grained (fine and medium) and retains its clean, well-sorted nature before merging with other similar sandstones in Virginia.

Cross-section B-B' (Figure 5) runs west to east across northern West Virginia to the eastern panhandle outcrop areas where the Williamsport was first named and described. The Williamsport is represented by several different types of facies in this cross-section, none of which is similar to the clean, well sorted, fine-grained sandstone facies of the Kanawha County area and southern cross-section.

In western Wood County a green shale is present above the McKenzie Limestone in this cross-section. In the Sandhill well in eastern Wood County green shale, gray sandy dolomite, and thin, fine-grained, gray sandstone beds occupy the Williamsport interval. Approximately 30 miles to the east the Williamsport undergoes a further facies change to a gray sandy dolomite with no sandstone beds. Another 25 or 30 miles east a thin sandstone is again present above the McKenzie. This sandstone is light gray and fine grained. At the eastern end of the cross-section siltstone and very fine-grained, silty, argillaceous gray and green sandstones similar to the Williamsport of the outcrop sections are present in deep wells above the McKenzie.

Cross-section CC' (Figure 6) was drawn from southwest to northeast, from the subsurface to surface exposures. At the southwestward end gray sandy dolomite is present at the top of the McKenzie below the Salina. In the area where the Williamsport is productive (Boone and Kanawha counties) it is represented by a light gray to white, fine-grained, rounded, well-sorted sandstone. Carbonates are interbedded in the lower half. These carbonates increase in number just to the northeast in Braxton County, near the edge of the sand body, until finally only sandy dolomite is present at the Williamsport level in the Lewis County

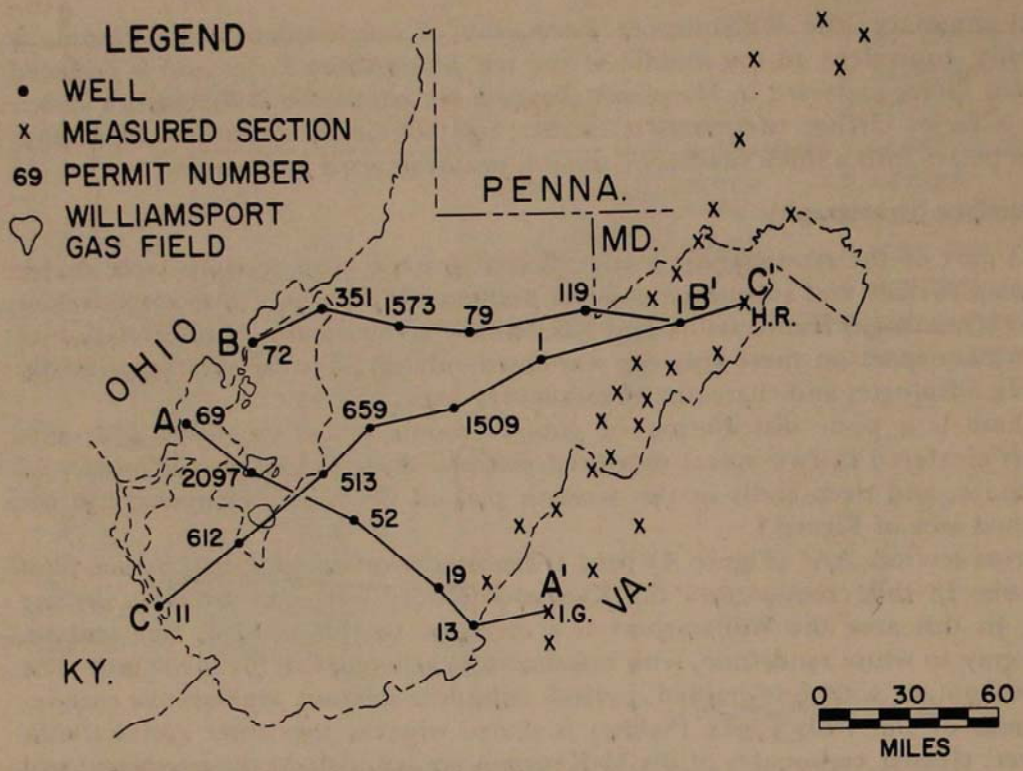

FIGURE 3. Cross-section locations.

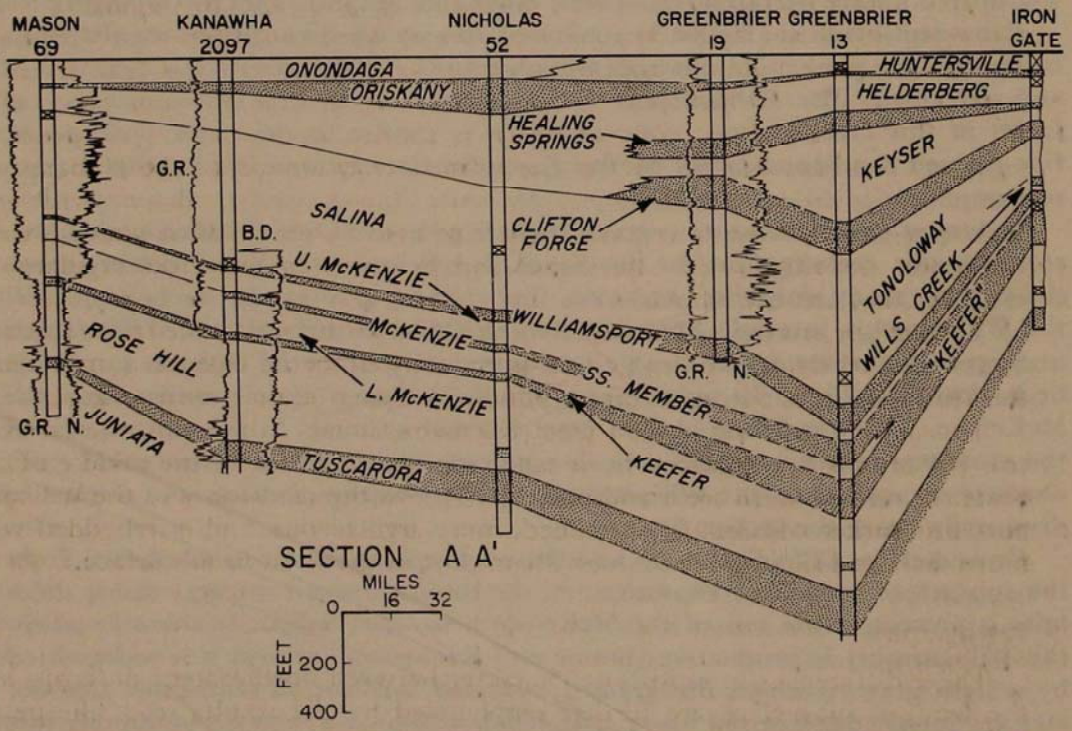

FIGURE 4. Cross-section AA' from Mason County, West Virginia southeastward to Iron Gate, Virginia.

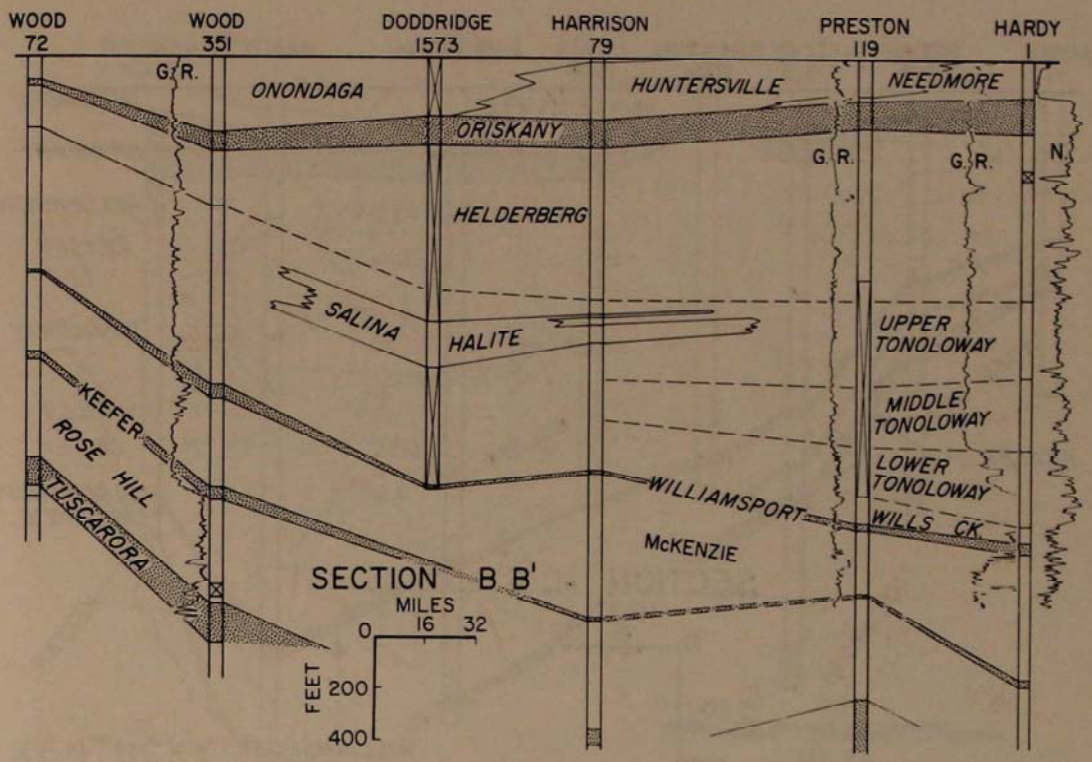

FIGURE 5. Cross-section BB' from Wood County eastward to Hardy County, West Virginia.

deep well. In wells at the northeastern end of the cross-section gray, brown and green siltstones, very fine-grained, argillaceous sandstones, and shales make up the Williamsport Formation. In the Hampshire County outcrop (Hanging Rock) red shale, siltstone, mudstone, and very fine-grained sandstones of the Bloomsburg have replaced the non-red Williamsport.

Subsurface Summary

In areas where it is productive the subsurface extension of the Williamsport Sandstone is recognized as a gray to white, fine-grained sandstone with gray carbonate beds in the lower half, occurring above a gray, coarse-grained, clean carbonate, the McKenzie Limestone, and below a darker, more argillaceous, pyritic carbonate, the Salina.

Toward the southeast (from Kanawha County) the sandstone facies thickens and retains its light color and clean, rounded, well-sorted character. In Virginia the Williamsport is part of a thicker Middle to Upper Silurian sandstone.

Toward the northeast (again from Kanawha County) the sandstone facies of the Williamsport is replaced by a sandy dolomitic facies in the middle of the State. In northeastern wells and outcrop sections the sandstones of the Williamsport are darker colored, finer grained, more argillaceous, and interbedded with more shale and siltstone than the Williamsport in the western subsurface.

Petrography

These differences in sandstone character between northeastern outcrops and the western subsurface are further emphasized by the results from the petrographic study. The samples for this part of the study came from outcrop sections in the northeast and southeast, and well cuttings and well cores located in the

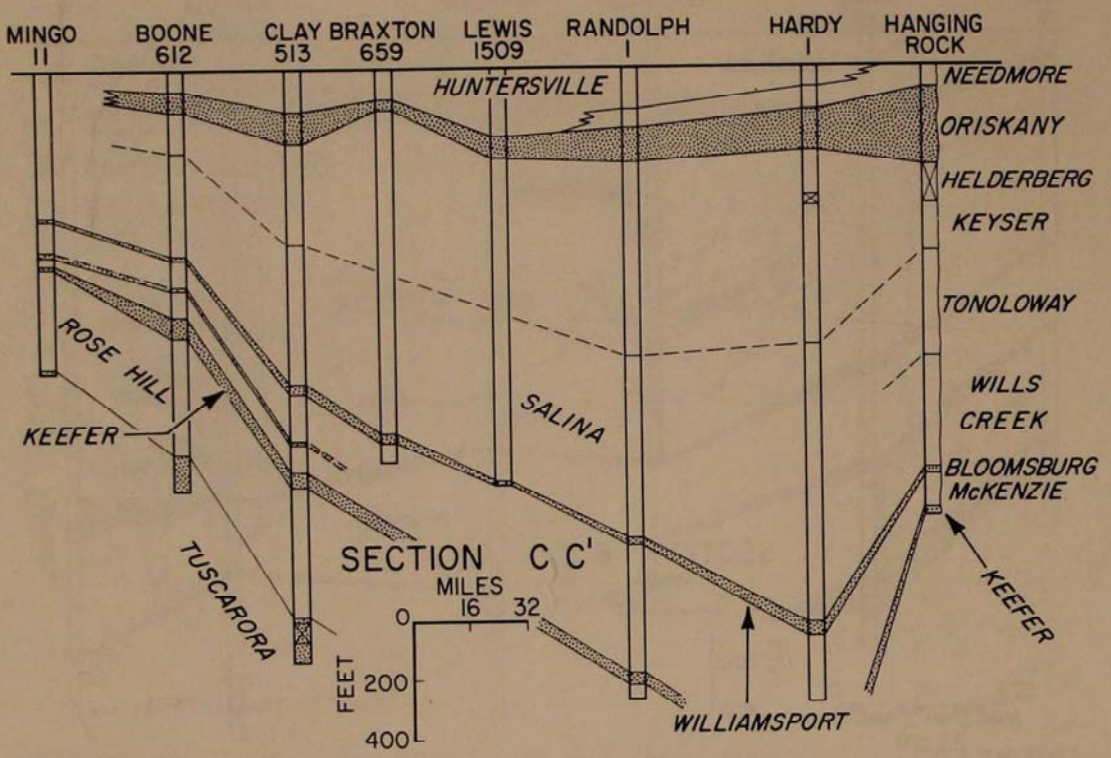

FIGURE 6. Cross-section CC' from Mingo County northeastward to Hampshire County, West Virginia.

productive areas (Figure 7). Point counts of thin sections from these cores were made to determine the textural and mineralogic properties of the sandstones. All of the data shown on Figures 8 and 9 are the result of point counts.

The results from a typical core in one of the Kanawha County fields are shown in Figure 8. Quartz grains are generally fine grained, well sorted, and subround to round. With the exception of two thin sections, clay matrix was absent. Due to the cleanness, good sorting, and high roundness most sandstone beds are texturally mature or supermature. Exceptions are the two argillaceous, immature beds and a poorly sorted submature bed.

The detrital grains are predominantly quartz, with feldspar and rock fragments rare or absent. Well-rounded zircon and tourmaline are the main heavy minerals. Thus, the mineralogy of the detrital grains in the Williamsport is quite simple.

The cements found in the Williamsport sandstone beds are more varied, however. Secondary quartz in the form of quartz overgrowths is prominent in the upper sandstone beds, whereas dolomite is more abundant in the lower sandstone beds. Anhydrite and barite are also present, generally in the upper half of the formation. Interstitial porosity, resulting from incomplete cementation, is greater in the upper siliceous beds and less in the lower dolomitic beds. All percentages on the bar graphs in Figures 8 and 9 are expressed as the percent of original pore space.

The same textural and mineralogic properties occur in the Williamsport Sandstone farther north in the Jackson County fields (Figure 9). With few exceptions quartz grains are of fine sand-size, well sorted, and subround to round. Clay matrix is absent or less than 5 percent in all slides. Therefore, due to the

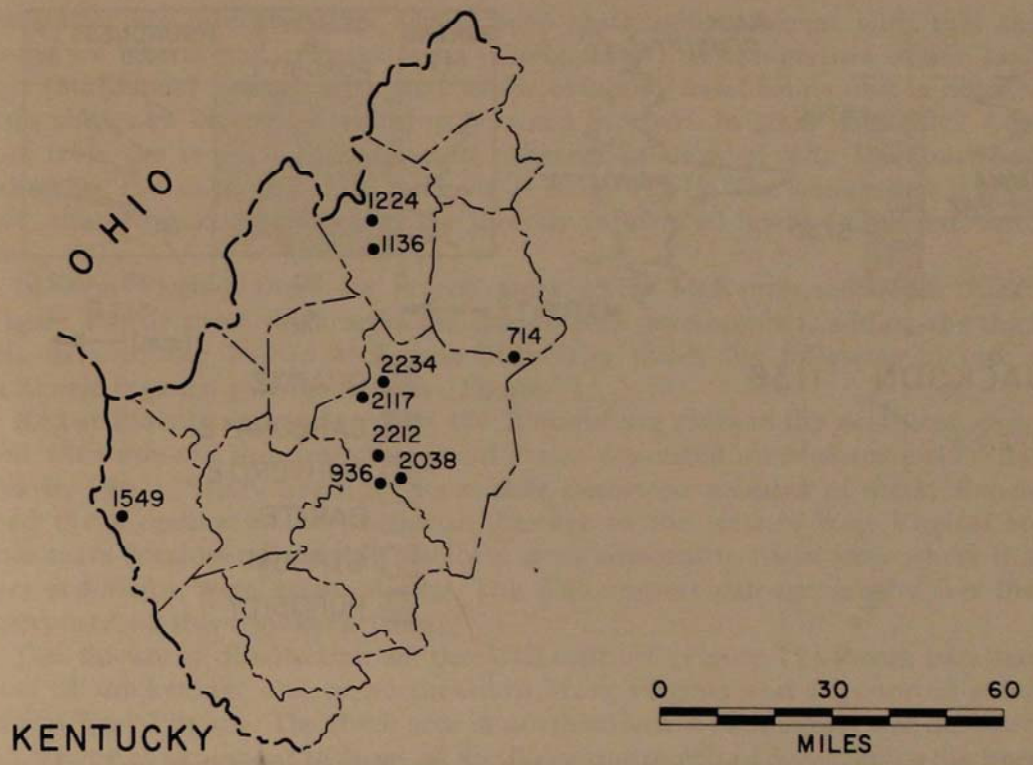

FIGURE 7. Location of Williamsport cores.

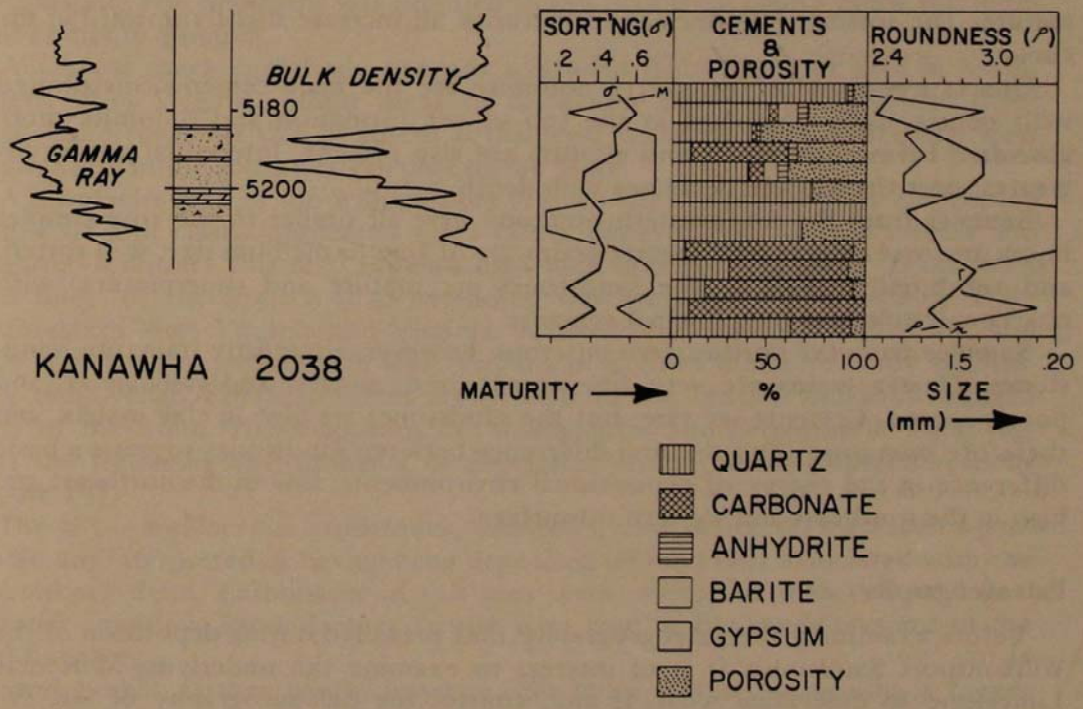

FIGURE 8. Textural and mineralogic properties of the Williamsport Sandstone, Kanawha County, West Virginia.

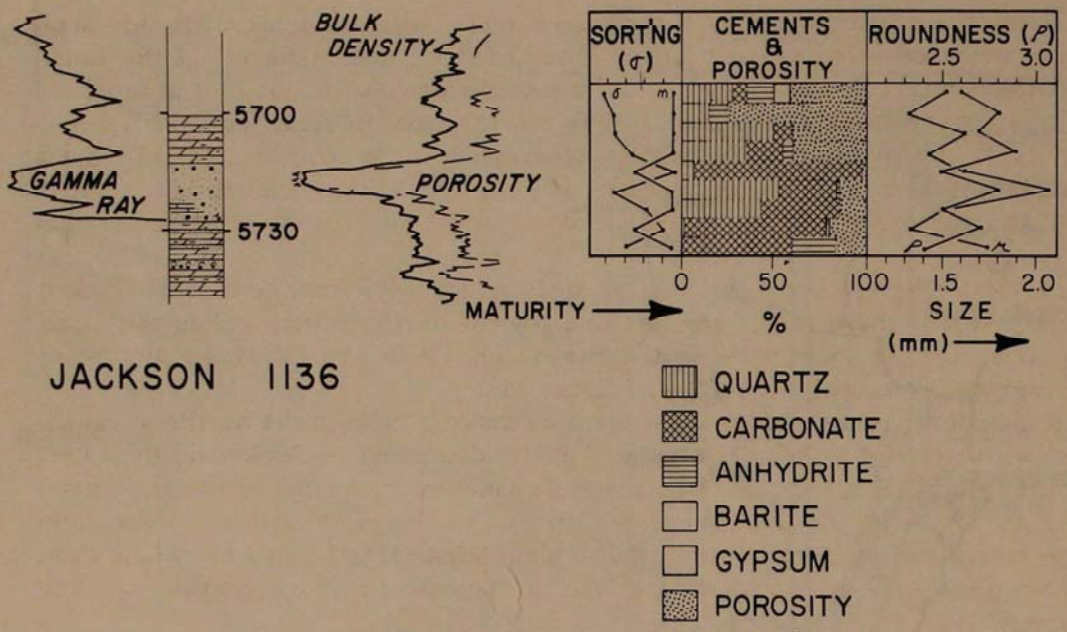

FIGURE 9. Textural and mineralogic properties of the Williamsport Sandstone, Jackson County, West Virginia.

cleanness, good sorting, and high rounding, the sandstones are mature and supermature. The sorting, roundness, and maturity all increase slightly upward in the core.

Quartz overgrowths and sparry dolomite are the main cements, distributed with quartz more abundant at the top of the formation and dolomite more abundant below. Anhydrite and gypsum are also present. Interstitial porosity is greatest near the top and decreases with depth.

Samples from the southeastern outcrops were all similar to the core samples in texture and mineralogy. Quartz grains are of fine to medium size, well sorted, and subround to round. The sandstones are mature and supermature, with quartz and dolomite the principal cements.

Samples from the northeastern outcrops, however, are mostly immature sandstones. Quartz grains are very fine to silt-sized, angular and subangular, and poorly sorted. Cements are rare, but the sandstones are high in clay matrix, and therefore immature. This textural difference between sandstones suggests a basic difference in the energy of depositional environments; low in the northeast and high in the southeast and western subsurface.

Paleogeography

Before examining the paleogeography that prevailed during deposition of the Williamsport Sandstone, it is of interest to examine the underlying McKenzie Limestone to determine what, if any, control the paleogeography of late Niagaran time exerted on the dispersal of lower Cayugan sediments.

In northern Ohio, areas with a thick accumulation of Niagaran (Lockport)

limestones are interpreted as having been reefs, whereas areas with thin sediments are interpreted as basin areas (Ulteig, 1964). A comparison of the Lockport (McKenzie) isopach with that of the overlying basal Salina unit in northern Ohio shows an inverse relationship between the two. In areas with thick Lockport reefs the overlying unit is thin, whereas in areas of thin Lockport basin sediments the overlying unit thickens (Ulteig, 1964). The conclusion is therefore, that Niagaran paleogeography directly influenced lower Salina sedimentation.

In West Virginia there are several areas where McKenzie sediments thicken (Figure 10). If these thick areas are due to reef development, adding the thickness data to the known McKenzie lithofacies yields the following picture of McKenzie regional paleogeography (Figure 11).

Red sediments accumulated on the Bloomsburg delta in the northeast associated with non-red thin limestones and shales deposited on McKenzie tidal flats (Travis, 1962). Sandy beaches (the middle sandstone member of the McKenzie) lined the shoreline in the southeast. Farther to the west in West Virginia and Ohio reefs devcloped on stable platform areas adjacent to basin areas where thin, finer sediments were accumulating. The Williamsport paleogeography was then superposed on this regional setting.

The thickness distribution of the Williamsport (Figure 12) shows two main areas of thickening: one in northeastern West Virginia and a second in southeastern West Virginia. The thick area in northeastern West Virginia was deposited in a marine environment in front of the Bloomsburg delta (Bloomsburg thickness is shown by the contour lines in the extreme northeast, reaching 80 feet in thickness). The source of Williamsport sediments there was from the deltaic system. The thick area in southeastern West Virginia was on the edge of the Williamsport sea. Sediment was supplied to this area from source lands and older sand bodies in Virginia.

A narrow sheet sand body extends westward from the thick area in southeastern West Virginia. Minor areas of thickening developed within this sheet body. Sandstones are thin or absent at this level in central and northcentral West Virginia and in the southwestern part of the State.

A lithofacies map of the Williamsport (Figure 13) was prepared by contouring sand/shale and clastic/nonclastic ratio values derived from sample studies and measured sections. This map shows a high sand area corresponding to the sheet sand body of the isopach map extending westward and northwestward from southeastern West Virginia and Virginia. A mixture of sandstone, siltstone, and shale is present in northeastern West Virginia in front of the more sandy Bloomsburg delta. High carbonate areas are present in the central and southwestern parts of the State. This map, plus the stratigraphic and petrographic data, suggests the following environments of deposition and sediment dispersal systems (Figure 14).

The silty, argillaceous sandstones, siltstones, and shales of the eastern panhandle are interpreted as having been deposited on mud flats associated with the Bloomsburg delta. Carbonates in this area were associated with this tidal flat-lagoonal complex. Sands farther to the west may be bar sands seaward of the tidal flat areas.

Sand bodies farther south, however, are more mature, suggesting a higher energy of deposition. One of the models (lower left) indicates that sand was swept westward and northwestward by marine currents and deposited as a large marine spit. The second model (upper left) is similar to the modern Gulf Coast

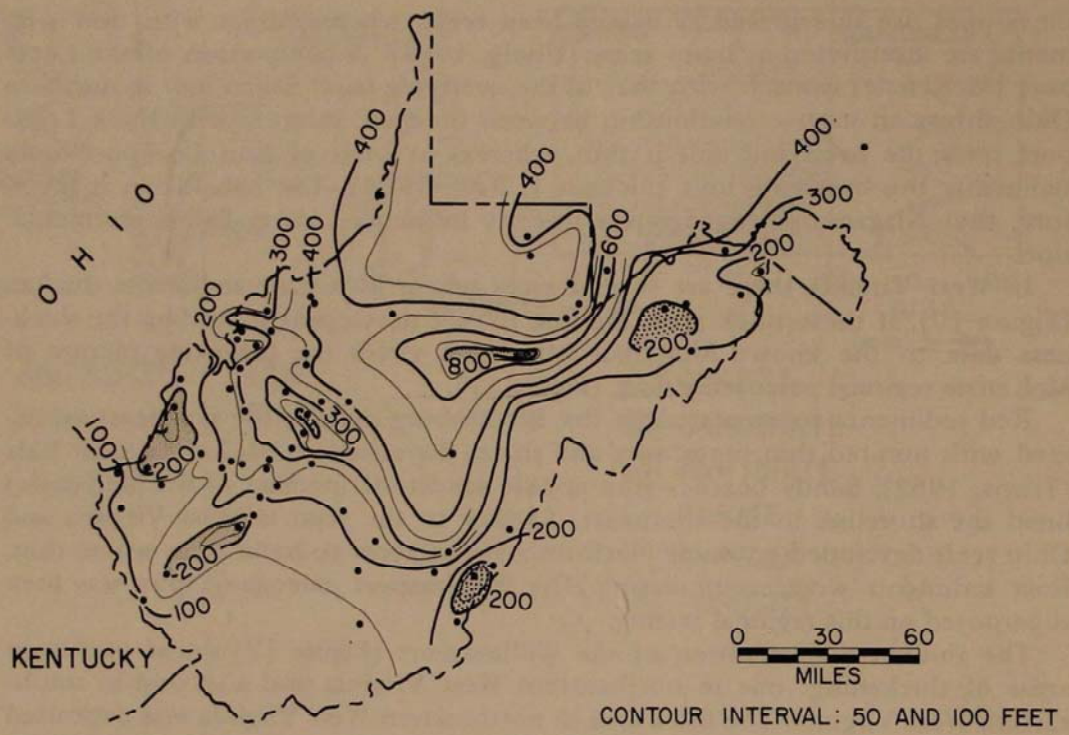

FIGURE 10. Isopachous map of the McKenzie Formation.

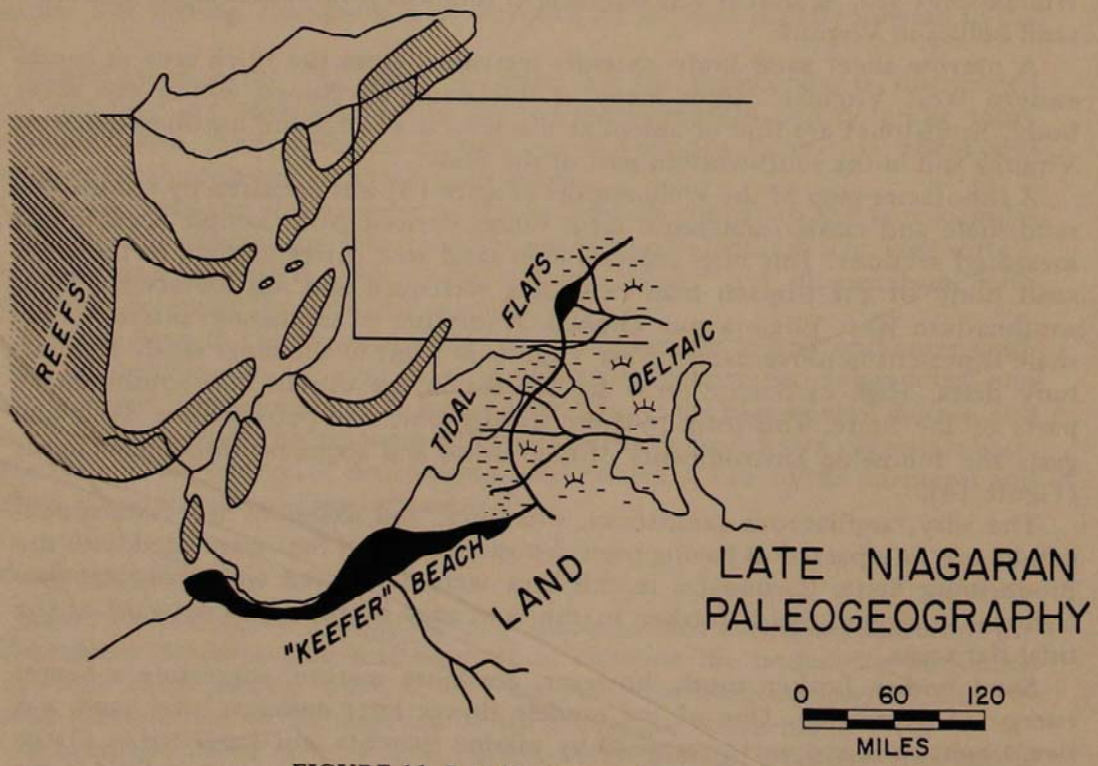

FIGURE 11. Late Niagaran paleogeography.

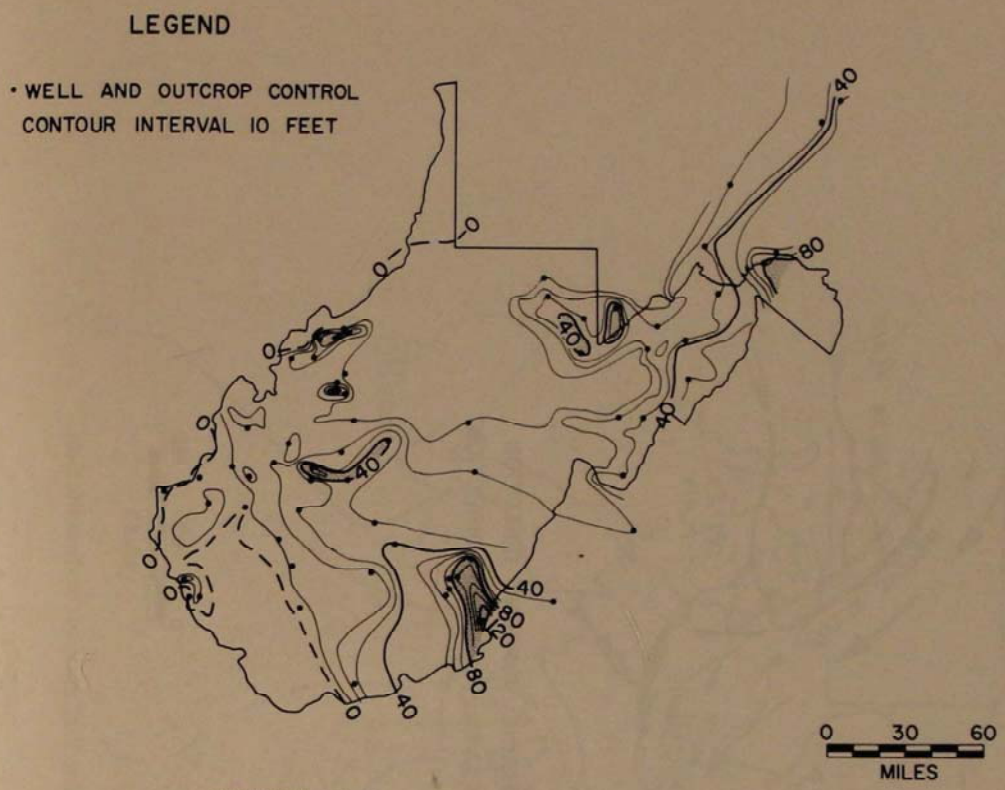

FIGURE 12. Isopachous map of the Williamsport Sandstone.

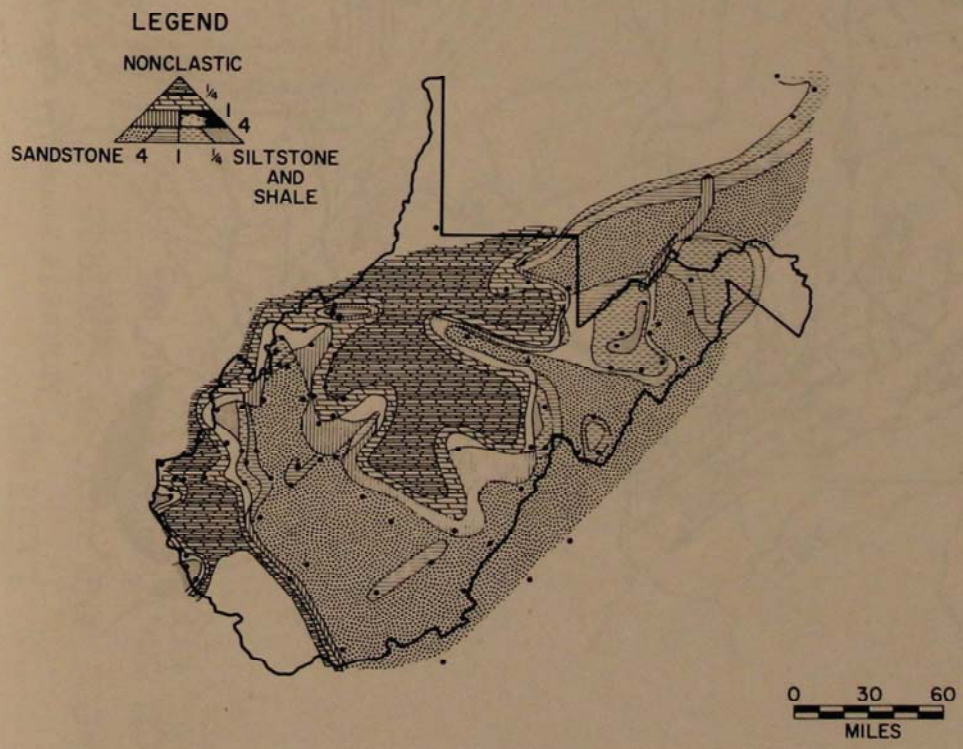

FIGURE 13. Lithofacies map of the Williamsport Sandstone.

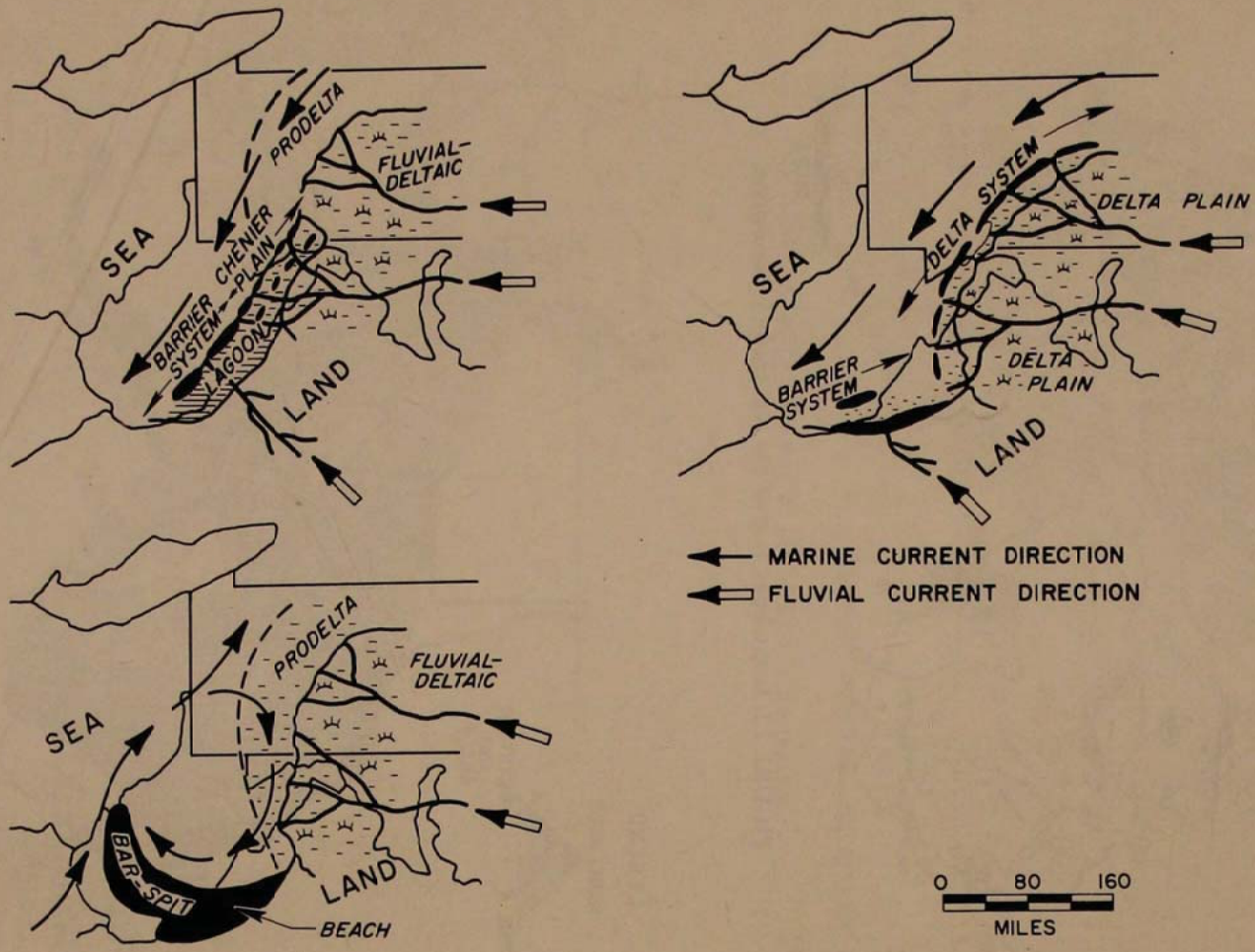

FIGURE 14. Summary of suggested models for Williamsport sedimentation.

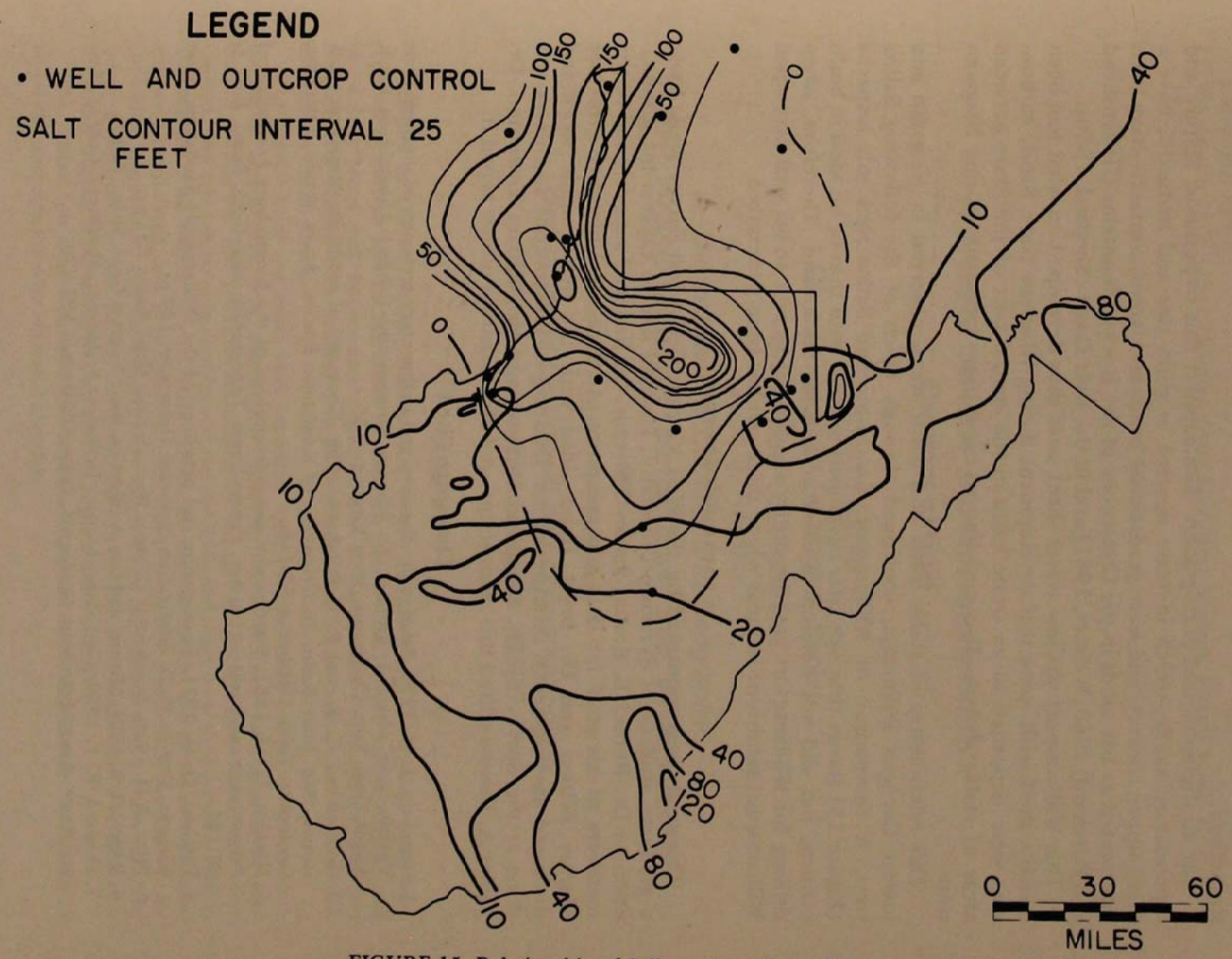

FIGURE 15. Relationship of Salina salt and basal Cayugan sand thickness.

area with a delta system, chenier plain, and barrier system. Thus, the marine currents in this model are reversed from the first model, placing the barrier system downcurrent from the delta. The third model, which is similar in the northeast to the present Nile delta, includes a beach-barrier system in the southeast. Regression of the shoreline would spread a sheet of sand westward and northwestward, with thicker sands developing during times of more stable strandlines.

The stratigraphic and petrographic data support this hypothesis. Mature and supermature sands—which increase upward in grain size and maturity, have a sharp upper contact, and have gradational lower and lateral contacts—have been interpreted as bar sands in the Cretaceous of the Rocky Mountains (Hollenshead and Pritchard, 1960; Weimer, 1961) and in the Gulf Coast (Shepard, 1960).

This Williamsport shallow water sheet sand thus developed on what had been a stable shelf with some reef development during Niagaran time. Sandy carbonates were deposited in an ovate basin in the central part of the State between areas of stable shelves. This area also received basin sediments during Niagaran time.

This relationship of stable shelf and basin areas, observed in Niagaran and lowest Cayugan sediments, continued through much of the following Salina time. A comparison of Williamsport Sandstone and Salina rock salt isopachs (Figure 15) shows that salt later developed in areas with thin or no sand in basin centers, but did not develop in shelf areas with thick sand. Therefore, when drilling for Williamsport gas, the driller should not expect to hit well-developed Williamsport sandstone in areas where thick salt has been penetrated.

Acknowledgments

This study was sponsored by the West Virginia Geological Survey while I was a graduate student at Syracuse University. I would like to express my appreciation to Dr. Robert B. Erwin, Survey Director, for financial support, and to the members of his staff for data and assistance. At Syracuse University Professor Murray Felsher and Dr. Bryce Hand aided with the petrographic work and discussed environmental interpretations. Drafting of illustrations and slides was done at the Survey by Mr. Raymond Strawser and Mr. William Townsend. Dr. James A. Barlow edited this manuscript, and Mrs. Jeanne Fullmer typed it.

Literature Cited

1. Dennison, J. M. 1970. Silurian stratigraphy and sedimentary tectonics of southern West Virginia and adjacent Virginia. In *Silurian Stratigraphy Central Appalachian Basin.* Appal. Geol. Soc., Charleston, West Virginia: 2-33.
2. Hollenshead, C. T., and R. L. Pritchard. 1960. Geometry of producing Mesaverde sandstones, San Juan Basin. In *Geometry of Sandstone Bodies.* Amer. Assoc. Petroleum Geologists, Tulsa, Oklahoma: 98-118.
3. Hoskins, D. M. 1961. Stratigraphy and paleontology of the Bloomsburg Formation of Pennsylvania and adjacent states. *Pennsylvania Topographic and Geol. Surv., Bull.* G 36:124.
4. Patchen, D. G. 1971. Stratigraphy and petrology of the Williamsport Sandstone, West Virginia. Unpub. Ph.D. dissertation, Syracuse University: 109 p.
5. Price, P. H. 1929. Pocahontas County. *West Virginia Geol. Surv.:* 531 p.
6. Reger, D. B. 1924. Mineral and Grant counties. *West Virginia Geol. Surv.:* 624 p.
7. Shepard, F. P. 1960. Gulf Coast barrier. In *Recent Sediments, Northwest Gulf of Mexico.* Amer. Assoc. Petroleum Geologists, Tulsa, Oklahoma: 197-220.

8. Travis, J. W. 1962. Stratigraphy and petrographic study of the McKenzie Formation in West Virginia. Unpub. M.S. thesis, West Virginia University: 137 p.
9. Ulteig, J. R. 1964. Upper Niagaran and Cayugan stratigraphy of northeastern Ohio and adjacent areas. *Ohio Geol. Surv., Rept. of Invest.*, no. 51: 48 p.
10. Weimer, R. J. 1961. Spatial dimensions of Upper Cretaceous sandstones, Rocky Mountain area. In *Geometry of Sandstone Bodies.* Amer. Assoc. Petroleum Geologists, Tulsa, Oklahoma: 82-97.
11. Woodward, H. P. 1941. Silurian System of West Virginia. *West Virginia Geol. Surv.* 14:326.

Analysis of Benzene- and Chloroform-Soluble Organics of Coal

Donald L. Streib
Ohio Division of Geological Survey
Columbus, Ohio 43212
John J. Renton
Department of Geology and Geography
West Virginia University, Morgantown, West Virginia 26506
and
Robert V. Hidalgo
West Virginia Geological and Economic Survey
Morgantown, West Virginia 26505

Abstract

Samples of the Pittsburgh, Bakerstown, Upper Freeport, and Kittanning coals were reduced in particle size to 325 mesh by successive use of a sturtevant laboratory roll mill and a Spex Mixer mill. Representative samples were obtained using a riffle splitter. The coal samples were leached with benzene in a Soxhlet extractor for 40 hours, then leached with chloroform for 30 hours.

The organic acids and bases were separated from the extracting solvent with potassium hydroxide and sulfuric acid, respectively, and the neutral oils were concentrated by controlled distillation. The fractions containing the organic acids and organic bases were neutralized, and ethyl ether was used to remove the acids and bases from their aqueous media. The organic acids were separated into weak and strong fractions by use of sodium bicarbonate, were neutralized, and were removed with ethyl ether. The ethyl ether was removed by controlled distillation, and the samples were weighed and then dissolved in carbon disulfide. Infrared spectroscopy was used to verify the indentity of the weak organic acids as phenolic, the strong organic acids as carboxylic, and the organic bases as amines.

The neutral oils were separated into aliphatics, aromatics, and asphaltenes by the use of liquid chromatography over activated alumina.

The purpose of this investigation was to quantitatively extract, separate, and identify various organic groups of coal (Figure 1). Samples of the Pittsburgh coal used in this study were collected from the Consolidation Coal Company Humphrey #7 Mine at Mt. Morris, Pennsylvania. Samples of the Bakerstown, Upper Freeport, and Kittanning coals were collected from outcrops in Preston County, West Virginia (Figure 2). Channeling, either of mine pillars or outcrops, was used to collect the samples after removal of the outer layer of coal to minimize contamination.

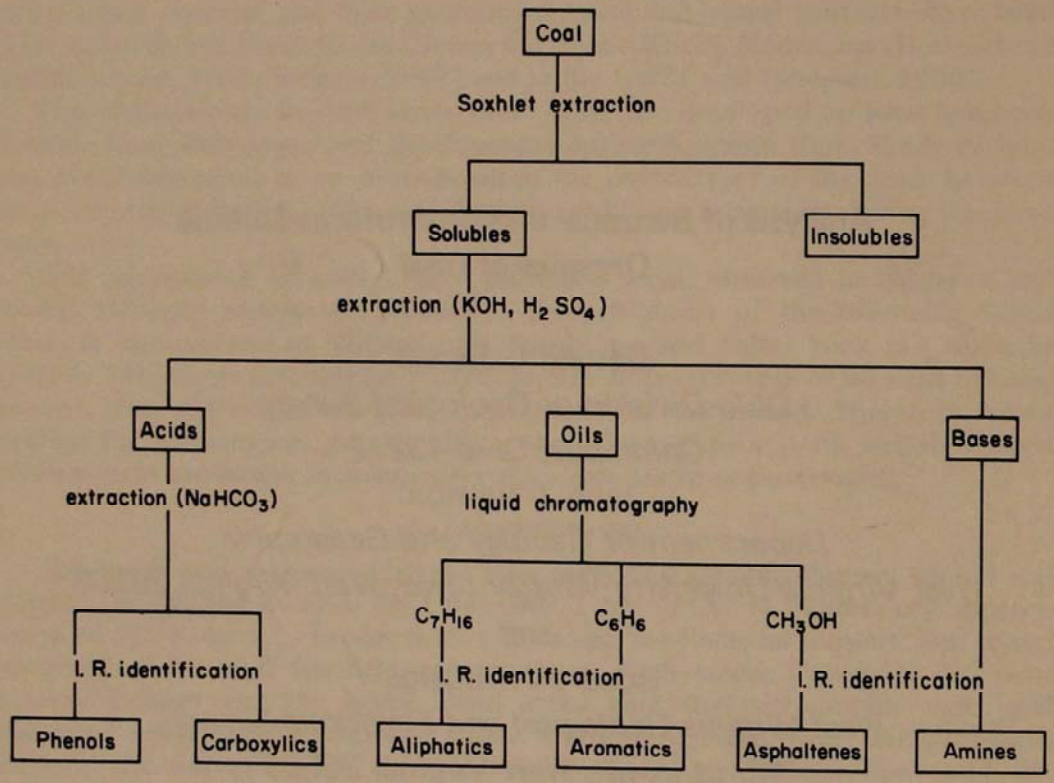

FIGURE 1. General Flow Chart

Materials and Methods

Each coal sample was reduced initially in a sturtevant laboratory roll mill to approximately 10 mesh, then reduced in particle size by a Spex Mixer mill to less than 325 mesh. A 5-minute grinding-cooling cycle was used in the Spex Mixer mill to prevent the buildup in the grinding vial of excessive heat which could result in thermal alteration of the organic components of the coal. After completion of the particle-size reduction process, a representative sample of 100 g was removed with a riffle splitter and weighed to 0.0000 g.

The soluble organic groups were leached from the coal by the use of a Soxhlet extraction technique. The advantages of Soxhlet extraction are that it need not be attended, the extracting solvent may be maintained at just below

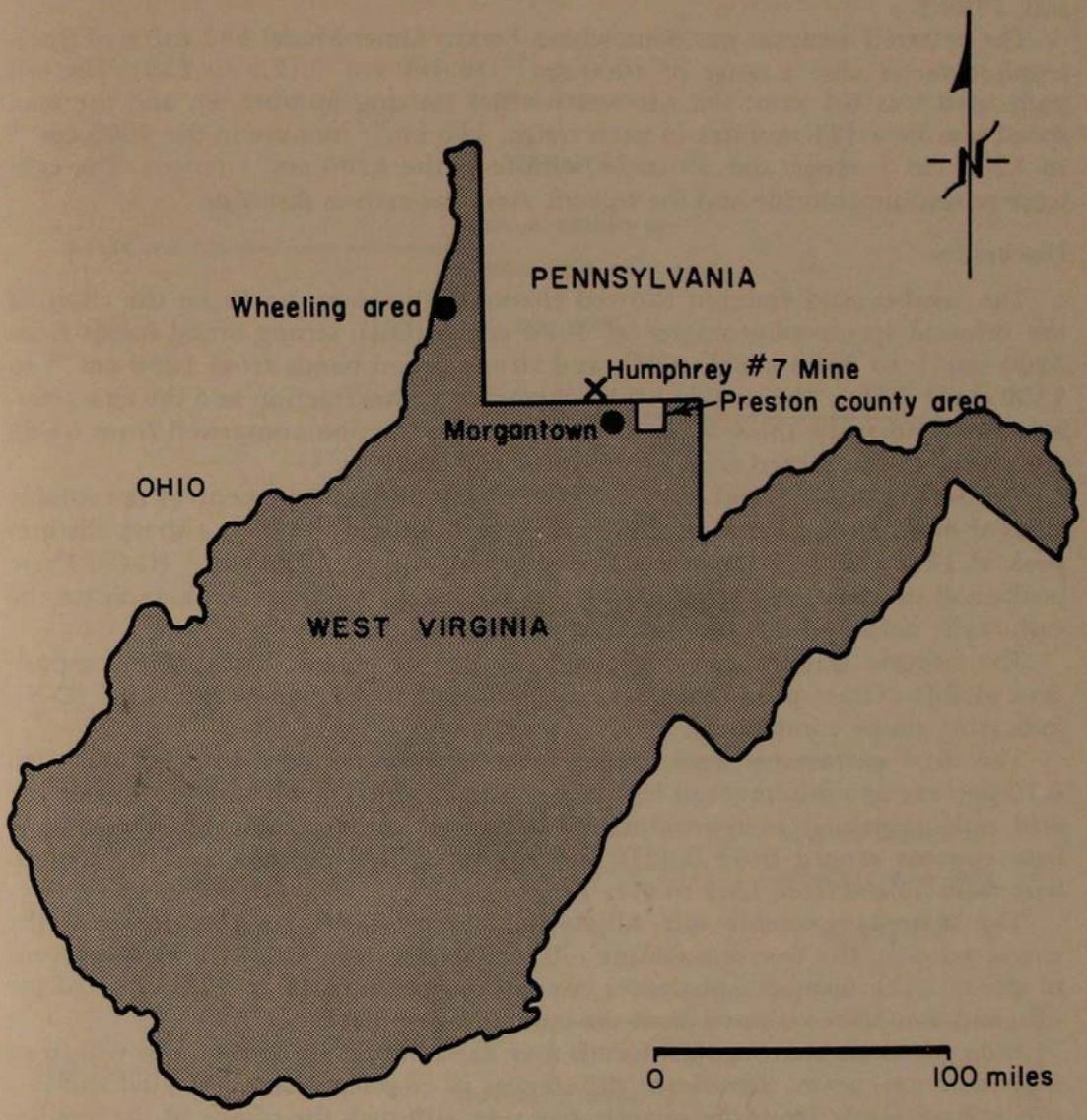

FIGURE 2. General location map of Morgantown and Wheeling sample areas.

the boiling point, and particulate contamination is kept at a minimum. The coal samples were first extracted with benzene for 40 hours, then with chloroform for 30 hours.

The organic acids were removed from the extracting solvent by treatment with potassium hydroxide, and the organic bases were removed by treatment with sulfuric acid (Figure 3 and 4) (Karr, *et al.*, 1966). The organic acids were separated into weak and strong acid fractions by treatment with sodium bicarbonate (Figure 3). The extracting solvent was removed by controlled distillation from the soluble oils remaining in solution after removal of acids and bases, and the oils were separated into three fractions using liquid-column chromatography. The concentrated oils were introduced into a layer of organic-free silica sand above a column packed with Alcoa F-20 80-200-mesh alumina, and liquids

of increasing polarity were eluted in sequence. (Figure 5) (Stevenson and Dickerson, 1969.)

The infrared analysis was done with a Perkin-Elmer Model 337 Infrared Spectrophotometer with a range of 4000 cm^{-1} to 400 cm^{-1} (2.5 to 25μ). The cell path used was 0.1 mm; the slit was normal (setting number 4), and the scan speed was slow (24 minutes in each range, 116 cm^{-1}/minute in the 4000 cm^{-1} to 1200 cm^{-1} range and 33 cm^{-1}/minute in the 1200 cm^{-1} range). The cells were potassium chloride and the solvent used was carbon disulfide.

Discussion

The weaker acid fraction showed characteristic sharp peaks on the chart of the infrared spectrophotometer at 3620 cm^{-1} (OH), strong broad bands from 3200 cm^{-1} to 3600 cm^{-1} (OH), and strong broad bands from 1230 cm^{-1} to 1300 cm^{-1} (C-O). The weakly acidic character of this fraction and the characteristic peaks identify these acids as phenols. The fraction comprised from 61-68 percent of the extracted acids in a total of 158 analyses.

The strong organic acid fraction, comprising 32 to 39 percent of the soluble acids showed strong bands at 2500 cm^{-1} to 3000 cm^{-1} (OH), a sharp distinct peak at 1740 cm^{-1} (C-O), and a strong broad peak at 1250 cm^{-1} (C-O). These peaks and the relatively strong acidity as compared to the phenols indicate the carboxylic nature of this fraction of the soluble acids.

The sulfuric acid extract contained the soluble organic bases. The composition of this extract produced peaks at 3400 cm^{-1} (N-H) and 1200 cm^{-1} (C-N), indicating amine compounds.

The total extractable acid ranged from a maximum of slightly greater than 0.10 percent to a minimum of less than 0.02 percent. The phenolic to carboxylic acid ratio remained at approximately 2:1 in all samples analyzed. The organic base content ranged from 0.0212 percent to 0.0078 percent, and the acid-to-base ratio ranged from 15:1 to 6:1.

The N-heptane-soluble oils, aliphatics, comprised 46 to 51 percent of the extracted oils. The benzene-soluble oils, aromatics, comprised 27 to 33 percent of the oil. The opaque asphaltenes constituted the final 16 to 27 percent of the oils, and they were stripped from the column using methanol.

Indications are that regional trends may exist in organic compounds within an individual coal seam. Significant differences in coal seams are indicated also in a preliminary study from the quantitative side, although the results of the qualitative analysis has been the same in all seams tested.

Acknowledgments

The authors would like to thank the West Virginia Geological and Economic Survey for the financial help that made this study possible.

Literature Cited

1. Karr, C., J. R. Comberiati, K. B. McCaskill, and P. A. Estep. 1966. Evaluation of low temperature coal tars by a rapid detailed essay based on chromatography: *J. Applied Che.*, vol. 16, no. 1, reprint.
2. Stevenson, D. L., and D. R. Dickerson. 1969. Organic geochemistry of the New Albany shale in Illinois: *Petrol. Bull.* Ill. Geol. Survey, 11 p.

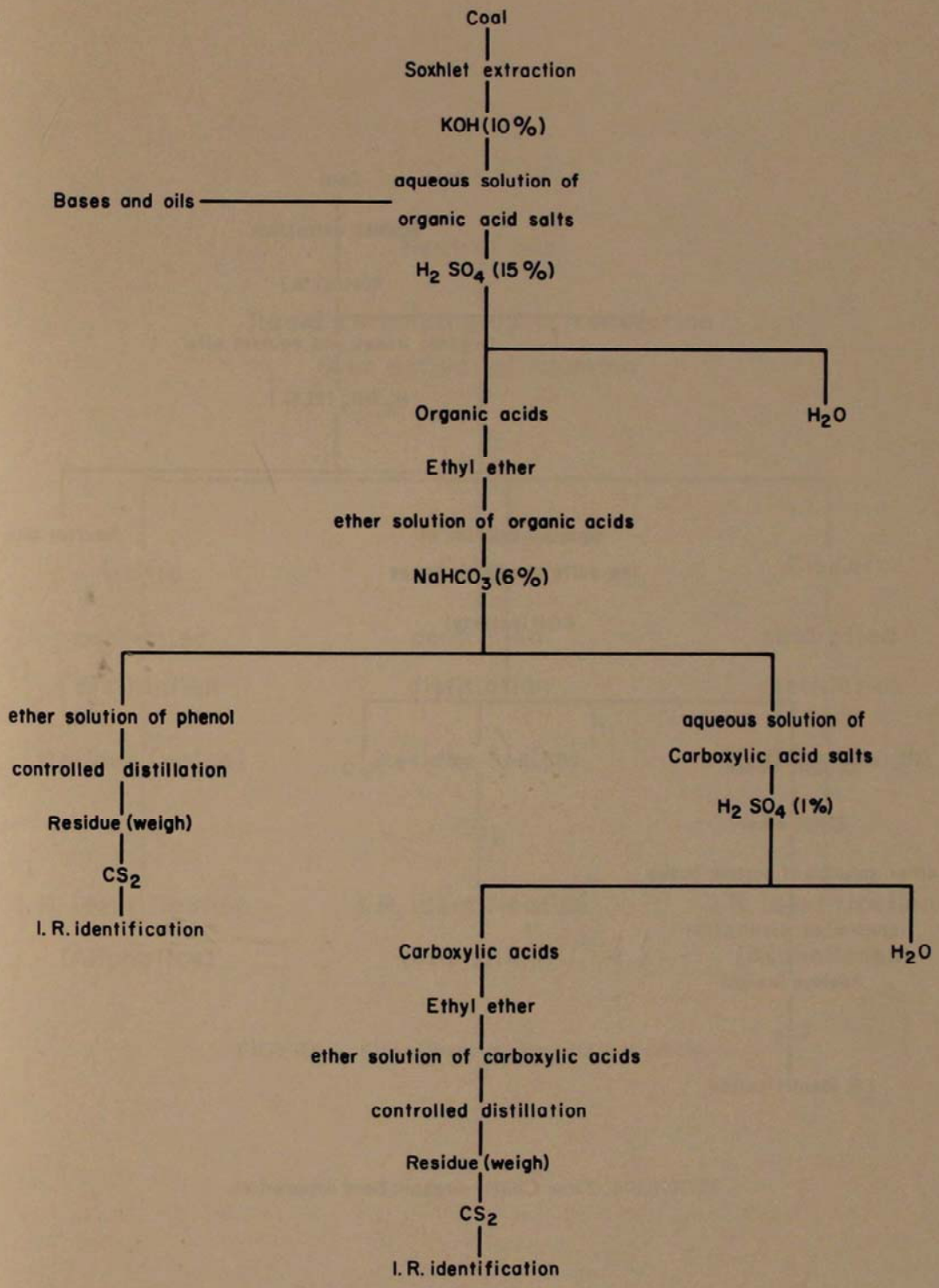

FIGURE 3. Flow Chart—organic acid separation.

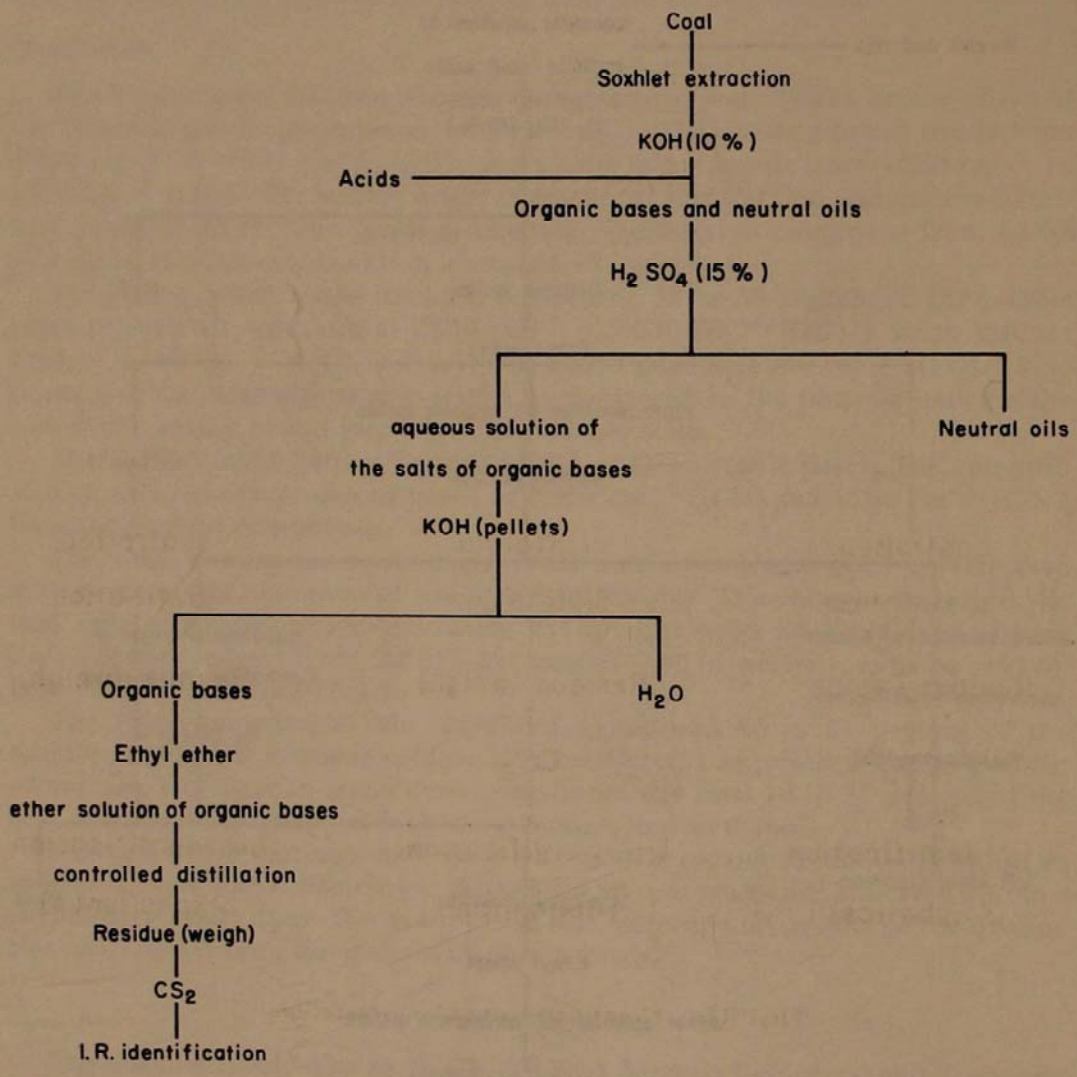

FIGURE 4. Flow Chart—organic base separation.

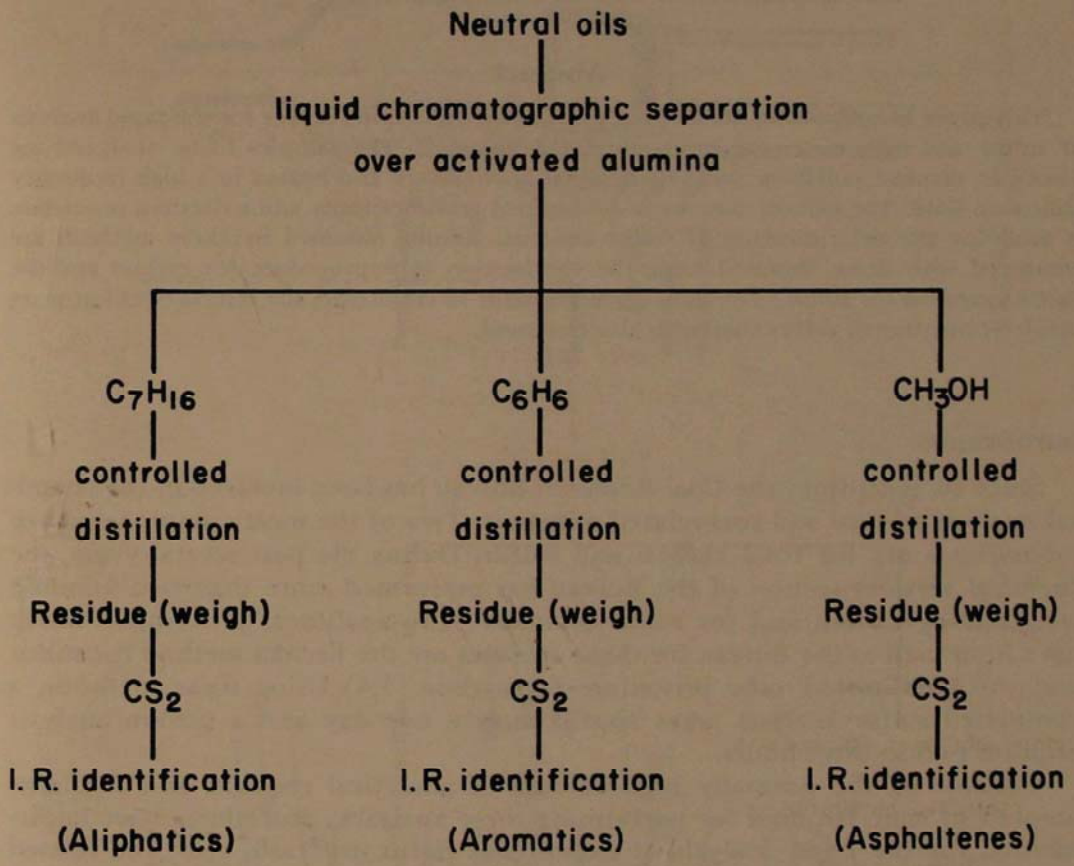

FIGURE 5. Flow Chart—neutral oil separation.

Procedures for the Rapid Determination of Carbon and Sulfur

Lionel L. Craddock
Coal Research Bureau, School of Mines
West Virginia University
Morgantown, West Virginia 26506

Abstract

This paper is a report on methods of utilizing an induction furnace for the rapid analysis of sulfur and carbon in coal and coal-related materials. The samples to be analyzed are placed in ceramic crucibles along with metal accelerators and heated in a high frequency induction field. The carbon content is determined gravimetrically and a titration procedure is used for the determination of sulfur content. Results obtained by these methods are compared with those obtained using the combustion tube procedure for carbon and the Eschka method for sulfur. The use of sodium azide to counteract the effects of chlorine on the determination of sulfur content is also discussed.

Introduction

Since its inception, the Coal Research Bureau has been involved in the chemical analysis of coal and coal-related materials. Two of the most common analytical requests are for total carbon and sulfur. During the past several years, the chemical services section of the Bureau has performed more than two hundred analyses for carbon and for sulfur annually. The analytical procedures which have been used at the Bureau for these analyses are the Eschka method for sulfur and the combustion tube procedure for carbon.(3,4) Using these methods, a completed sulfur analysis takes approximately one day and a carbon analysis requires two to three hours.

Because of the normally high volume of analytical requests and the large amount of time required for performing these analyses, procedures were implemented for the rapid analysis of carbon and sulfur in flyash, coal, and related materials utilizing an induction furnace.(6) These procedures utilize the equipment and techniques developed by the Laboratory Equipment Corporation (LECO) for the analysis of carbon and sulfur in steel and steel alloys.

Experimental Procedures

Induction Heating

An alternating electrical current, I(t), flowing through a conducting coil sets up a time-varying magnetic field, H(t), along the axis of the coil (Figure 1). When a metal is placed inside the coil, eddy currents are formed in the conductor. The amount of heat produced in the metal by the eddy currents is a function of the current, the current frequency, the reciprocal of the distance between the coil and the metal, and the permeability and resistivity of the metal. Large coil currents and high frequencies produce greater temperatures.

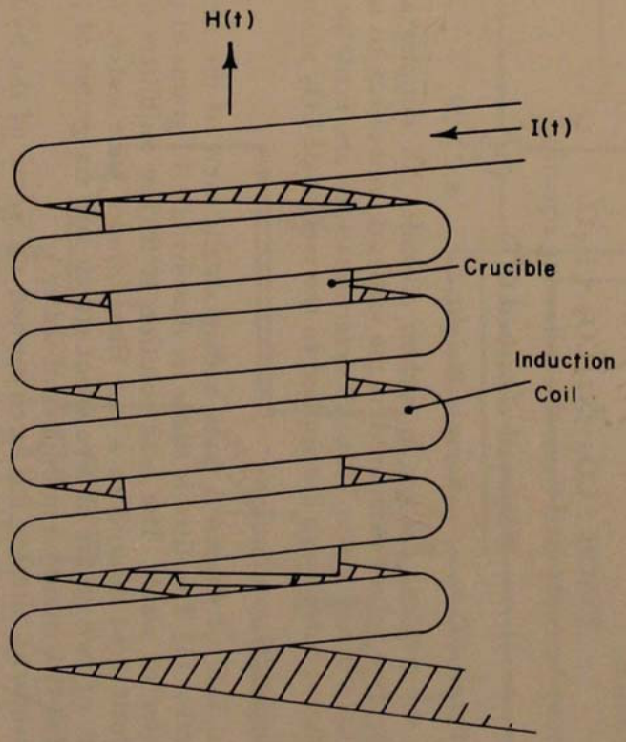

FIGURE 1. The induction coil.

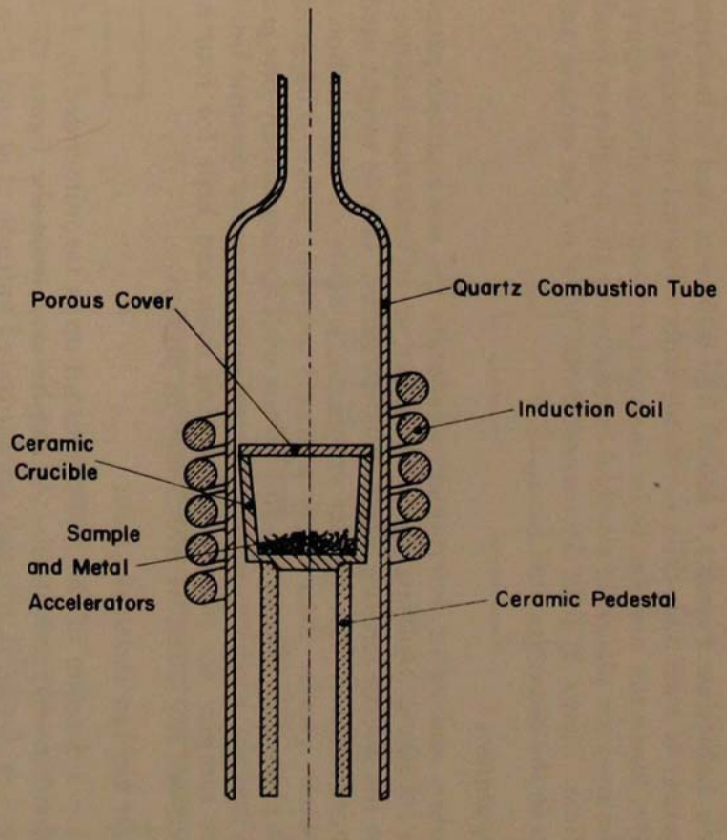

FIGURE 2. Cross-sectional view of the induction coil.

The Leco Induction Furnace,* Model 523-000, was used in this study. The source of power is a vacuum-tube oscillator with a normal operating frequency of 13.4 MHz. Since the samples to be analyzed are non-metallic in composition, metal accelerators are placed in physical contact with the samples to produce the necessary heat. Figure 2 gives a cross-sectional view of the sample and metal accelerators in the induction coil.

Sample Preparation

Both carbon and sulfur determinations require the same sample preparation. All samples are run in duplicate and are weighed on an analytical balance with an accuracy to the fourth decimal place. The maximum sample weight used in this study is approximately one-quarter gram; the weights of high carbon samples (carbon content greater than thirty percent) are kept below 0.05 grams. The samples are placed in ceramic crucibles along with approximately one gram each of the iron and tin accelerators and covered with a porous ceramic lid. Prior to analysis the samples are placed in a drying oven and kept for four hours at 105°C to remove any moisture which may be present.

Procedure for Carbon Determinations

Figure 3 is a diagram of the equipment set-up as recommended by LECO for carbon and sulfur determinations. As can be seen from the figure, commercial grade oxygen is bubbled through concentrated sulfuric acid and then passed through ascarite to remove trace amounts of moisture and carbon dioxide.

The right-hand side of Figure 3 depicts the gas flow for carbon determinations: Excess oxygen and gases from the combusting sample pass through a cloth dust trap, a sulfur trap containing manganese dioxide, a catalyst furnace which converts carbon monoxide to carbon dioxide, a moisture trap of magnesium perchlorate, and finally through an ascarite absorption bulb where the carbon dioxide is collected. The carbon dioxide is absorbed by the ascarite according to the following reaction:

$$2NaOH + CO_2 \rightarrow Na_2CO_3 + H_2O.$$

Percent carbon may be computed from the following equation:

$$\text{Percent C} = \frac{\text{Weight of absorbed } CO_2}{\text{Sample Weight}} \times 27.29,$$

where 27.29 is the percent carbon in carbon dioxide. All samples are run in duplicate and the two values compared; if the values do not check to within five percent, the sample is run again. "Blank" determinations are made periodically and, when necessary, corrections are applied to the weight of CO_2 absorbed.

Procedure for Sulfur Determinations

The left-hand side of Figure 3 gives a diagramatic view of the LECO automatic sulfur titrator.(5) The titre is made by dissolving 1.11 grams of potassium iodate in one liter of water. The acid solution is fifteen milliliters of concentrated hydrochloric acid diluted to a one liter volume with water. The starch solution consists of two grams of arrowroot starch and six grams of potassium iodide dissolved in two hundred milliliters of water.

After the automatic titrator has been turned on, some of the hydrochloric

*Use of trade names does not imply endorsement by the Coal Research Bureau.

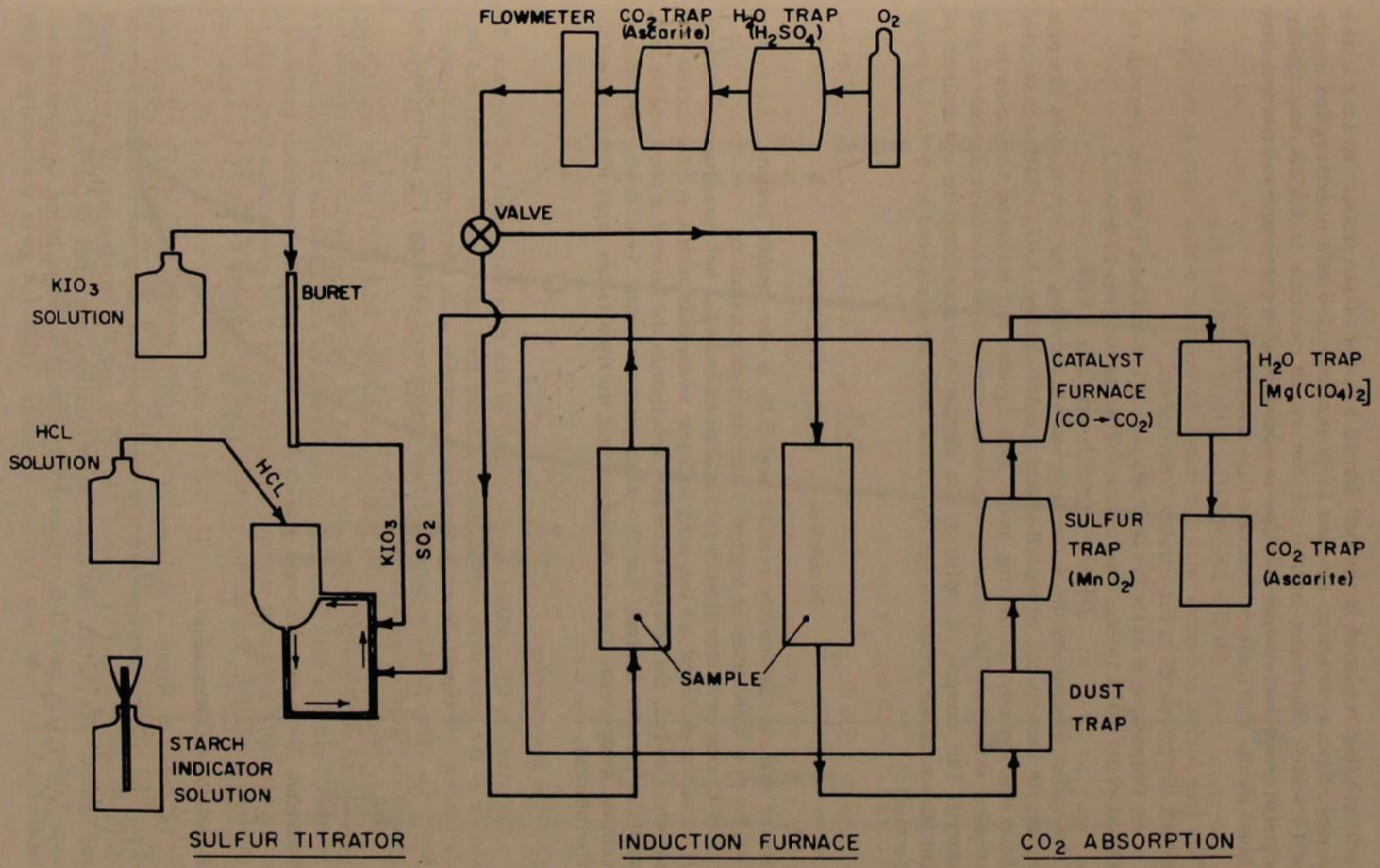

FIGURE 3. Schematic diagram of apparatus for determination of carbon and sulfur.

acid solution is placed in the bell-shaped housing of the titrator and the level is noted. Next a measured amount (approximately 0.6 mls as determined by the self-leveling dispensing bottle) of the starch solution is added; and finally, enough potassium iodate solution is added to give the liquid a "medium dark blue" color. The chemical reaction that takes place is:

$$6HCl + 5KI + KIO_3 \rightarrow 3H_2O + 6\ KCl + 3I_2.$$

The free iodine combines with the starch to produce a blue color in the liquid, which the photocell in the titrator "remembers."

As the sample is heated, sulfur dioxide is formed and is carried through the liquid in the bell housing, causing the following reaction to occur:

$$2H_2O + I_2 + SO_2 \rightarrow H_2SO_4 + 2HI.$$

The sulfur dioxide oxidizes the free iodine, reducing the intensity of the blue color. As soon as the photocell senses a color change, KIO_3 solution is released from the burette, producing more free iodine and restoring the color to its original intensity. This process continues until no more sulfur dioxide is produced. The amount of sulfur in the sample is proportional to the amount of potassium iodate added to the liquid and may be computed from the following formula:

$$\text{Percent S} = \frac{\text{B.R.}}{\text{S.W.}} \times 0.2500,$$

where B.R. is the burette reading and S.W. is the sample weight. If a sample weight of 0.2500 grams is used, the burette is direct reading.

After one determination, liquid is drained from the bell housing until its level is equal to the level of the acid solution when first added. A new measure of starch is added, the level of the KIO_3 solution in the burette is returned to zero, and the titrator is ready for the next determination. As with the carbon procedure, samples are run in duplicate and the two values must check to within five percent.

Chlorine Interference

Chlorine, as Cl_2, added to the liquid in the titration vessel will replace the iodine in the potassium iodide, causing more free iodine to be formed and thus darkening the liquid. Since some of the samples with which the Coal Research Bureau is concerned contain significant amounts of chlorine, the ability to counteract this interference is needed.

It was determined that the addition of sodium azide(1,2) to the starch solution would sufficiently negate the effect of chlorine on sulfur determinations. Synthetic samples with four percent sulfur and varying amounts of chlorine were prepared. These samples were analyzed for sulfur using the procedure previously described both with and without the addition of 2.00 grams of sodium azide to the starch solution. The results of these tests are depicted in Figure 4.

Results and Discussions

In order to obtain a measure of the accuracy of the analytical procedures described herein, identical samples were analyzed using the induction furnace methods and the Eschka method for sulfur and the combustion tube procedure for carbon. The carbon and sulfur determinations are listed in Tables I-A and I-B and Tables II-A and II-B, respectively. The procedures being investigated are labeled I.F. or Induction Furnace Methods. Table I-A gives the results of the

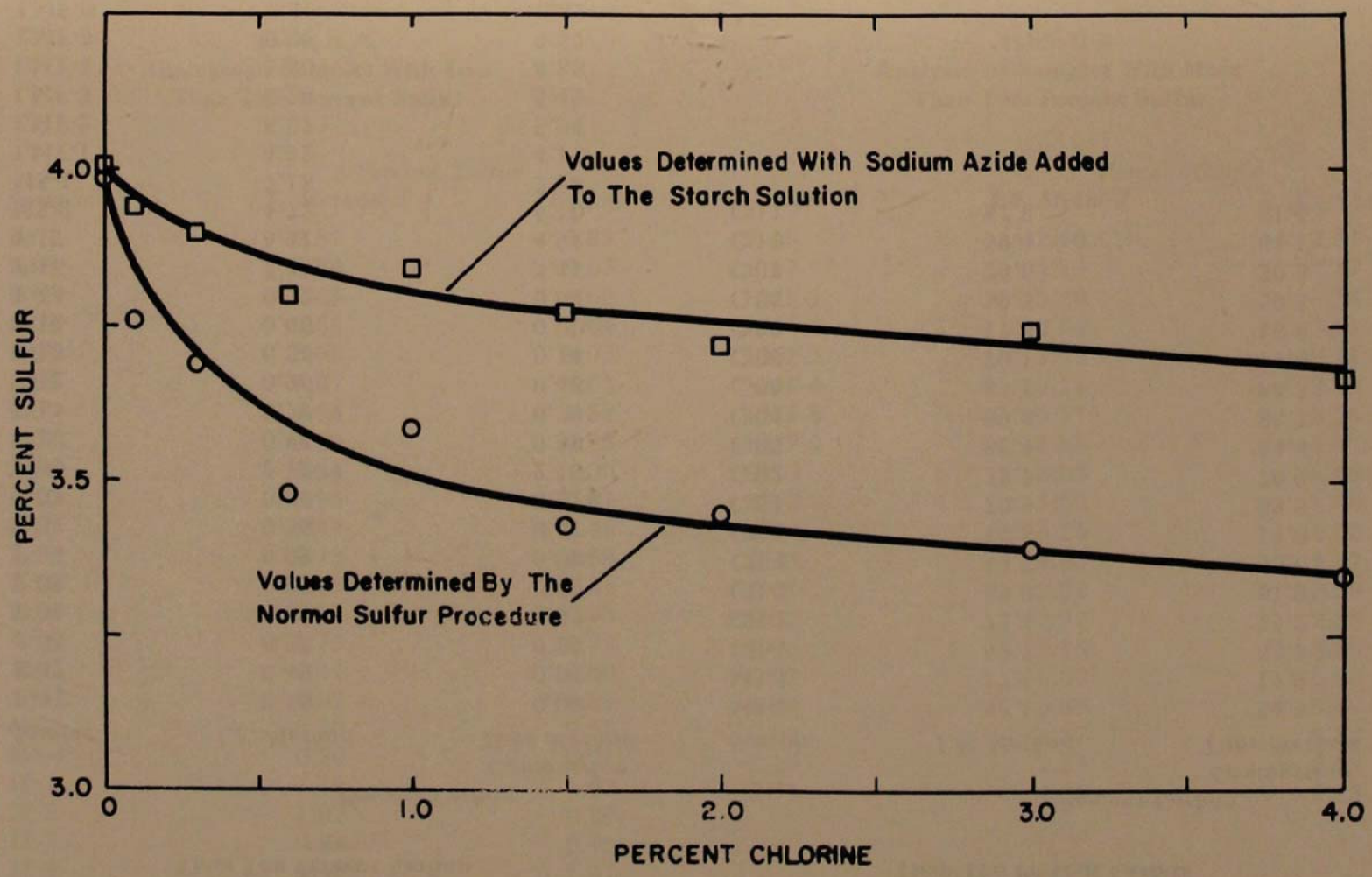

FIGURE 4. The effect of chlorine on sulfur determinations for synthetic samples with four percent sulfur.

Table I-A.
Analyses of Samples With Less Than Ten Percent Carbon

	Percent Carbon	
Sample	*I.F. Method*	*Combustion Tube Method*
F-01	0.10	0.00
F-02	0.49	0.54
F-03	0.20	0.25
F-04	0.54	0.63
F-05	0.85	0.92
F-06	0.09	0.00
F-07	0.36	0.41
F-08	0.20	0.22
F-09	2.12	2.16
F-10	0.84	0.89
F-11	0.79	0.79
F-12	0.96	0.46
F-13	0.24	0.14
F-14	0.00	0.00
F-15	0.53	0.64
F-16	3.44	3.41
F-17	5.31	4.91
MS-2	4.72	5.10
MS-4	7.18	7.28
LMF-1	4.32	4.17
LMF-2	6.27	5.94
LMF-3	6.28	5.49
LMF-4	5.80	4.88
LMF-5	9.22	9.67
LMF-6	2.30	2.22

Table I-B.
Analyses of Samples With More Than Ten Percent Carbon

	Percent Carbon	
Sample	*I.F. Method*	*Combustion Tube Method*
MS-1	32.1	34.5
MS-3	17.8	17.9
CH-1	52.7	53.7
CH-2	73.5	75.2
CH-3	59.9	61.9
CH-4	54.7	55.6
CH-5	14.8	14.0
C-01	70.9	69.9
C-02	72.7	70.9
C-03	82.4	84.4
C-04	89.8	85.7
C-05	83.1	80.3
C-06	70.1	71.8
C-07	17.3	16.8
C-08	59.3	59.3
C-09	29.6	30.3
C-10	59.4	64.1
C-11	57.8	61.4

Table II-A.
Analyses of Samples With Less Than Two Percent Sulfur

Sample	Percent Sulfur I.F. Method	Eschka
F-01	0.87	0.88
F-02	0.64	0.63
F-03	0.65	0.62
F-04	0.65	0.64
F-05	0.93	0.90
F-06	0.67	0.67
F-07	0.64	0.58
F-08	0.80	0.79
F-09	0.94	1.00
F-10	0.96	0.97
F-11	0.47	0.46
F-12	0.73	0.69
F-13	0.71	0.71
F-14	0.73	0.73
F-15	0.75	0.76
MS-1	0.44	0.40
MS-2	0.07	0.09
MS-3	0.30	0.33
MS-4	0.20	0.21
IF-1	1.10	1.02
IF-2	1.02	0.95
IF-3	0.98	0.95
IF-4	1.45	1.41
IF-5	0.89	0.95
LMF-5	1.20	1.27
C-03	0.60	0.64
C-04	0.54	0.67
C-05	0.57	0.63

Table II-B.
Analyses of Samples With More Than Two Percent Sulfur

Sample	Percent Sulfur I.F. Method	Eschka
F-16	2.46	2.61
F-17	3.19	3.17
LMF-1	3.20	3.34
LMF-2	2.86	3.01
LMF-3	9.42	9.71
LMF-4	9.21	9.39
LMF-6	5.11	5.25
LMF-7	4.68	5.02
CH-1	6.68	6.99
CH-3	3.56	3.68
CH-4	5.25	5.52
CH-5	4.85	4.77
C-01	2.92	2.99
C-02	2.97	2.88
C-06	3.15	3.25
C-07	6.00	5.86
C-08	5.69	5.69
C-09	5.37	5.44
C-10	2.53	2.63
C-11	4.05	4.28

carbon determinations of samples with less than ten percent carbon while Table I-B lists all other carbon results. Table II-A shows the percent sulfur in samples with less than two percent sulfur, while Table II-B lists the percent sulfur of all other samples. The samples are divided into these categories to facilitate statistical testing.

The designations of the samples listed in the tables are as follows:

F—flyash;
IF—incinerator flyash;
LMF—limestone modified flyash;
MS—miscellaneous samples;
CH—coal char; and
C—coal materials.

The miscellaneous samples category includes mine floor and strip mine floor samples. The coal materials include run-of-mine and treated coal samples.

When the first of the incinerator flyashes was analyzed for sulfur, the titration solution became darker in color without addition of potassium iodate. The presence of chlorine in all the incinerator flyashes was confirmed by treating these samples with nitric acid, precipitating the solute with silver nitrate, and then dissolving the precipitate with ammonium hydroxide. A procedure using sodium azide added to the starch solution was then devised to overcome the problems caused by the presence of chlorine. The sulfur content of the incinera tor flyashes was then determined using this procedure and is reported in Table II-A.

A paired t-test(7) was performed on the data in each of the above mentioned tables. In all cases the null hypothesis (H_o) is that there is no significant difference in the two methods, and the alternative hypothesis (H_a) is that there is a significant difference. The test statistic (computed t-value) is equal to the average of the differences of the data pairs divided by the standard deviation of those differences. The test of significance is the comparison of the computed t-value with the tabulated t-value at the 5% probability level. The results of these four tests are reported in the table below:

RESULTS OF PAIRED t-TESTS

Table	*Degrees of Freedom*	*t-Values*		
		Computed	*Tabulated*	*Result*
I-A	24	0.267	2.064	H_o Accepted
I-B	17	0.259	2.110	H_o Accepted
II-A	27	0.008	2.052	H_o Accepted
II-B	19	0.853	2.093	H_o Accepted

Tables III and IV give the results of what might be termed "reproducibility tests" of the two procedures described in this report. Seventeen determinations of the percent carbon in graphite (100% carbon) are reported in Table III. In Table IV are reported the values of fourteen determinations of the sulfur in a flyash material and twelve determinations of the sulfur in a coal char material. It should be noted that the values reported in Tables III and IV are results of individual runs and not the averages of duplicate determinations.

Table III.
The Carbon Content of Graphite by the I.F. Method

Run #	*Percent Carbon*
1	97.7
2	96.6
3	106.3
4	107.1
5	100.8
6	98.2
7	101.6
8	101.3
9	99.3
10	103.4
11	97.5
12	97.2
13	98.2
14	102.5
15	102.6
16	98.5
17	101.0
Average Value:	100.6
Standard Deviation:	3.1
Standard Error:	0.78

Table IV.
The Sulfur Content of a Flyash Sample and a Coal Char Sample by the I.F. Method

	Percent Sulfur	
Run #1	*Flyash F-5*	*Char CH-3*
1	0.888	3.55
2	0.889	3.53
3	0.907	3.59
4	0.904	3.39
5	0.954	3.68
6	0.889	3.56
7	0.947	3.63
8	0.964	3.56
9	0.958	3.48
10	0.941	3.68
11	0.944	3.49
12	0.948	3.54
13	0.945	
14	0.926	
Average Value:	0.929	3.56
Standard Deviation:	0.028	0.08
Standard Error:	0.007	0.02

Conclusions

Since standard samples with carbon and sulfur percentages covering the ranges of interest are not readily available, it is difficult to determine exactly the accuracy of the procedures described in this report. However, for the Coal Research Bureau, the induction furnace is satisfying the purpose for which it was intended—that of providing rapid carbon and sulfur determinations. After sample preparation, the time lapse for completing a carbon or sulfur analysis is generally from fifteen to twenty minutes. When compared to conventional procedures (one day for sulfur by the Eschka method and up to three hours for carbon by the combustion tube procedure) the savings in time and personnel are substantial.

Acknowledgments

The author wishes to acknowledge the assistance of Richard Muter, Gerald Moore, Edna Rogers, and Pam Trainer in the development of the analytical procedures. Special thanks go to David Akers, Pam Trainer, and Richard Muter for reviewing the manuscript. Also, thanks to Charles McFadden who drew the figures and to Sally See who typed the paper.

Literature Cited

1. Bremanis, E., Deering, J. R., Meade, C. F., and Keyworth, D. A. 1967. "Elimination of nitrogen and chloride interferences in the Iodometric Determination of Sulfur as Sulfur Dioxide," *Materials Research and Standards,* 7:459-60.
2. Fassett, David W., and Irish, Don D., eds. 1963. *Industrial Hygiene and Toxicology,* second revised edition (Sutton, William L., "Azides" pp. 2208-13), Interscience Publishers.
3. Furman, N. Howell, ed. 1966. *Standard Methods of Chemical Analysis,* vol. 1, 6th edition, D. Van Nostrand Co., Inc., Princeton, New Jersey.
4. Gaseous Fuels: Coal and Coke. 1967. *1967 Book of ASTM Standards,* Part 19, American Society for Testing and Materials, Philadelphia.
5. LECO Application Booklet, Form No. 133A, Laboratory Equipment Company, St. Joseph, Michigan.
6. Lozinskii, M. G. 1969. *Industrial Applications of Induction Heating,* Pergamon Press, New York.
7. Snedecor, George W., and Cochran, William G. 1967. *Statistical Methods,* 6th edition, The Iowa State University Press, Ames, Iowa.

Gravity Profile Across Massanutten Synclinorium at Bedington, West Virginia: A Study in Gravity Modeling of Near-surface Structure in the Central Appalachians

Jay R. Byerly
Department of Geology and Geography
West Virginia University
Morgantown, West Virginia 26506

Abstract

A gravity profile was surveyed across Massanutten Synclinorium in northern Berkeley County, West Virginia. The profile extends from Hainsville through Bedington, and terminates just west of the confluence of Opequon Creek and the Potomac River. A station spacing of 500 to 1000 feet was used. Station elevations have an absolute accuracy of plus or minus 0.25 feet while neighboring stations generally have a greater relative accuracy. Measurements of the vertical component of the gravitational field were made with a Prospector model of the Worden gravimeter. The instrument constant was 0.0941(3) milligals per scale division, with a reading accuracy of approximately 0.01 milligals. The individual stations were looped to a base station reoccupied at two-hour intervals. The terrain-corrected Bouguer gravity values have cumulative errors no greater than approximately 0.1 milligal.

The Martinsburg Shale is the youngest formation found in Massanutten Synclinorium in West Virginia. It and all older Ordovician units present in the local geologic column were incorporated into gravity-modeled cross-sections. Density values were assigned from Jolly balance measurements of surface samples, from estimated densities based on published and unpublished descriptions of lithologies, and from preliminary modeling results. All but three units are predominantly limestone and have densities around 2.70 to 2.71 gm/cm^3. Two high-density zones exist in the local Ordovician column. One zone consists of the Martinsburg Shale with densities from 2.740 to 2.755 gm/cm^3. The other, older zone consists of the Pinesburg Station Dolomite and the dolomitic upper Rockdale Run Formation, with an average density of 2.82 to 2.83 gm/cm^3.

Two-dimensional modeling was undertaken with the aid of a computer program. The program is based on an integral that calculates variations in the vertical component of gravity for sets of two-dimensional, plane laminae. Gravity intensities could thereby be calculated for cross-sectional models consisting of a series of polygons representing various groupings of bodies with variable masses and an infinite extent in the third dimension.

A significant gravity high exists over the portion of Massanutten Synclinorium underlain by the high-density dolomite zone. The intensity of this high ranges from 1.5 to 1.8 milligals above the regional background intensity and has a width of nearly 3.5 miles.

Accurate density values were impossible to obtain for the Martinsburg Shale without modeling. Nettleton profiling and actual sample measurements (featuring a statistical search for water-saturated weight limits) suggest low densities (2.70 to 2.71 gm/cm^3) because of weathering. Bulk-density logs and well cores are not commonly taken from the Martinsburg Shale. Where the profile crosses several small synclines within the Massanutten Synclinorium, the Martinsburg Shale produces rounded gravity peaks with an amplitude of approximately 0.30 milligals on the broader gravity high due to the dolomite zone.

Small but excessive gravity lows appear to exist where the Chambersburg, New Market, and Row Park Limestones crop out on the limbs of the Synclinorium and on two intervening small anticlines. The increased mass deficiency is best explained as the effect of ground water solutioning of these units. Estimates of available thickness (30 to 100 feet) and

density (2.565 gm/cm^3 for five percent solutioning) of the anticlines fit well in the modeling process. Solutioning appears necessary to provide reasonable models of at least two points on the profile.

A combination of geological mapping by previous investigators and the results of gravity modeling indicate that the folds in Massanutten Synclinorium are asymmetrical. Folds near the overturned eastern limb of the Synclinorium appear to be overturned. One anticline may be cut by at least one small thrust fault. The gravity modeling has also shown that the most sensitive geometric variable in this gravity profile is the thickness of the dolomite zone. Observed gravity intensities, when fit to subsurface models, do not indicate any significant thinning of the dolomite zone eastward across the Synclinorium.

Mathematical Analysis of Hammer Zones Used in Terrain Corrections for Gravimeter Stations

Jay R. Byerly
Department of Geology
and
Henry W. Gould
Department of Mathematics
West Virginia University
Morgantown, West Virginia 26506

Abstract

Computation of terrain correction factors in Hammer zones is based on the formula $\varepsilon = 2\pi\gamma\sigma\left[R - r + (r^2 + h^2)^{1/2} - (R^2 + h^2)^{1/2}\right]$ for the gravitational attraction of a vertical hollow cylinder at a point on the axis and in the plane of one end of the cylinder, where r and R are the inner and outer radii, h is the height of the cylinder (average height of terrain), γ is the gravitational constant, and σ is the density of the surface material. Hammer's system uses thirteen zones, A through M. The innermost zone, A, is seldom used unless the station is situated on or near a very sharp topographic feature. For zone A, r=0 and this circumstance makes the behavior of the corrections for that zone differ from those for the remaining zones. We illustrate by comparing and contrasting zones A and B. Precise tables of values and graphs are given which may be of interest and use to those working with these zones.

When the topography around a gravimeter station departs considerably from a horizontal plane, the observed value of gravity is reduced, since both the mass above the station level, and the deficiency of mass below, contribute a negative effect. A terrain reduction to be added to the observed value is most often found by dividing the region around the station into standard zones, bounded by concentric circles and radii, estimating the mean difference in elevation of each

zone from that of the station, and then applying a correction for each zone, based on this difference and on the density of the surface material.

Two systems have been used to construct templates of zones. These are the systems of John F. Hayford and Sigmund Hammer. Hammer's system is described in his original paper [2] and both systems are described in Garland's paper [1]. Hammer's system is used commonly when the effects of more distant features may be ignored. In each system, each zone is divided into a number of compartments and correction factors are found for each compartment. Table 1 below gives the description of the zones for both systems. The outer radius of a given zone is the inner radius of the next.

Table 1. Standard Zones for Terrain Corrections

	Hayford Zones			*Hammer Zones*	
Zone	*Outer radius (meters)*	*No. of Compts.*	*Zone*	*Outer radius (feet)*	*No. of Compts.*
A	2	1	A	6.56	1
B	68	4	B	54.6	4
C	230	4	C	175	6
D	590	6	D	558	6
E	1280	8	E	1280	8
F	2290	10	F	2936	8
G	3520	12	G	5018	12
H	5240	16	H	8578	12
I	8440	20	I	14662	12
J	12400	16	J	21826	16
K	18800	20	K	32490	16
L	28800	24	L	48365	16
M	58800	14	M	71996	16
N	99000	16			
O	166700	28			

It will be observed that the inner zone in both systems is of radius 2 meters, a very small zone. Unless the gravity station is situated in a very peculiar spot the effects of such a small zone may be neglected. However, there are instances where this zone is of use.

Gravity stations must be situated at points of known elevation for the proper reduction of the observed gravity data. Many times elevation points are located on natural or manmade topographic features with extreme relief within zone A of Hammer's system. Usually points of reference elevation located at positions with localized, but irregular and excessive, relief are bypassed by surveying to more suitable station positions nearby. The solitary field observer of a gravity survey can not follow this procedure, and the simple use of a handlevel for approximate elevations may not be accurate enough or even feasible under certain circumstances. The use of existing elevation points may also be expedient when the amount of time available for field work is a limiting factor. The accurate measurement and recording of variations in relief in zones A and B with templates printed on recording sheets allow for the determination of average elevations for use with the calculated tables.

Tables of correction factors are based on the well known formula

(1) $$g = 2\pi\gamma\sigma\left[R - r + (r^2 + h^2)^{1/2} - (R^2 + h^2)^{1/2}\right]$$

for the gravitational attraction of a vertical hollow cylinder at a point on the axis and in the plane of one end of the cylinder, where r and R are the inner and outer radii and h is the height of the cylinder (average height of the terrain), γ is the gravitational constant, and σ is the density of the surface material.

Table 2. Values of g_1 and g_2 With r = 6.56, R = 54.6

h	$g_1(h)$	$g_2(h)$	*h*	$g_1(h)$	$g_2(h)$
0	0	0	10.1	4.6166	4.5572
1	0.92421	0.06665	10.2	4.6326	4.6228
2	1.70189	0.26141	10.21	4.6342	4.6294
3	2.34657	0.57103	10.218	4.6355	4.6346
4	2.87667	0.97693	10.2185	4.6356	4.6349
5	3.31175	1.45975	10.219	4.6356	4.6353
6	3.66992	2.00138	10.2195	4.635704	4.635636
7	3.96659	2.58651	10.22	4.6358	4.6360
8	4.2143	3.2027	10.25	4.6405	4.6557
9	4.4230	3.8402	10.3	4.6484	4.6885
10	4.6004	4.4914			
11	4.7524	5.1505			
12	4.8839	5.8129			
13	4.9986	6.4751			
14	5.0993	7.1344			
15	5.1883	7.7887			
20	5.5116	10.9406			
30	5.8511	16.4499			
40	6.0256	20.8901			
60	6.2025	27.2731			
80	6.2915	31.4521			
100	6.3451	34.3200			
200	6.4524	40.8286			
400	6.5060	44.3847			
1000	6.5385	46.5720			
∞	6.56	48.04			

Table 3. Values of $g_2''(h)$.

h	$g_2(h)$
5	0.058603
10	0.007726
11	0.00323
11.5	0.00138
11.85	0.000225
11.92	0.0000061
12	-0.00024
13	-0.00292

For zone A, formula (1) becomes

(2) $g_1(h) = r + h - (r^2 + h^2)^{1/2}$,

while for zone B it becomes

(3) $g_2(h) = R - r + (r^2 + h^2)^{1/2} - (R^2 + h^2)^{1/2}$,

where, in the hammer zones, r = 6.56 and R = 54.6. Here we have also dropped the multiplicative constant in formula (1) to simplify our work. Throughout the remainder of this paper, and in the tables and graphs, this factor must be restored to get the true values.

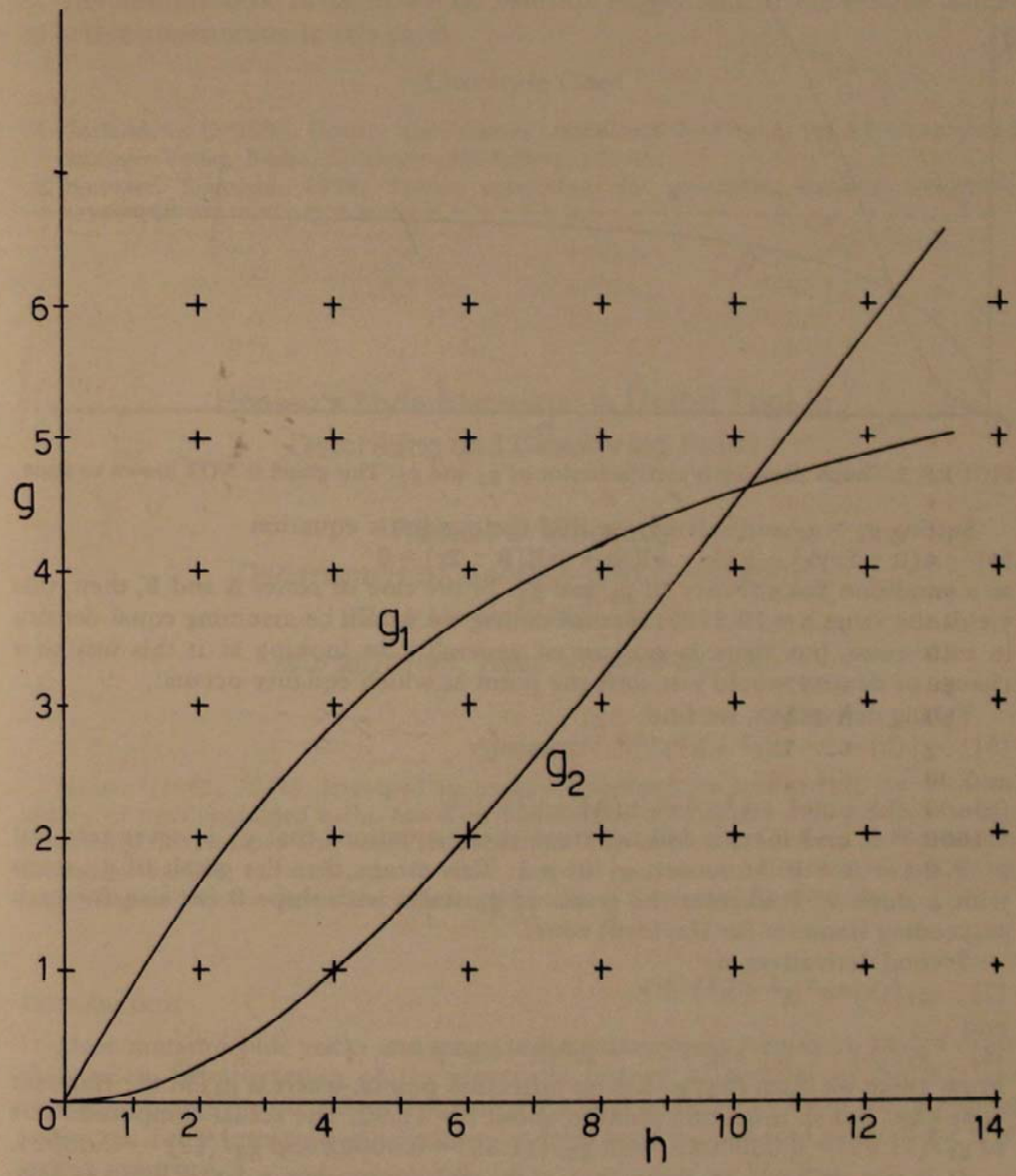

FIGURE 1. Graphs of g_1 and g_2 for $0 \leqslant h \leqslant 13$ traced from a scale drawing.

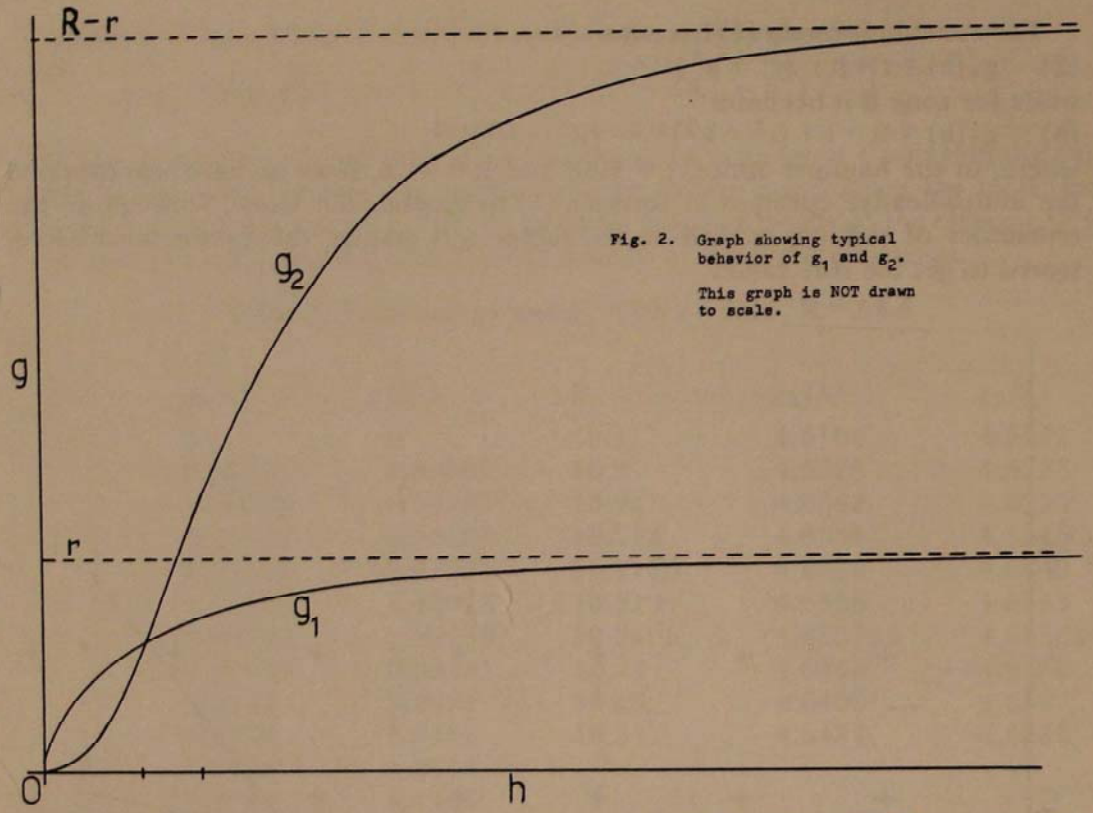

Fig. 2. Graph showing typical behavior of g_1 and g_2.

This graph is NOT drawn to scale.

FIGURE 2. Graph showing typical behavior of g_1 and g_2. This graph is NOT drawn to scale.

Setting $g_1 = g_2$ and solving, we find the quadratic equation

(4) $4(R - 2r)h^2 + R(4r - 3R)h + 4rR(R - 2r) = 0$

as a condition for equality of g_1 and g_2. In the case of zones A and B, then, this yields the value h = 10.2195. Here of course we would be assuming equal density in each zone, but there is no loss of generality in looking at it this way as a change of density would just shift the point at which equality occurs.

Taking derivatives, we find

(5) $g_1'(h) = 1 - h(r^2 + h^2)^{-1/2}$

and

(6) $g_2'(h) = h(r^2 + h^2)^{-1/2} - h(R^2 + h^2)^{-1/2}$

Since $r \neq 0$, and $R > r$, it follows from these equations that g_1' is never zero but $g_2' = 0$ for $h = 0$. Moreover, $g_1'(0) = 1$. This means that the graph of g_1 starts with a slope of 1 whereas the graph of g_2 starts with slope 0 (so also for each succeeding Hammer (or Hayford) zone.

Second derivatives are

(7) $g_1''(h) = -r^2(r^2 + h^2)^{-3/2}$

and

(8) $g_2''(h) = r^2(r^2 + h^2)^{-3/2} - R^2(R^2 + h^2)^{-3/2}$.

From these we learn that g_1 has no inflection points, whereas g_2, in the Hammer zone case, has an inflection point at about h = 11.92. The actual computed value of $g_2''(11.92) = 0.0000061$, with $g_2''(11.85) = 0.00022$ and $g_2''(12) = -0.00024$.

It is not difficult to show that each g(h) approaches a fixed limit as h increases without bound, so that g(h) is bounded. In fact we have

(9) $\lim_{h\to\infty} g_1(h) = r$ and $\lim_{h\to\infty} g_2(h) = R - r$.

For our case of the zones A and B these limits are 6.56 and 48.04 respectively. This information along with the table of values given below enables us to draw the graphs presented below. All computations have been rounded to four or five decimals, some special cases are given to six or seven.

The outstanding difference between the graphs is that g_1 begins at once to rise rapidly, but is soon overtaken by the slower g_2 which then rises rapidly and levels off at a value considerably higher than the limiting value of g_1. It is possible to give an intuitive explanation of these variant curves, but the graphical analysis makes it most clear.

The authors wish to acknowledge valuable suggestions of the referee leading to better presentation in this paper.

Literature Cited

1. Garland, G. D. 1956. Gravity and Isostasy. *Handbuch der Physik*, vol. 47, Geophysik I, Springer-Verlag, Berlin, Göttingen, Heidelberg. 202-45.
2. Hammer, Sigmund. 1939. Terrain corrections for gravimeter stations. *Geophysics* 4:184-94.

Hansen's Style Elements: A Useful Tool in Describing and Classifying Folds

Russell L. Wheeler
Department of Geology and Geography
West Virginia University
Morgantown, West Virginia 26506

Abstract

Hansen (1962, 1971) developed an improved approach to interpreting the structural history of multiply-folded rocks, based on classification of folds into style groups according to detailed fold shapes and fabric relationships. This approach has been field-tested by several workers in six map areas in three orogens, and seems well-suited for use in the poorly-exposed metamorphic and sedimentary rocks of the central Appalachians.

Introduction

Most metamorphic rocks and many sedimentary rocks have been folded more than once. Interpretation of the structural history of such rocks requires (1) recognition and distinction of folds that formed at different times, (2) grouping individual folds into fold generations, and (3) ordering the fold generations into a time sequence.

Usually folds have been grouped into generations by evaluations of their shapes and of their relationships to fabric elements such as schistosity, cleavage, and mineral lineation. The time sequence in which fold generations formed has

usually been deduced from observations of superposition relationships such as refolding and crosscutting. However, in many multiply-folded areas, superposition relationships may be rare. In studies of such areas, fold shapes and relationships to fabric have often been subjectively evaluated and vaguely reported.

A method was needed to describe folds exactly, reproducibly, completely, and in detail, yet quickly and simply enough to be usable in field work. Hansen (1962, 1971) has done this by developing the concept of strain facies and the method of style elements. Over the past decade his approach has been field-tested in four medium-grade metamorphic terrains in the infrastructure of the Norwegian Caledonides (Hansen, 1962, 1971; Scott, 1967; Brueckner, 1968, 1969; Wheeler, 1973), in one high-grade metamorphic terrain in the infrastructure of the Coast Ranges of southern British Columbia (Reamsbottom, 1971), and in the Martinsburg Formation at the Delaware Water Gap (Wheeler, unpublished results).

Strain facies

The strain-facies concept asserts that similar rocks folded under similar conditions will acquire folds of the same shape. Application of the strain-facies concept to multiply-folded rocks consists of (1) distinguishing folds of different shapes, and then (2) inferring that they developed under different conditions (Wheeler, 1973).

Style elements

Distinguishing folds of different shapes involves describing the style elements of individual folds and looking for style groups, that is, groups of folds with the same style elements. A style element is a field-observable part of a fold's shape or fabric relationships. The style elements used in the areas cited above are (1) the overall geometry of the fold in profile section (similar or concentric), (2) curvature of the hinge, (3) curvature of the limbs, (4) height-width ratio (roughly, the ratio of amplitude to wavelength), (5) harmonicity (whether the fold extends through many or few layers), (6) length of the hinge line, (7) curvature of the hinge line, (8) cylindricity, (9) relationship to planar fabric-elements, and (10) relationship to linear fabric-elements. Most of these style elements can be evaluated in profile section. Usually, but not always, harmonicity and relationships to schistosity or cleavage were the style elements most useful in classifying folds into style groups (for example, see Reamsbottom, 1971, and Wheeler, 1973).

Deformation variables that can affect folds' overall shape and individual style elements include (1) gross lithology, (2) layer anisotropy, (3) local chemical and textural inhomogeneities, (4) boundary effects, (5) older structures, (6) subsequent deformations, (7) changes in metamorphic grade, (8) changes in relative flow-rate, and (9) non-contiguous outcrop areas (Wheeler, 1973). Of these variables, the first four are expressions of rock type, the second four of the rocks' orogenic history, and the last of exposure. If all these variables can be controlled, then and only then may one make the deceptively simple statement that folds with different style elements formed at different times.

Once the individual folds have been classified into style groups, that is, into groups of folds with roughly the same style elements, then if a fold of one style group is seen superposed on a fold of another style group, the time sequence in which all folds of the two style groups formed is established.

As an example, all deformation variables were controlled during three summers of field work in an area of medium-grade schists and gneisses in central Norway (Wheeler, 1973). The method of style elements classified several hundred minor folds into four style groups. Refolding relationships observed in six outcrops ordered the four style groups into three folding episodes. Traditional, more qualitative methods would have found this difficult.

As described above, the method of style elements has been used to interpret multiple foldings in metamorphic rocks after the deformation variables listed above had been controlled. In the following paper will be described the first attempt (King, 1973) to apply this approach to sedimentary rocks that have been folded only once, in an attempt to investigate the effects of individual deformation variables.

Literature Cited

1. Brueckner, H. K. 1968. The relationships of anorthosites, ultramafic rocks, and eclogites to the country rocks of the Tafjord area, southwestern Norway. Unpublished Ph.D. dissertation, Yale University, Geology Department, 149 p.
2. ———. 1969. Timing of ultramafic intrusion in the Core Zone of the Caledonides of southern Norway. *American Journal of Science* 267:1195-1212.
3. Hansen, E. C. 1962. Strain facies of the metamorphic rocks in Trollheimen, Norway. Unpublished Ph.D. dissertation, Yale University, Geology Department, 206 p.
4. ———. 1971. Strain facies. Springer-Verlag. New York, 207 p.
5. King, G. L. 1973. Geometric analysis of minor folds in sedimentary rocks. Unpub. M.S. thesis, West Virginia Univ., 80 p.
6. Reamsbottom, S. 1971. Structural geology of the Mount Breakenridge-Cairn Needle area, southern Coast Ranges, British Columbia (approximate title). Unpublished M.S. thesis, University of British Columbia, Department of Geology, ? p.
7. Scott, W. H. 1967. Evolution of folds in the metamorphic rocks of western Dovrefjell, Norway. Unpublished Ph.D. dissertation, Yale University, Geology Department, 111 p.
8. Wheeler, R. L. 1973. Folding history of the metamorphic rocks of eastern Dovrefjell, Norway. Unpub. Ph.D. dissertation, Princeton Univ., 233 p.

Hansen's Style Elements: Application to Minor Folds in Sedimentary Rocks

Gary L. King and Russell L. Wheeler
Department of Geology and Geography
West Virginia University
Morgantown, West Virginia 26506

Abstract

Application of the concept of strain facies and of the method of style elements, via cluster analysis, to folded, silty shales of the Appalachian High Plateau reveals three style groups of minor folds. The style groups would probably not be resolvable using more traditional methods. The minor folds formed by flexural slip, were modified by flexural

flow and wedging, and resemble major folds in the Plateau and Valley and Ridge Provinces in orientation and in shape.

The preceding paper (Wheeler, 1973b) summarizes the development and field-testing of the concept of strain facies and of the method of style elements, as tools to detect and distinguish style groups, in the decade since Hansen (1962, 1971) formalized them for interpretation of structural histories of folded metamorphic rocks. This companion paper summarizes the first attempt to apply the strain-facies concept and the style-element method to folded sedimentary rocks (King, 1973).

In order to investigate whether style groups exist and can be resolved in sedimentary rocks, one road cut on Interstate 64 in Greenbrier County, West Virginia, was studied (see King, 1973, for location). The rocks are silty shales of the Devonian Brallier Formation, and are in the hinge zone of the major Browns Mountain anticline, near the anticline's southern terminus (Cardwell, Erwin, and Woodward, 1968), and within Gwinn's (1964) High Plateau.

Methods

One hundred minor folds were examined. Most are chevron-shaped, upright, and northeast-trending. Variations in fold shapes are attributed to two of the nine deformation variables listed by Wheeler (1973a, 1973b): local mechanical inhomogeneities and layer anisotropy. For each fold, as many as feasible of the following were evaluated or measured: five style elements (type of geometry, height/width ratio, harmonicity, limb curvature, and hinge curvature: see Wheeler (1973a, 1973b) or King (1973) for definitions), orientation of hinge line or of fold axis (as defined by Dennis, 1967), orientation of axial surface, and shear sense. Style groups were detected by cluster analysis based on the five style elements (see King, 1973, for details). Material movements within individual folds were analyzed using the approach of Donath and Parker (1964). Shapes and orientations of minor folds were compared to those of major folds of the central Appalachians.

Results

Cluster analysis detected three style groups. To the unaided eye, typical folds from each of the three style groups are not strikingly different in shape. However, the three possible pairs of style groups can be tested for significant differences, by comparing pairs of histograms of cumulative frequencies for each of the five style elements. Using the Kolmogorov-Smirnov test (Siegel, 1956; Miller and Kahn, 1962), eleven of the fifteen possible comparisons reveal differences that are significant with a probability greater than or equal to 0.95: each style group is distinguished from each of the other two style groups by three or four diagnostic style elements, at the 0.05 significance level. Each of the five style elements is diagnostic in at least two of the three comparisons of style groups.

Therefore, the method of style elements, applied via cluster analysis, has detected real differences in fold shape that would probably have escaped normal, visual inspection. The three style groups, whose folds resemble each other in overall shape but differ significantly in terms of individual style elements, are considered to have formed in different subfacies of the same strain facies. The different subfacies are suggested to have arisen because of anisotropies in the deformation environment at the time of folding.

The minor folds of this study have axes, hinge lines, and axial surfaces that

are sub-parallel to those of the major Browns Mountain anticline in and near the study outcrop. Faill's (1973) descriptions of the shapes of major folds in the Valley and Ridge Province in Pennsylvania resemble the style elements of the minor folds studied here. No minor fold was seen to fold another minor fold. Accordingly, minor and major folds may have formed under approximately the same deformation conditions, and perhaps coevally. (The last statement assumes that the four lithology-related deformation variables of gross lithology, boundary effects, layer anisotropy, and local mechanical inhomogeneity (Wheeler, 1973b) operated in analogous ways on major and minor scales.)

Features observed in outcrop (see King, 1973) suggest that the minor folds formed mainly by the flexural-slip mechanism of Donath and Parker (1964). In addition, material moved from limbs into hinges by flexural flow and by wedging (Cloos, 1961, 1964), possibly because of the inherent volume increase that arises in sharp hinges of flexural-slip folds (Dewey, 1965). In Donath and Parker's (1964) scheme, the minor folds thus appear to have formed when the rocks possessed low to moderate average ductility and a low to moderate ductility contrast. If some of the wedging pre-dated folding, as suggested by Cloos (1964), the resulting local mechanical inhomogeneities could have localized subsequent initiation of folding.

Literature Cited

1. Cardwell, D. H., R. B. Erwin, and H. P. Woodward, compilers, 1968. Geologic map of West Virginia. W. Va. Econ. Geol. Surv., Morgantown, W. Va.
2. Cloos, E. 1961. Bedding slips, wedges, and folding in layered sequences. *Extrait des C. R. de la Soc. Geol. de Finlande* 33:106-22.
3. ———. 1964. Wedging, bedding plane slips and gravity tectonics in the Appalachians. In Lowry, W. D., editor. Tectonics of the southern Appalachians. VPI Dept. Geol. Sci. Mem. 1, 114 p. See p. 63-70.
4. Dennis, J. G., editor. 1967. International tectonic dictionary. Am. Assoc. Petr. Geol. Mem. 7, 196 pp.
5. Dewey, J. F. 1965. Nature and origin of kink-bands. *Tectonophysics* 1:459-94.
6. Donath, F. A., and R. B. Parker. 1964. Folds and folding. *Geol. Soc. Am. Bull.* 75:45-62.
7. Faill, R. T. 1973. Kink-band folding, Valley and Ridge Province, Pennsylvania. *Geol. Soc. Am. Bull.* 84:1289-1314.
8. Gwinn, V. E. 1964. Thin-skinned tectonics in the Plateau and northwestern Valley and Ridge Provinces of the central Appalachians. *Geol. Soc. Am. Bull.* 75:863-900.
9. Hansen, E. C. 1962. Strain facies of the metamorphic rocks in Trollheimen, Norway. Unpub. Ph.D. dissertation, Yale Univ., 206 pp.
10. ———. 1971. Strain facies. Springer Verlag, N. Y., 220 pp.
11. King, G. L. 1973. Geometric analysis of minor folds in sedimentary rocks. Unpub. M.S. thesis, West Virginia Univ., 80 pp.
12. Miller, R. L., and J. S. Kahn. 1962. Statistical analysis in the geological sciences. John Wiley and Sons, Inc., N. Y., 483 p. See p. 464-70.
13. Siegel, S. 1956. Nonparametric statistics for the behavioral sciences. McGraw-Hill Book Co., N. Y., 312 pp.
14. Wheeler, R. L. 1973a. Folding history of the metamorphic rocks of eastern Dovrefjell, Norway. Unpub. Ph.D. dissertation, Princeton Univ., 233 pp.
15. ———. 1973b. Hansen's style elements: a useful tool in describing and classifying folds. *Proc. W. Va. Acad. Sci.* 45:289-291.

Possibilities for Uranium, Vanadium, Copper, and Silver in the Pennsylvanian System in West Virginia

John M. Dennison
Geology Department
University of North Carolina at Chapel Hill
Chapel Hill, North Carolina 27514

Abstract

Most United States commercial deposits of uranium are associated with feldspathic fluvial sandstones as a result of geochemical cell concentration from groundwater circulation. Sedimentary and stratigraphic criteria are presented which lead to the conclusion that the Pottsville Group, Allegheny Formation, and Conemaugh and Monongahela Groups in West Virginia have moderate potential for uranium. The Dunkard Group is highly favorable for uranium prospecting.

Geochemical cells can concentrate other elements besides uranium, including vanadium, copper, and silver. Geochemical sampling should be done for these elements, especially associated with the red shales and siltstones of the Dunkard, Monongahela, and Conemaugh Groups and Allegheny Formation.

Most commercial deposits of uranium in the United States occur in fluvial sandstones. Uranium protore sandstone is characteristically arkosic or feldspathic and is usually reddish or brownish in color, associated with oxidation of originally carbonaceous or pyritiferous sandstones (Adler, 1970). The ore bodies form by reduction and precipitation at the downward circulation limit of oxidizing groundwater (Figure 1), with concentrations along channel margins.

Based on these criteria, the Pottsville Group, Allegheny Formation, and Conemaugh and Monongahela Groups in West Virginia are rated to have moderate potential for uranium. Plant and pyritic material is abundant in the sandstones, but feldspar content is lower than desirable. The Pocahontas Formation is more feldspathic than the overlying New River and Kanawha Formations of the Pottsville Group. The greater thickness of the Pottsville in the south and reports of brownish or reddish colors for scattered outcrops of the Dotson and Lower Nuttall sandstones also suggest that the southern region is the most favorable site for uranium. Reddish shales and siltstones seem totally absent in the Pottsville, however. Regional tilts to the northwest would favor uranium-cell potential from groundwater circulation in southern West Virginia. Nonmarine deltaic deposits alternate with some marine zones.

The upper Allegheny Formation has definite reddish shale and siltstone streaks from Wayne to Clay counties, but no red sandstones are reported. Average depositional strike extended along a line from Wayne to Mineral County, with the Allegheny strata being alluvial plain deposits and low-rank graywacke sandstone channels formed by streams flowing northwestward toward occasional marine embayments in Ohio and the Northern Panhandle of West Virginia.

Conspicuous red shales and siltstones occur in Conemaugh Group cyclothems, but none of the fresh sandstones are oxidized reddish in unweathered exposures

GEOCHEMICAL WEATHERING CELLS

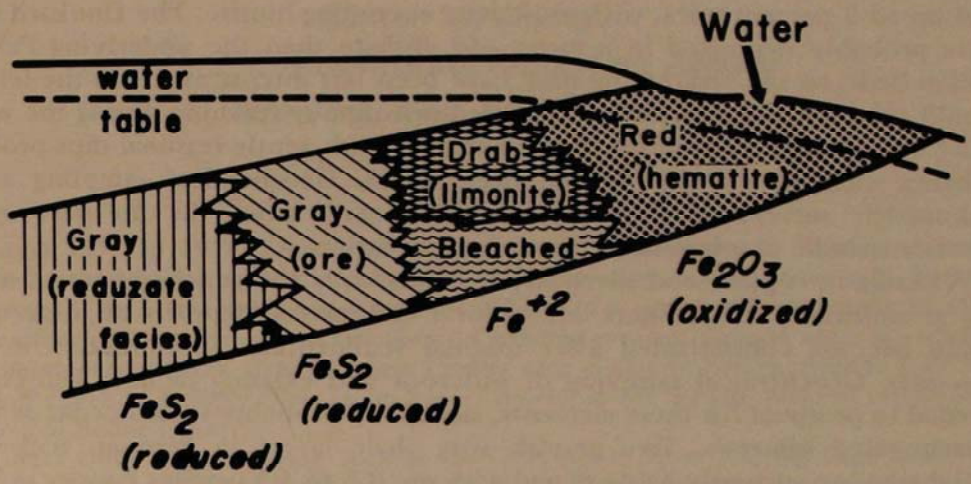

Reduced	Oxidized
Fe^{+2}	Fe^{+3}
U^{+4}	U^{+6}
Cu^{+1}	Cu^{+2}
Ag^{0}	Ag^{+1}
$V^{+3 \text{ or } +2}$	$V^{+4 \text{ or } +5}$
S^{-2}	S^{+6}

FIGURE 1. Cross-section diagram of geochemical cell mechanism which can concentrate uranium and other elements by changes in oxidation potential of circulating ground water systems. The most common occurrence of element valence state is indicated for the reduced and oxidized portion of the cell. (Chiefly after Adler, 1970 and Rackley, Shockey, and Dahill, 1968.)

of the ancient stream channels. Southward and eastward increase in redbed abundance, decrease of marine shale and limestone zones in the same direction, and limited paleocurrent information on the low-rank graywacke sandstones suggest paleoslopes toward the north and northwest.

The Monongahela Group lacks marine fauna in West Virginia. Regional facies patterns with marked increase of red shale and siltstone toward the south (Arkle, 1959), along with limited paleocurrent information suggest streams flowed northward to northwestward and deposited low-rank graywacke channel sandstones. No oxidizing facies sandstones occur in the Monongahela Group.

The Dunkard Group is rated as highly favorable for uranium prospecting. Red shales and siltstones become especially pronounced in the south (Arkle, 1959).

There are no confirmed reports of oxidizing facies reddish sandstones, but they should be expected in southern localities. Limited paleocurrent data (Jones and Clendening, 1968; Martin and Henniger, 1969) confirm a northern paleoslope pattern for the streams which deposited sandstones with up to 5 percent feldspar and up to 5 percent mica, with muscovite exceeding biotite. The Dunkard strata were probably deposited in a more arid climate than the underlying Pennsylvanian beds, so the weathering may have been less intense and thus the feldspar would tend not to have lost its associated uranium by leaching during the weathering cycle before deposition. Broad expanses with gentle regional dips probably enhance chances for uranium-cell occurrences. Geochemical sampling and/or radiometric surveys of fresh cuts and well cores would be the best way to identify specific uranium occurrences for evaluation.

Vanadium, copper, and silver all are affected by the geochemistry of oxidizing groundwater cells (Figure 1), so local commercial deposits of these metals could become concentrated after original sedimentary accumulation in trace amounts. Geochemical sampling of outcrops and existing or new drill cores is needed to prospect for these elements, since they probably would occur as finely disseminated minerals. Two grayish silty shale layers in Permian redbeds of Oklahoma are currently being mined with ore 0.5 to 4.5 percent copper in layers up to 1.5 feet thick (Johnson and Ham, 1972). Chalcocite occurs there in the subsurface, altered to malachite near the outcrop. Comparable deposits should be sought in West Virginia, especially in Dunkard, Monongahela, and Conemaugh Groups and Allegheny Formation red shales and siltstones. The Dunkard Group, of these stratigraphic units, has by far the largest volume of favorable strata, and the Dunkard rocks are most favorably situated for open-cut mining, so they are the best target for copper exploration.

Acknowledgments

This paper is an outgrowth of work done for a compilation evaluation of uranium protore potential in southeastern United States (Dennison and Wheeler, 1972), supported by the United States Atomic Energy Commission under Contract AT(30-1)-4168.

Literature Cited

1. Adler, H. H. 1970. Interpretation of color relations in sandstone as a guide to uranium exploration and ore genesis, *in* Uranium exploration geology. International Atomic Energy Agency. Vienna. 331-44.
2. Arkle, T., Jr. 1959. Monongahela Series, Pennsylvanian System, and Washington and Greene Series, Permian System, of the Appalachian basin. *Geol. Soc. America,* Guidebook for field trips, Pittsburgh meeting, Field trip 3:115-41.
3. Dennison, J. M., and W. H. Wheeler. 1972. Precambrian through Cretaceous strata of probable fluvial origin in southeastern United States and their potential as uranium host rocks. U. S. Atomic Energy Commission open-file report GJO-4168-1, 211 p.
4. Johnson, K. S., and W. E. Ham. 1972. Permian copper-shale deposits of southwestern Oklahoma. *Geol. Soc. America,* Abstracts with programs 4:555.
5. Jones, M. L., and J. A. Clendening. 1968. A feasibility study for paleocurrent analysis in lutaceous Monongahela-Dunkard strata of the Appalachian basin. *Proc. W. Va. Acad. Sci.* 40:255-61.
6. Martin, W. D., and B. R. Henniger. 1969. Mather and Hockingport Sandstone Lentils (Pennsylvanian and Permian) of Dunkard basin, Pennsylvania, West Virginia, and Ohio. *Amer. Assoc. Petroleum Geologists Bull.* 53:279-98.
7. Rackley, R. I., P. N. Shockey, and M. P. Dahill. 1968. Concepts and methods of uranium exploration. *Wyo. Geol. Assoc. Guidebook,* Twentieth Annual Field Conference :115-24.

Development of Fresh Water Aquifers near Salt Water in West Virginia

Benton M. Wilmoth
U. S. Environmental Protection Agency
Wheeling, West Virginia 26003

Abstract

During 1971 to 1973, more than a dozen small communities in Logan and Boone counties, West Virginia, started development of public water supplies from wells. Existing water supply problems are being solved by utilizing the cumulative experience of other communities and the history of operation of existing systems. Ground water is currently being developed in valley areas of Logan County such as Man to Lorado, Essie to Big Creek and Huff Creek to Mallory. New ground-water developments are also planned for the Ashford area of Boone County.

In areas along major streams, such as the Guyandotte River and Big Coal River, salt water is present in places at depths of only 60 to 150 feet beneath the river channel. Before test drilling is done in these areas, it is prudent to obtain expert advice on subsurface conditions. Such guidance can be useful in test drilling and well-field development and operation. A geologist can also help to prevent large monetary losses and failure of good existing systems from poor aquifer management.

In the next few years, many new communities and industries in West Virginia will have to develop water supplies and some existing communities and industries will need to consider additional sources of supply because of increases in water use.

Ground water has historically been regarded as a quantitatively minor water source with the principal users being rural residents. In fact, however, ground water represents more than 90 percent of the available fresh water in the State. Ground-water systems are used by 301 communities and most rural residents, which totals 55 percent of the State's population. In addition, some 400 industries and 8,000 businesses, institutions, and dairy farms also utilize ground-water sources for all requirements. Although ground water is known by geologists to be an imperative in water resources development, this major resource is, at times, not considered by developers (Lehr, 1972). Reasons for this appear to be that ground water cannot be seen or estimated during initial planning and reconnaissance and that subsurface hydrologic conditions present a strange and bothersome unknown. This unfortunate lack of knowledge on the part of water-development planners is being corrected as rapidly as possible by those involved in ground-water work such as scientists, competent drilling contractors, and the programs of the National Water Well Association.

One important aspect of the water conservation effort is to determine the amounts of ground water that can be obtained from the available local aquifers on a sustained basis. The yield of wells depends upon the local hydrogeology. Most important is the permeability and storage capacity of the rocks, but topography and the shape of the water table also have an effect.

Relatively shallow rocks of Pennsylvanian age in the western half of the State

have been invaded in the geologic past by connate brine (Price, et al., 1937). The magnitude of this salt-water encroachment has been realized from the development and operation of industrial and public water supply wells. Examples of fresh ground-water development near salty ground water in western West Virginia include both natural occurrences of salt water and unnatural encroachment of salt water caused by the stresses placed on the subsurface environment by man. Salt-water encroachment into existing fresh-water aquifers is usually the result of some industrial activity. Both vertical and lateral encroachment can be caused by (1) reduction of fresh-water head due to pumping, (2) drilling too deep and intercepting salt-water zones, and (3) imposing greater head on salt-water zones from waste brine disposal, repressuring, and hydraulic fracturing at oil and gas operations (Wilmoth, 1970). The general extent of brine intrusion into shallow aquifers in the western part of the State is known and can be described in order that drillers and developers can plan the construction of a well field in advance. It is important to know the depth of the shallowest salt water in an area before a production well is constructed.

During 1971 to 1973, several small communities in Logan and Boone counties, West Virginia, started development of new water systems from ground-water sources. A considered major factor was that the cost of treated ground water at the household tap is only 10 to 30 percent of the cost of treated surface water at the tap.

The important water-bearing rocks in these counties are the massive coarse-grained sandstones and conglomerates that dominate the geologic section of the Pottsville Group of Pennsylvanian age. The coarseness of grain size and porosity of these rocks are favorable to the storage and transmission of large amounts of ground water. Good fracture permeability also contributes significantly to their water-bearing character. Yields of individual wells range from less than 50 to more than 1,000 gallons per minute, but the average yield of high-capacity industrial and public supply wells is about 200 gpm. Supplies as large as 0.5 to 1 million gallons per day are developed locally with well fields of only 3 to 5 wells (Wilmoth, 1972b).

Ground water is usually more abundant in valley areas, but along the Guyandotte River and the Coal River natural salty ground water is present at depths of only 60 to 150 feet beneath the river channel. The presence of this salt-water interface imposes some limitations on the availability of fresh ground water from a single well.

In the Man to Kistler area of Logan County, the salt-water interface lies at about 600 to 625 feet above mean sea level. Therefore, wells can be drilled no deeper than about 150 feet to avoid intercepting salt water. Along Buffalo Creek tributary to the Guyandotte River in the Accoville to Amherstdale area, wells can be drilled as deep as 200 feet. In the Lorado area, wells as deep as 500 feet have not encountered salt water. This tends to substantiate the general concept that the river channels act as areas for the natural discharge of all ground water and that the salt-water interface tends to cone up toward the channel.

In the Essie to Big Creek area of Logan County, along the Guyandotte River, the salt-water interface is extremely shallow and lies at about 550 feet above mean sea level. Consequently, most fresh-water producing wells must be no deeper than about 80 feet if they are located near Route 10. In order to obtain a greater fresh-water aquifer thickness, wells can be located at higher elevations away from streams.

In the Huff Creek to Mallory area of Logan County, the salt-water interface

lies at about 125 to 150 feet below the channel of Huff Creek. Consequently, wells cannot be drilled much deeper than about 100 feet.

In higher areas of tributaries such as Riddle Branch, however, wells can be drilled as deep as 200 to 250 feet and still produce fresh water. Similar elevation of land surface, depths of wells, and quality of ground water relationships exist along other topographically higher tributaries of Huff Creek.

At Ashford, Boone County, along Big Coal River, the salt-water interface lies at about 570 to 580 feet above mean sea level. Wells initially penetrated the interface as much as 50 feet or more, depending on the topographic location of the wells. Each well in the field is pumped at a sustained rate of 250 gallons per minute. Records of chloride content during 1971 show that chloride increased from 880 mg/l to 933 mg/l at one well and from 630 mg/l to 938 mg/l at another well. In order to reduce salt-water encroachment, consideration has been given to experimentally decreasing the pumping rates perhaps to as low as 25 gallons per minute. In order to have the same amount of water available, pumping time will be longer, storage facilities will be enlarged, and more wells may have to be considered.

In the Charleston area of Kanawha County, withdrawal of large amounts of fresh water from the principal aquifer was a significant factor in accelerated encroachment of salt water. In 1930, the interface was about 400 feet above mean sea level but by 1950, it had moved upward by 75 to 100 feet beneath major pumping centers. The chloride content of ground water increased from less than 100 mg/l to more than 300 mg/l in several well fields and to more than 1,000 mg/l at individual wells (Wilmoth, 1972a).

Planning, design, and construction of a well field require detailed hydrogeologic data. Before the initial test drilling is started, expert advice on local subsurface hydrologic conditions should be obtained. This will help to assure successful development where shallow salt water is present. Large monetary losses and failure of test wells have been common where this guidance was not utilized. Also, some initially successful well fields have decreased in value because of water quality deterioration from excessive pumping rates. Where well-field withdrawals are properly managed, upward migration of the salt water is not a problem.

Along the coastal areas of the United States, the amount of salt water available for contamination of fresh water is essentially unlimited. In West Virginia, however, the amount of connate brine that can contaminate is limited to the amount originally in the rocks. With proper controls in subsurface activities, much salt-water contamination of fresh-water zones can be prevented.

Literature Cited

1. Lehr, J. H. 1972. Ground water—an imperative in water resources planning. The Well Log, National Water Well Association. pp. 26-31.
2. Price, P. H., and others. 1937. Salt brines of West Virginia. West Virginia Geological Survey, 203 pp.
3. Wilmoth, B. M. 1970. Occurrence of shallow salty ground water in West Virginia. *Proc. West Virginia Academy of Science* 42:202-208.
4. ———. 1972a. Salty ground water and meteoric flushing of contaminated aquifers in West Virginia, *Ground Water* 10:99-106.
5. ———. 1972b. Ground water development for communities and industries in West Virginia. *West Virginia Academy of Science* 44:149-154.

Lake Lynn, West Virginia: A Review of Recent and Current Geologic Research

Robert G. Corbett
Department of Geology
The University of Akron
Akron, Ohio 44325

Abstract

Lake Lynn, West Virginia, has been and continues to be the site of geologic and geochemical investigation. Studies of water chemistry of the reservoir and the local tributaries indicate that five streams draining old disturbed areas in the Pittsburgh seam are of the poorest quality, the reservoir itself is degraded, and some tributaries from relatively undisturbed ground are of high quality. Constituents normally sought in potable water analysis and other selected elements are reported.

Attention is called to related studies of the bottom sediments.

The reservoir officially named Lake Lynn, but widely recognized as Cheat Lake, is one of the few acidic impoundments in the United States. Ability of the water to corrode aluminum boats or marine engine parts is recognized by area inhabitants.

The reservoir provides unusual environments, in that local tributaries ranging from very low to high pH mix with the low pH reservoir water. Distribution of sediment by acid extractable trace element content (Knox, 1972) and by size (Hall, 1966; Hall and Corbett, 1966) has been studied.

The serious degradation of water quality has been documented (Corbett and Kulander, 1964; Environmental Protection Agency, 1971, p. 55, 57, 59). Studies of the spatial and seasonal variations in water quality of the reservoir (Stilson, 1969; Dannemiller, 1972; Houghton, in preparation) are described in this paper. Extreme differences in water quality of local tributaries are documented and related to the extent of strip mining (Corbett, 1973).

Water Quality Studies

Acid discharges, the most clearly recognizable form of acid mine drainage, are generally characterized by a pH between 2 and 4.5, dissolved iron content of between 500 and 10,000 PPM, and significant amounts of manganese (Hill, 1968, p. 5 and 8). Such distinctions were used by Stilson (1969) who monitored approximately monthly water quality of the reservoir at 8 stations (46 individual samples) and at 16 tributaries. He analyzed the samples for total iron by the 2,2' bipyridine method, for manganese by atomic absorption spectrophotometry, and pH at the collection site using a portable meter. In addition, he recorded temperature and dissolved oxygen.

The data allow characterization of Lake Lynn waters (annual averages for 1968) as pH of 4.25, total iron of 1.6 PPM and manganese of .04 PPM. More revealing, however, is the seasonal and spatial variation. From opposite the town of Canyon to the dam, the reservoir stratifies thermally and compositionally

during the summer, whereas uplake from Canyon the reservoir remains more nearly homogeneous. Characteristics of the water by season are summarized in Tables 1 and 2.

Table 1. Seasonal Water Characteristics of Lake Lynn Based Upon Stations From Opposite Town of Canyon to the Dam.

Season (Condition)	*Temp. °F.*	*pH*	*Total Iron (PPM)*	*Manganese (PPM)*
Winter (Homogeneity)	40.1	4.6	0.97	0.17
	(34.8 to 43.4)	(3.5 to 5.4)	(0.32 to 2.6)	(0.04 to 0.25)
Summer (Upper Water when Stratified)	75.6	4.0	0.33	0.63
	(65.8 to 81.2)	(3.6 to 4.8)	(0.09 to 0.82)	(0.31 to 0.84)
Summer (Lower Water when Stratified)	61.7	3.7	4.5	0.79
	(55.3 to 69.0)	(3.3 to 4.5)	(0.82 to 21.00)	(0.47 to 1.10)

Table 2. Seasonal Water Characteristics of the Cheat River Based Upon Station Adjacent to Quarry Run.

Season	*Temp. °F.*	*pH*	*Total Iron (PPM)*	*Manganese (PPM)*
Winter	41.4	5.3	2.0	0.16
	(40.3 to 42.6)	(5.0 to 5.5)	(1.6 to 3.6)	(0.10 to 0.20)
Summer	72.5	4.1	0.80	0.59
	(63.5 to 79.5)	(3.6 to 5.0)	(0.33 to 3.3)	(0.21 to 0.98)

Stilson's data indicate most tributaries fall into only two groups (Table 3). Preliminary geologic maps of the area (Reppert, 1972, written communication) confirm that the low pH (2.3–3.1), high iron (53–1100 PPM) and relatively high manganese (5.1–32 PPM) waters drain areas from which Pittsburgh (and Sewickley) coal has been extensively mined. The better quality waters of moder-

ate pH (5.2—8.2), low iron (up to .68 PPM) and low manganese (up to .13 PPM) drain from less-disturbed, stratigraphically lower areas.

Table 3. Water Characteristics of Tributary Streams.

	pH	*Total Iron (PPM)*	*Manganese (PPM)*
Streams from east bank or south of town of Canyon. (Minor to no strip mining of Lower Kittanning, Bakerstown or Upper Freeport coals)	7.3 (5.2 to 8.25)	0.18 (0.00 to 0.68)	0.04 (0.00 to 0.13)
Streams from west bank, town of Canyon to the dam (Extensively stripped Pittsburgh coal)	2.7 (2.3 to 3.1)	520. (53. to 1100.)	15. (5.1 to 32.)

These data suggest that the most interesting seasonal and spatial variations in the reservoir water occur late in the fall season where the water column is thickest. In order to characterize more completely these variations, the water chemistry near the dam has been studied (Dannemiller, 1972; Houghton, in preparation). These studies were of shorter duration (4 months in late summer to winter, 1971), involved fewer samples (one station, 9 samples), but sought many more constituents as compared to Stilson's work.

Constituents normally sought in potable water were determined by Dannemiller using U.S. Geological Survey analytical methods, Hach kit techniques and atomic absorption spectrophotometry as appropriate. Selected trace elements were determined by Houghton using atomic absorption spectrophotometry.

Dannemiller's data are converted to milliequivalents per liter and plotted in Figure 1, a Piper Diagram (Hem, 1970, p. 268-70; Piper, 1944). The high proportion of sulfate among the anions and the low proportion of sodium and potassium in the cations cause the water to be characterized as secondary salinity greater than 50%. Only two bottom water samples deviate from the cluster of results by having a slightly higher proportion of sodium and potassium.

Houghton's data are plotted in Figure 2, a logarithmic scale, and show the general range and some individual extreme values for the selected elements. The diagonal line is for reference and represents a zone clearly separating the acid discharges from the areas of strip mining in the Pittsburgh seam from most other tributary data (see Figure 4).

The tributary streams have been analyzed for major and selected trace elements (Corbett, 1973). Samples 2, 5, 6, 7, and 8 indicated in Figure 3, a Piper Diagram, are rather similar to the water samples from the reservoir. Each of these five samples is from a stream draining areas of strip mining in the Pittsburgh coal north of Canyon on the west side of Lake Lynn. Diversity characterizes the other samples, some falling into the type secondary alkalinity exceeding 50%.

The samples draining the disturbed areas of Pittsburgh coal are also distinctive

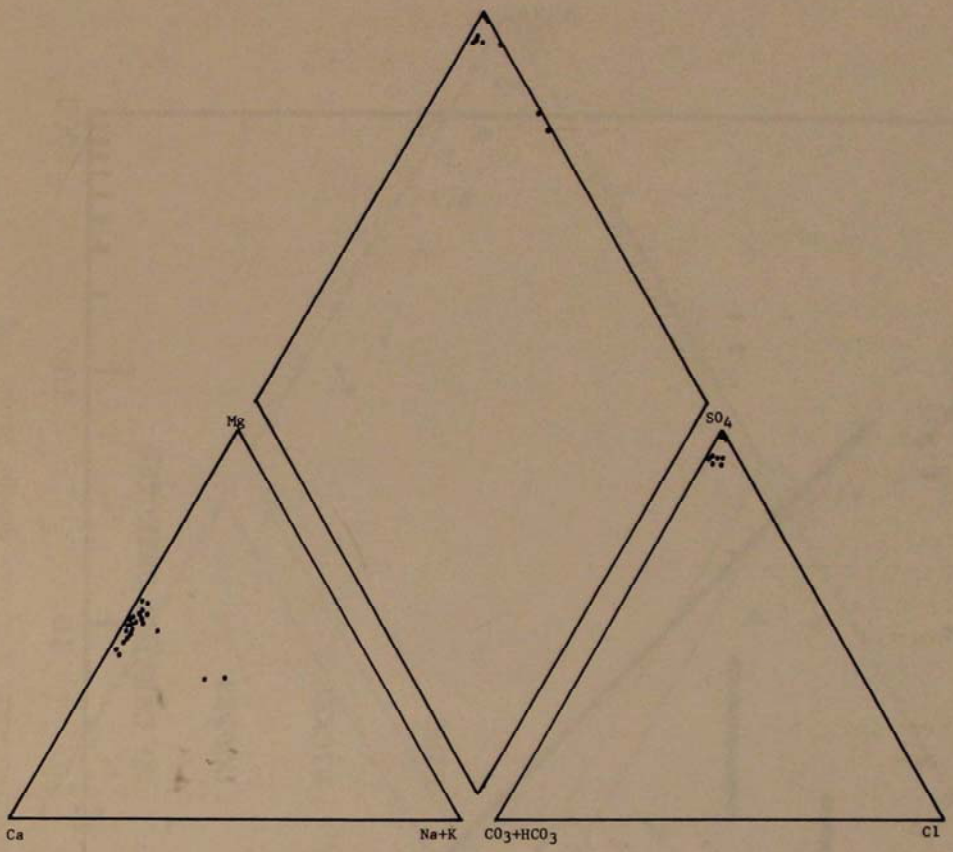

FIGURE 1. Piper diagram of reservoir water from nine depths, before and after fall overturn. Samples collected near the dam. Duplicate values omitted. Point represents percent of total milliequivalents per liter; concentration of sample not plotted.

in trace element composition (Figure 4). These samples are generally one to two orders of magnitude higher in the constituent determined, and the heavy diagonal line distinguishes them from better quality stream samples.

Conclusions

The reservoir waters are not uniform, but vary in composition with the location and the season. The greatest uniformity follows fall overturn.

The chemical quality of streams emptying into Lake Lynn ranges from high quality to very poor. The former tend to improve the water quality of Lake Lynn, but unfortunately have little quantitative effect, as indicated by the similarity in Piper Diagrams of the poor quality tributaries and the reservoir waters.

The poorest quality streams drain areas in which there has been extensive mining of Pittsburgh coal. These streams not only have the low pH, high iron and aluminum, and relatively high manganese normally ascribed to such water, but generally average one order of magnitude or more higher in such elements as silicon, chromium, zinc, nickel, copper and cadmium when compared to waters from less disturbed terrain in the area.

Acid generation from the decomposition of iron sulfide minerals, and the availability of acid-soluble trace elements in the disturbed material combine to provide the chemical composition described here.

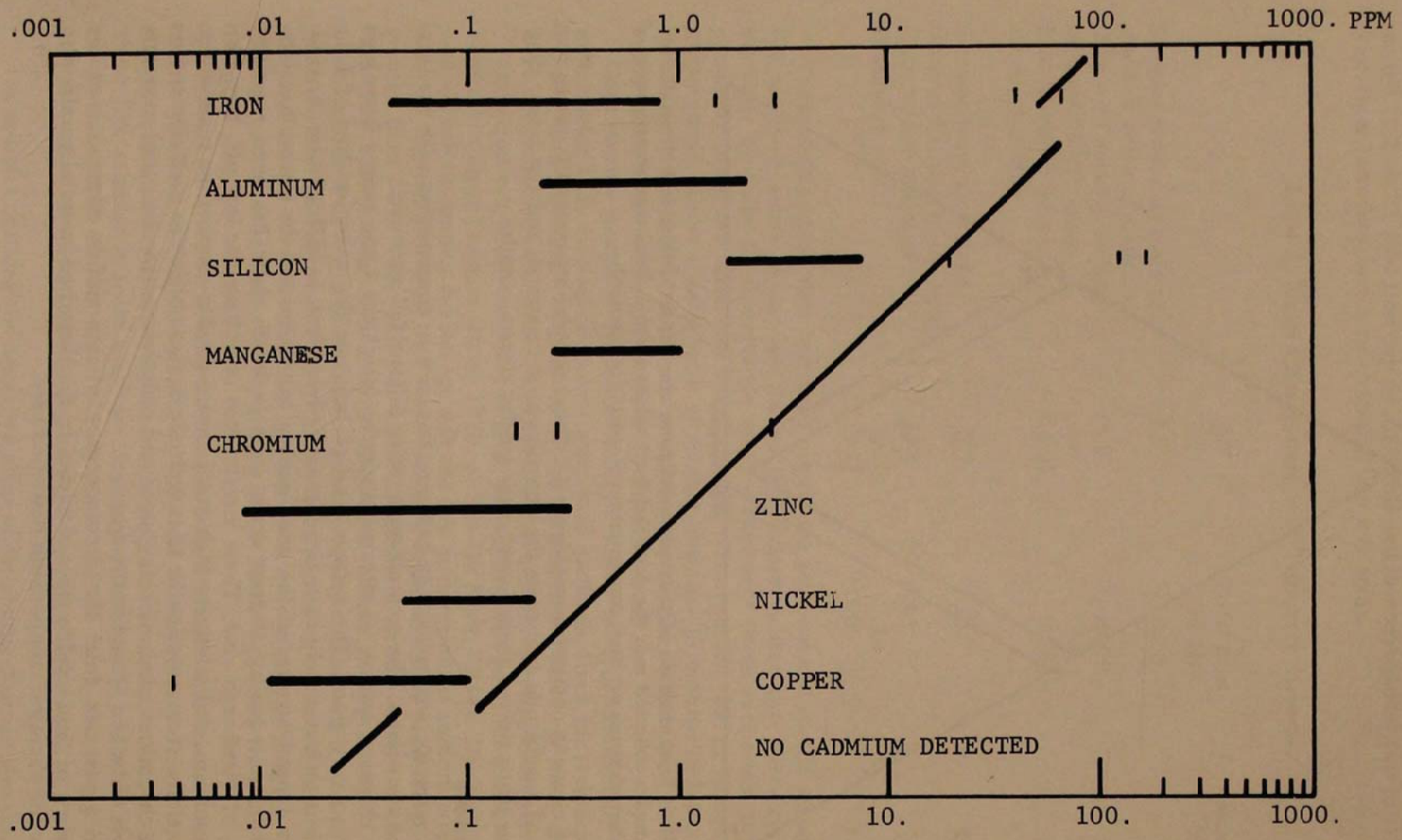

FIGURE 2. Trace element determinations of reservoir water from nine depths, before and after fall overturn. Samples collected near the dam. Diagonal bar from figure 4 included for reference.

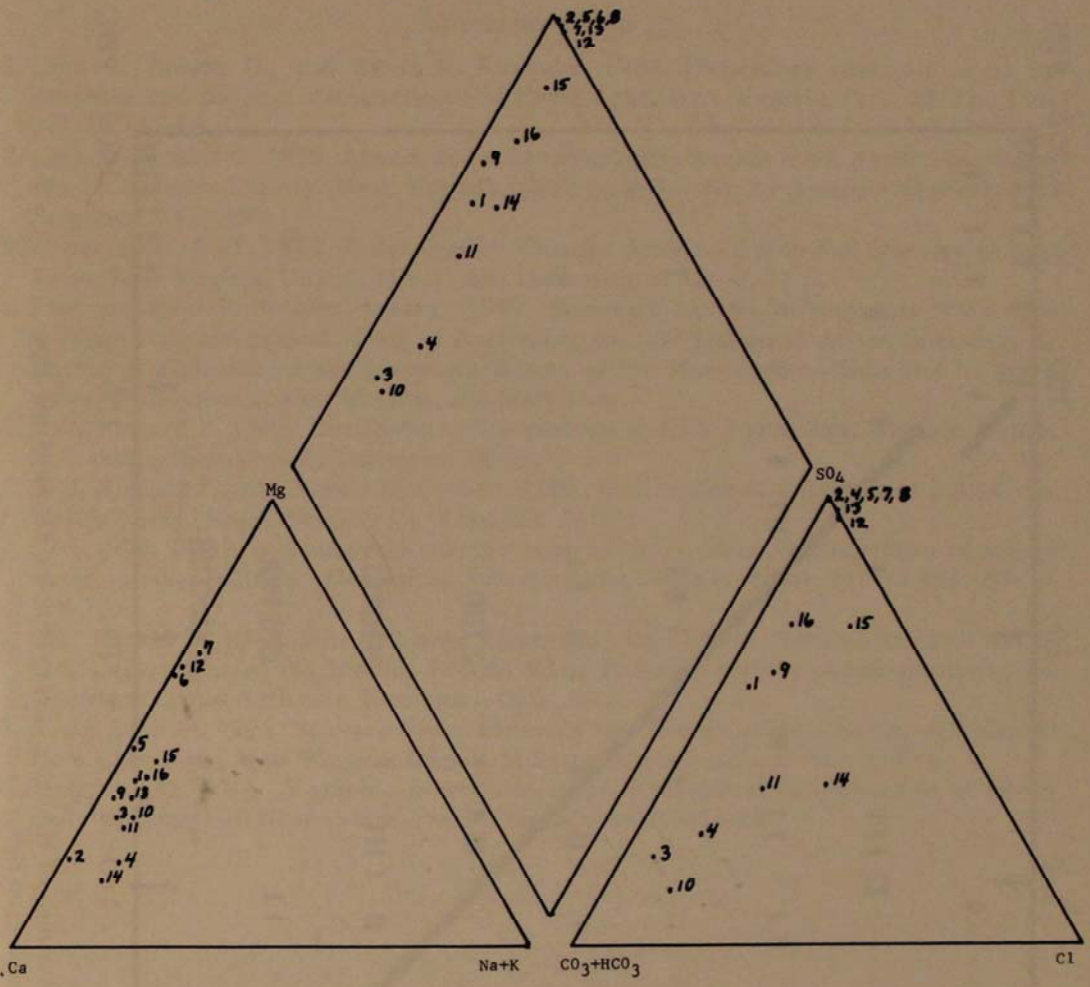

FIGURE 3. Piper diagram of tributary streams entering Lake Lynn. Point represents percent of total milliequivalents per liter; concentration of sample not plotted.

Acknowledgments

Much of the effort of these studies was enthusiastically provided by former and current graduate students at West Virginia University and The University of Akron. I gratefully acknowledge Richard T. Hall, Howard W. Phillips and John H. Knox for their efforts in collecting or analyzing bottom sediments. I also acknowledge William P. Stilson, Gary Dannemiller and Leroy K. Houghton III, for their significant contributions to the water quality studies. Members of my geochemistry classes over the years assisted in acquisition of data, but the list is too extensive to cite in detail. My appreciation, however, is clearly evident.

Robert S. Reppert, of the West Virginia Geological and Economic Survey, has kindly provided me with preliminary geologic maps and sections of the Morgantown North and Lake Lynn 7.5 minute Quadrangles.

Parts of this study have been supported by the Water Research Institute of West Virginia University as part of the project "Geochemical Behavior of Iron and Manganese in a Reservoir (Lake Lynn, West Virginia) Fed by Streams Containing Acid Mine Drainage." I am grateful for the opportunities this support provided.

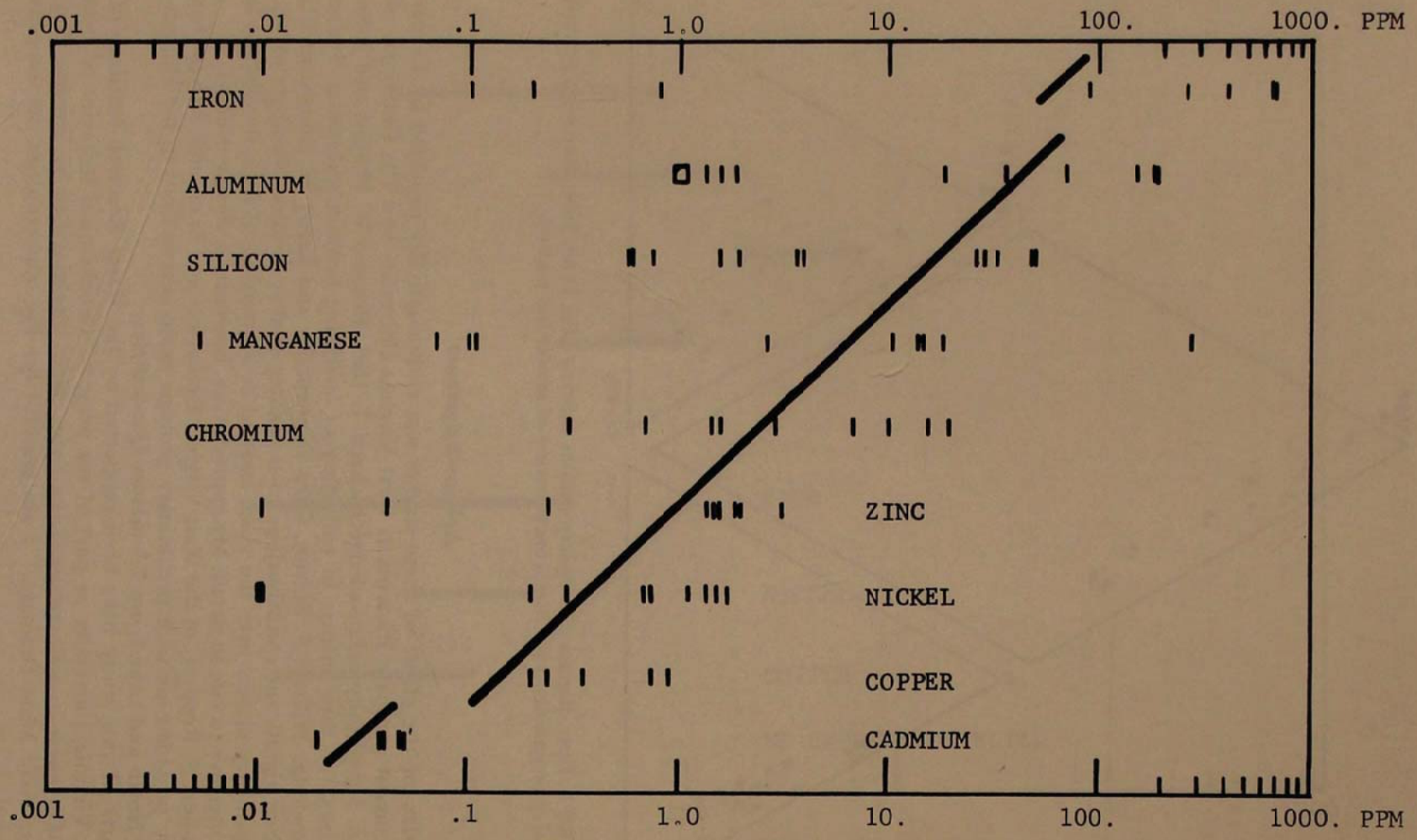

FIGURE 4. Trace element determinations of tributary stream samples. Diagonal bar separates obvious acid mine drainage samples (on right) from other samples.

Literature Cited

1. Corbett, Robert G., and Byron R. Kulander. 1964. Preliminary observations on the chemical and physical characteristics of Cheat Lake, West Virginia. *Proc. W. Va. Acad. Sci.* 36:143-46.
2. Corbett, Robert G. 1973. Abandoned strip mines: effects upon water quality, northeastern Monongalia County, West Virginia. *Geological Society of America Abstracts with Programs.* 5 (5):390.
3. Dannemiller, G. T. 1972. Water Quality Changes Associated with Fall Overturn at Lake Lynn, West Virginia. Unpub. M.S. thesis, University of Akron, 77 p.
4. Environmental Protection Agency. 1971. Summary report, Monongahela River mine drainage remedial project: 1-46. *In* Proceedings Second Session of the Conference in the Matter of Pollution of the Interstate Waters of the Monongahela River and its Tributaries—Pennsylvania, West Virginia, and Maryland.
5. Hall, Richard P. 1966. Distribution of Sediments at Lake Lynn, West Virginia. Unpub. M.S. thesis, West Virginia University, 66 p.
6. Hall, Richard P., and Robert G. Corbett. 1966. Distribution of sediments at Lake Lynn, West Virginia (Abs.). *Proc. W. Va. Acad. Sci.* 38:158.
7. Hem, John D. 1970. Study and interpretation of the chemical characteristics of natural water, second edition. *Geological Survey Water–Supply Paper* 1473:1-363. See p. 268-70.
8. Hill, Ronald D. 1968. Mine Drainage Treatment, State of the Art and Research Needs. U.S. Department of the Interior Federal Water Pollution Control Administration Mine Drainage Control Activities, Cincinnati, Ohio, 99 p.
9. Knox, John H. 1972. Selected Trace Elements and Fixed Carbon Content of Sediment from Lake Lynn, West Virginia. Unpub. M.S. thesis, University of Akron, 69 p.
10. Piper, A. M. 1944. A graphic procedure in the geochemical interpretation of water-analyses. *American Geophysical Union Transactions* 25:914-23.

Geological Data for Sanitary Landfills

Peter Lessing
West Virginia Geological Survey
Morgantown, West Virginia 26505

Abstract

The planning of sanitary landfills requires geological input so that pollution potential is minimized. New site locations should be evaluated for topography, bedrock geology, hydrology, and soil. Topography is important because landfills should be above the groundwater table. A knowledge of the bedrock allows one to avoid permeable layers such as limestone and sandstone. It also permits location of landfills on shale, which under most circumstances is quite impermeable and provides a satisfactory landfill base. Leachate pollution of the surface water and groundwater is the most severe problem. Leachate must avoid contact with the local hydrological system, and this usually requires collection and treatment of the leachate. Daily covering of a landfill is required by law and adequate supplies of soil or ripped shale bedrock must be available. Landfills can be located in geologically acceptable sites that will minimize pollution and comply with the existing State Health laws. The State Geological Survey is prepared to assist anyone in West Virginia in locating sites for sanitary landfills.

Introduction

Solid waste is the residue of man's affluence. Its presence takes many forms, such as: bottles, plastics, wood, cars, refrigerators, garbage, gob piles, manure, crop wastes, slag dumps, and yesterday's newspapers. The annual accumulation of solid waste in the United States ranges from 4 to 12 billion tons and is ever increasing. Such wastes accumulate because of the consumer's demand for convenience, the myth of unlimited resources, affluence, and economics. As Flawn (1970, p. 126) has succinctly stated, "Our affluence has reached the point where thrift costs too much."

Mining and agriculture account for approximately 90 percent of our solid waste in the U.S. (Lyons and Morrison, 1971) while the remainder is contributed as municipal waste. This municipal waste (300 million tons per year) amounts to nearly 5 billion dollars as an annual expense. If dumped on West Virginia, the State would be covered by a 1-foot blanket in 145 years; and little Rhode Island would be inundated in 7 years!

The disposal of municipal waste is presently receiving its fair share of publicity, primarily in the form of sanitary landfills (Figure 1). State Health Laws recognize landfills as the major method of disposal and as a major alternative to the common open dump. Landfilling is not a panacea to the solid waste problem, but it does offer a remedy when properly located, managed, and maintained. This paper is principally aimed at the geologic aspects of site location for sanitary landfills. It will show that the geologic setting for a landfill is critical if pollution abatement and State Health standards are to be maintained.

The Problem

The basic idea of a sanitary landfill is to bury and cover compacted solid waste. In principle it is a satisfactory method of disposal. However, in practice,

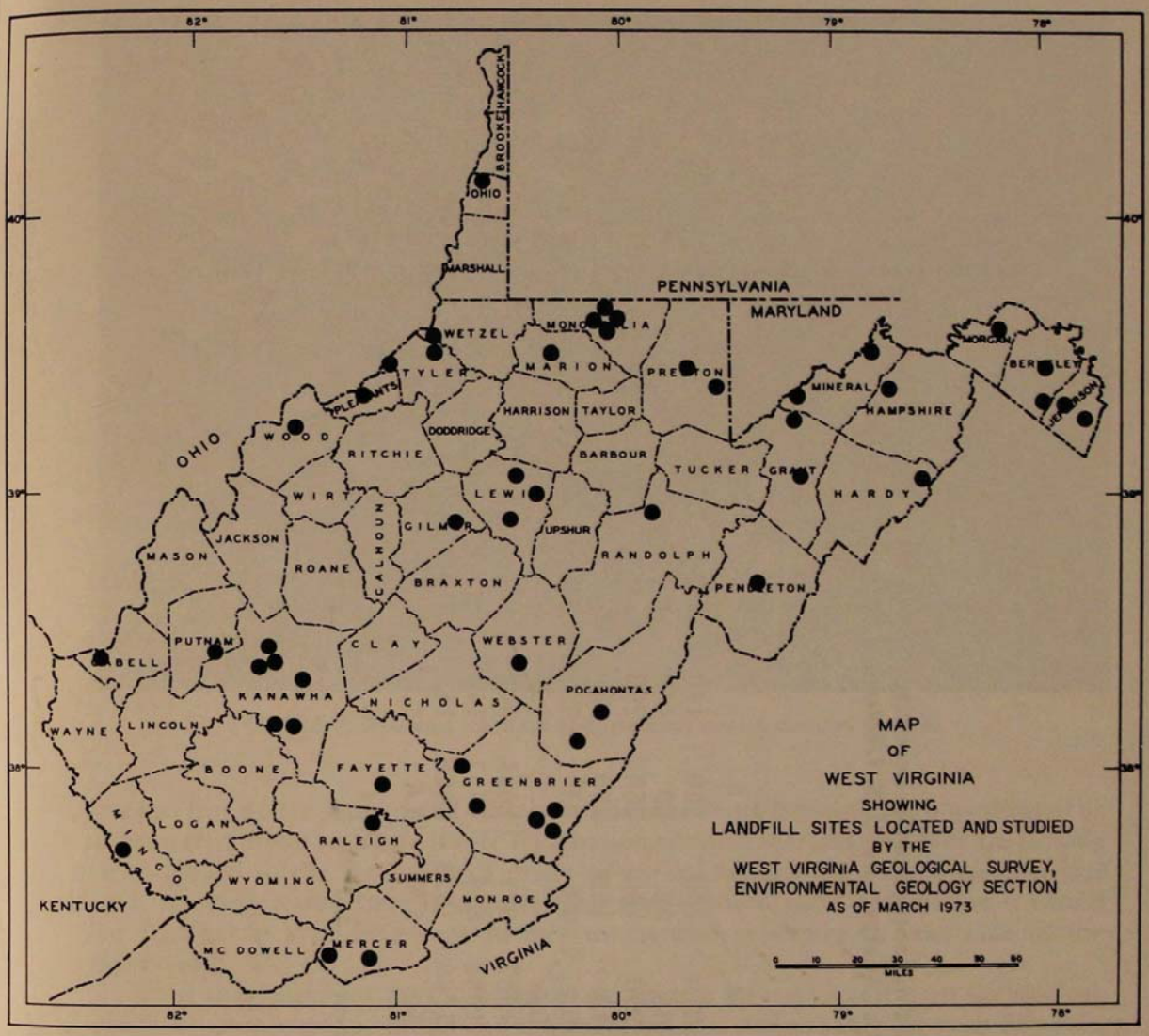

FIGURE 1. Map of West Virginia showing landfill sites located and studied by the West Virginia Geological Survey, Environmental Geology Section as of March, 1973.

the method is not fool-proof because garbage decomposes and the result is a noxious liquid referred to as leachate or effluent (Figure 2). When water passes through a landfill it removes, or leaches, any material it can, either in solution or as suspended solid matter. The amount of leachate will depend upon how much water is allowed to pass through the landfill. In the humid east it is impossible to halt the generation of leachate, and in fact, it can be expected 2 to 12 months after landfill operations begin. Leachate is the primary pollutant generated in a landfill, and its introduction into the hydrologic system must be avoided.

Leachate from sanitary landfills contains organic and inorganic material as well as gases, and their concentrations are far above all recommended and required health limits for potable water (Lessing, 1972). Few chemical analyses of leachate are available, but those that have been run attest to its unsanitary nature (Table 1). "The answer to pollution is dilution" may apply in this case, but unfortunately we do not have the data to support such a hypothesis. Furthermore, we do not know how much time is required to disperse toxic pol-

Table 1. Selected Chemical Concentrations in Leachate From a West Virginia Landfill in ppm Except pH. (Analyses by U. S. Geological Survey, 1971-72)

	1	*2*	*3*	*4*	*5*	*6*	*7*	*8*	*9*	*10*	*U.S. Public Health Service values for drinking water*
Iron	–	110	18	210	130	260	140	440	820	–	0.3
Manganese	–	70	5.8	45	32	60	44	70	95	–	0.05
Chloride	110	410	26	270	190	260	290	220	390	250	250
Sulfate	44	270	10	19	160	390	280	–	30	0.2	250
Fluoride	0.2	0.6	0.1	0.2	0.6	1.0	0.1	2.3	1.0	–	0.5-1.5[1]
Dissolved Oxygen	–	2.5	4.0	0.0	–	1.5	1.6	–	–	4.3	5[2]
Alkalinity	894	1394	176	1287	671	1591	902	1673	3018	1861	
Hardness	785	1960	161	1088	814	1537	1137	1578	2849	1519	200[3]
Dissolved Solids	1146	2678	247	1768	1335	2628	1813	2165	3992	2320	500
pH	6.1	5.6	6.3	5.5	5.5	5.6	5.7	5.9	5.5	5.4	6.5[4]

[1] Fluoride concentration is temperature dependent.
[2] Minimum for most fish.
[3] Value of 200 is considered hard.
[4] General minimum for aquatic animals.

FIGURE 2. Noxious leachate and old tires near a sanitary landfill.

lutant, nor do we know what distances leachate must travel to become diluted or attenuated down to a safe limit. To compound the uncertainties, data are lacking with regard to the retention of many of these chemicals in plants, animals, and soil. At the present time it is quite clear that without such information it would be fool-hardy and dangerous to rely on natural processes to take care of the problem.

Thus it is apparent that in order to maintain a sanitary landfill, in the manner that its name implies, the prime requirement is a site suitable for such disposal. With this in mind, the West Virginia Geological Survey has issued Environmental Geology Bulletin No. 1 (Lessing and Reppert, 1972) that discusses the site evaluation from a geological viewpoint. These authors have also written six other Bulletins that include maps for landfill sites in all 55 counties of West Virginia. Other nearby states have also investigated the relations of geology to landfill sites (Otten, 1972; Hughes and others, 1971; Miller and Maher, 1972) and bibliographies covering various phases of solid waste are available (Landers and Lessing, 1973) or from the U.S. Environmental Protection Agency.

Topography

Topography is probably the first consideration in evaluating an area as a possible sanitary landfill site. Ideally, a landfill should be located a sufficient distance from groundwater and surface water to avoid any possibility of pollution. No State Laws define this distance in West Virginia. However, it is known that the distance between landsurface and groundwater table is greatest in the higher topographic situations (Figure 3). Furthermore, the major lakes and rivers are located in topographic lows. Thus, for a starting point, sites on topographic highs will provide the maximum protection of the hydrologic system. There are,

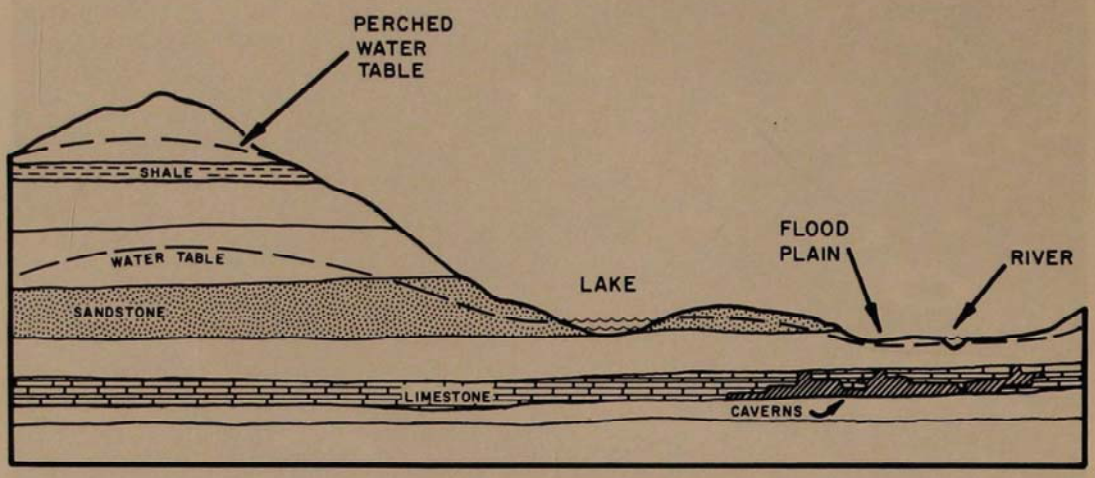

FIGURE 3. Schematic cross-section illustrating several geologic conditions discussed in text.

of course, exceptions that will be discussed later, but stream valleys, flood plains, and other low areas should not generally be considered for landfill sites.

Bedrock Geology

Bedrock characteristics which are critical to suitable sanitary landfill sites are those that control permeability. Permeable rocks, such as sandstone and limestone, permit leachate to flow through them and thus can lead to groundwater contamination. This natural characteristic is particularly evident in cavernous limestone where flow rates are measured in miles per day. Severe health hazards may result if leachate-polluted groundwater is used for a domestic supply. Although flow rates in cavernous limestone are certainly the highest, similar health conditions can develop if the bedrock is sandstone.

Based on many studies, including our own, we believe that shale or siltstone is the best available bedrock for landfill sites. Two major reasons justify this choice: (1) shale or siltstone is the most impermeable common rock category in the State, and (2) shale or siltstone bedrock can be ripped for satisfactory cover material. An impermeable bedrock minimizes the potential groundwater pollution, but it will not totally eliminate the possibility of pollution. If we combine a shale bedrock with a relatively high topographic situation, the chances of pollution are further minimized.

However, rock type alone is not the only criteria that must be evaluated. There are several geologic factors that would negate a site where shale is the bedrock. One of these factors is the existence of numerous fractures in the bedrock, whereby the original permeability would be greatly increased. Such cases are not uncommon in West Virginia, and the resulting open network of fractures may provide a permeability equal to cavernous limestone. In many cases the fractures in shale extend into under-lying limestone or sandstone and consequently may create insurmountable pollution problems.

As an impermeable rock type, shale can also be situated so as to create what is called a perched water table (Figure 3). In such case the shale prevents the downward movement of water and thus isolates it from the true water table. In such a hydrologic system the shale bedrock located near the top of a hill would *not* be a recommended landfill site.

Cover

Soil is a factor controlling landfill sites because State law requires daily cover of 6 to 8 inches and a final cover of 2 feet (Figure 5). Thus, an adequate supply must be available for proper management. It has been generally accepted that soil used for cover should be impermeable clay, so that precipitation would not percolate through the landfill and generate leachate. Two problems arise using this axiom: (1) soil is not generally plentiful enough to supply a properly managed landfill, and (2) such clay soil is extremely difficult to move in cold and wet weather.

An alternative to an impermeable cover material is ripped shale bedrock from the landfill site. Although ripped shale is a permeable material, it offers many advantages.

1. It would eliminate the possibility of gas accumulation within the landfill.
2. Water would not pool on the surface.
3. It is easily worked under adverse weather conditions.
4. Rain water could soak through the landfill rapidly, and the decay of garbage would be completed in a shorter period of time.
5. It would eliminate the stripping of nearby hillsides for soil cover.

One particular type of site that has proved to be potentially excellent for landfills is old surface mines (Figure 4). First, the spoil banks make excellent cover and it is readily available. Second, a trench is usually present and with little work can be made ready for disposal. And finally, it provides an excellent method of reclamation that few will object to.

Leachate Collection

The use of a porous cover will naturally cause the production of more leachate. However, we recommend, regardless of all other factors, that a tile drain system be constructed on an impermeable base prior to commencing operations. This tile drain under the waste will collect the leachate and direct it to a treatment facility, which is also recommended. The under-dump drain system and treatment facility further protects the surface water and groundwater. We believe such safeguards are necessary if a sanitary landfill is to live up to its name.

Hydrology

Hydrology has entered into a considerable portion of this paper. Indeed if it were not for the hydrologic implications, landfills would not present many of the problems they do (Schneider, 1970). Surface waters are relatively easy to avoid or divert, be they surface runoff, small streams, or ponds. This is not the case with groundwater, which, if polluted, may take years to naturally flush clean. The discussion thus far has emphasized groundwater for this precise reason.

One method occasionally used to purify leachate is to permit it to seep or percolate through a soil mixture under the assumption that the deleterious materials will be adsorbed on, or exchanged with, chemicals in the soil. The process is called ion-exchange and works much like a water softener. In theory, the leachate would be purified naturally and when it eventually reached the groundwater or surface water it would no longer be toxic or noxious.

Although this method is quite satisfactory under ideal conditions, there are several assumptions involved and there is also a considerable amount of data we do not have: First, it requires a soil with the correct chemistry and mineralogy

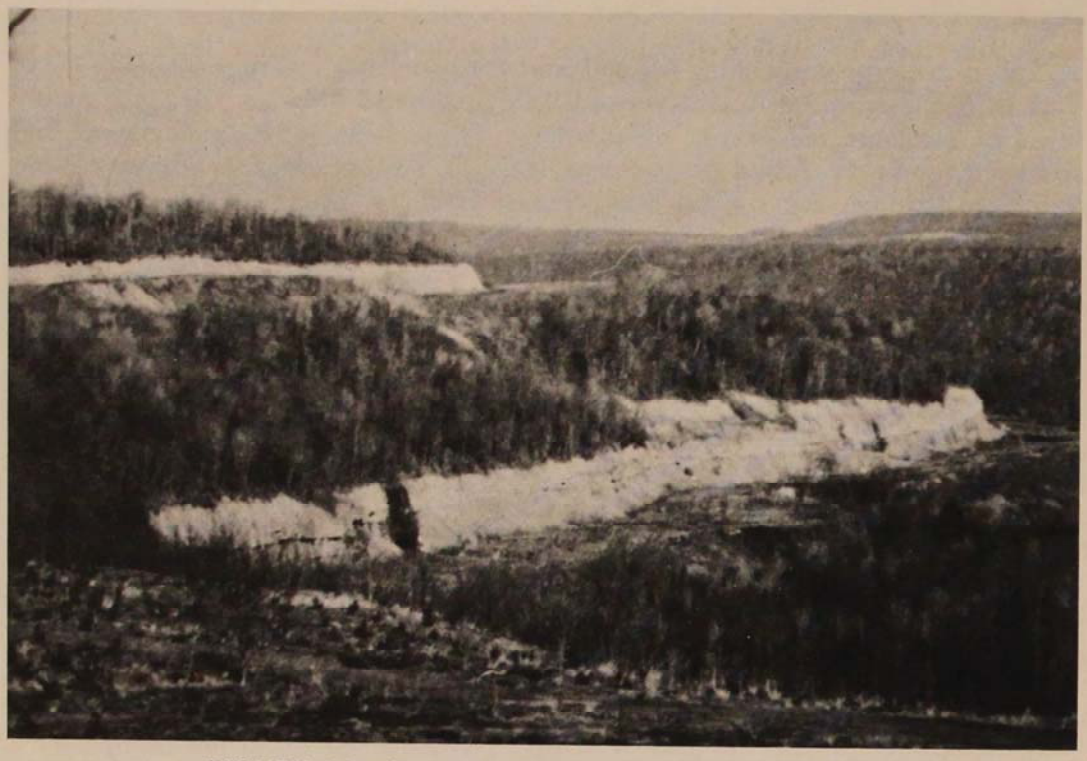

FIGURE 4. Surface mine as potential sanitary landfill site.

FIGURE 5. Heavy equipment used to cover landfill.

for exchange to take place. Second, the leachate must travel a sufficient distance through this soil for complete exchange. Third, if leachate travels as laminar flow greater flow distances are required than if flow is turbulent. Fourth, leachate cannot intersect the normal hydrologic system prior to purification. And fifth, the exchange capacity of the soil must be maintained for the duration of leachate generation. There are little or no data regarding these five conditions for natural sites in West Virginia and consequently we believe that it is better to collect and treat leachate than to rely on Mother Nature.

Conclusions

Despite the considerable number of necessary geological considerations involved in selecting a sanitary landfill site, there are many areas in West Virginia that qualify. It is certainly true that besides the geology, there are social, health, and economic factors that enter the picture. Geology should not outweigh these other vital parameters; it must be a team effort to properly evaluate a landfill site, design it, and then manage and maintain it to insure that a sanitary landfill is created.

The Environmental Geology Section of the West Virginia Geological Survey stands ready to serve the people of this State. We will geologically evaluate any site if so requested by State government, local government, or any interested non-profit agency, organization, or person.

Acknowledgments

I wish to thank Drs. Robert Erwin and James Barlow for critically reading the manuscript and offering valuable suggestions for its improvement.

Literature Cited

1. Flawn, P. T. 1970. Environmental geology. New York, Harper and Row, 313 p.
2. Hughes, G. M., R. A. Landon, and R. N. Farvolden. 1971. Hydrology of solid waste disposal sites in northeastern Illinois. U.S. Envirn. Protection Agency, publ. SW-12d, 154 p.
3. Landers, R. A., and Peter Lessing. 1973. Bibliography of environmental geology in West Virginia. *West Virginia Geol. Survey, Environ. Geol. Bull.* 8, (in press).
4. Lessing, Peter. 1972. Geology and the environment. *West Virginia Geol. Survey, 16th Newsletter,* p. 4-10.
5. Lessing, Peter, and R. S. Reppert. 1972. Geological considerations of sanitary landfill site evaluations. 2nd edition, *West Virginia Geol. Survey, Environ. Geol. Bull.* 1:33.
6. Lyons, C. J., and D. L. Morrison. 1971. Solid waste 1, Where does it all come from? *Battelle Research Outlook* no. 3, 3:3-7.
7. Miller, R. A., and S. W. Maher, 1972. Geologic evaluation of sanitary landfill sites in Tennessee. *Tennessee Geol. Survey, Environ. Geol. Ser.* 1:38.
8. Otton, E. G. 1972. Solid-waste disposal in the geohydrologic environment of Maryland. *Maryland Geol. Survey, Rept. Inv.* 18, 59 p.
9. Schneider, W. J. 1970. Hydrologic implications of solid-waste disposal. *U.S. Geol. Survey Circ.* 601-F, 10 p.